



No. 111 – March 2003

Inward Bound: Studying the Galactic Centre with NAOS/CONICA

T. OTT¹, R. SCHÖDEL¹, R. GENZEL^{1,2}, A. ECKART³, F. LACOMBE⁴, D. ROUAN⁴, R. HOFMANN¹, M. LEHNERT¹, T. ALEXANDER⁵, A. STERNBERG⁶, M. REID⁷, W. BRANDNER^{8,9}, R. LENZEN⁸, M. HARTUNG⁸, E. GENDRON⁴, Y. CLÉNET⁴, P. LÉNA⁴, G. ROUSSET¹⁰, A.-M. LAGRANGE¹¹, N. AGEORGES⁹, N. HUBIN⁹, C. LIDMAN⁹, A.F.M. MOORWOOD⁹, A. RENZINI⁹, J. SPYROMILIO⁹, L.E. TACCONI-GARMAN⁹, K.M. MENTEN¹², N. MOUAWAD³

¹MPI für Extraterrestrische Physik (MPE), Garching, Germany; ²Dept. of Physics, Univ. of California, Berkeley, USA; ³1. Physik. Institut, Univ. Köln, Germany; ⁴Obs. de Paris-Meudon, France; ⁵Faculty of Physics, Weizmann Institute of Science, Rehovot, Israel; ⁶Dept of Astronomy and Astrophysics, Tel Aviv Univ., Israel; ⁷Center for Astrophysics, Cambridge, USA; ⁸MPI für Astronomie, Heidelberg, Germany; ⁹ESO, Garching, Germany; ¹⁰Office National d'Etudes et de Recherches Aérospatiales (ONERA), Chatillon, France; ¹¹Obs. de Grenoble, Grenoble, France; ¹²MPI für Radioastronomie, Bonn, Germany

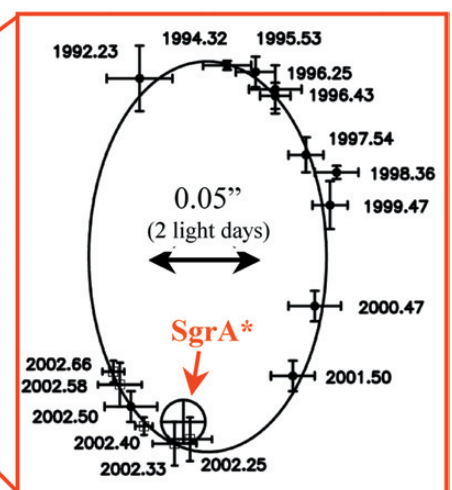
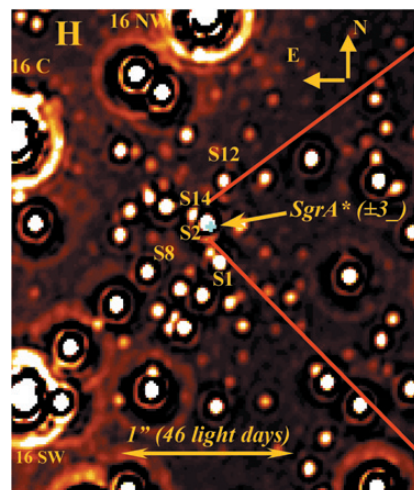
Introduction

Because of its proximity (see footnote on page 2) the centre of the Milky Way is a unique laboratory for studying physical processes that are thought to occur generally in galactic nuclei. The

central parsec of our galaxy is known to contain a dense and luminous star cluster, as well as several components of

neutral, ionized and extremely hot gas. For two decades, evidence has been mounting that the Galactic Centre har-

Figure caption: Orbit of the star S2 around SgrA* (from Schödel et al. 2002, 2003). Left: Wiener filtered, H-band NAOS/CONICA image (40 mas resolution) of the central 2". The light blue cross denotes the position of SgrA*, and its 3 σ error bar. Several of the blue 'S'-stars in the SgrA*-cluster are marked, as well as three of the bright IRS16 stars. The right inset shows the orbital data and best keplerian fit of S2 around the position of Sgr* (circle with cross). Filled circles are measurements with the SHARP speckle camera on the 3.5-m NTT, and open squares are the new NAOS/CONICA measurements. Error bars are conservative estimates, including systematic uncertainties.



bours a concentration of dark mass associated with the compact radio source SgrA* (diameter about 10 light-minutes), located at the Centre of the nuclear star cluster. SgrA* thus may be a supermassive black hole. High-resolution observations offer the unique opportunities of stringently testing the black hole paradigm and of studying stars and gas in the immediate vicinity of a black hole, at a level of detail that will never be accessible in any other galactic nucleus.

At visible wavelengths, the Galactic Centre is hidden behind 30 magnitudes of Galactic foreground extinction. Optical and ultraviolet observations are impossible or exceedingly difficult. Our knowledge of the Milky Way Centre thus derives from observations at both shorter (X- and γ -rays) and longer wavelengths (infrared and radio) that can penetrate through this obscuration. Near-infrared observations from large ground-based telescopes are particularly useful for studying the stellar component. Stars are excellent test particles of gravity. Stellar motions are ideal tools for significantly improving the constraints on the concentration and location of the central mass inferred from earlier observations of gas velocities. For this purpose, over the past decade a group of us at the Max-Planck-Institut für Extraterrestrische Physik (MPE) has been using the high-resolution, near-infrared camera SHARP, employed as a regular visiting instrument on the 3.5-m ESO NTT. The primary goal of the NTT observations was to detect stellar proper motions in the immediate vicinity of SgrA* by exploiting the excellent imaging properties and seeing of that telescope for diffraction limited H- and K-band, speckle imaging of the Galactic Centre. A second experiment used the novel '3D' near-IR integral field spectrometer for measuring Doppler velocities on the 2.2-m ESO/MPIA telescope.

When the first SHARP and 3D results of the stellar dynamics emerged 6 years ago (Eckart & Genzel 1996, 1997, Genzel et al. 1996, 1997) they provided a compelling case for the presence of a compact, central mass. The stellar velocity dispersion increases towards SgrA* from 20" to < 1" with a Keplerian law ($\sigma_v \propto R^{-1/2}$). Several stars in the 'SgrA* cluster' within 1" of the radio source exhibit velocities in excess of 10³ km/s. Shortly thereafter, the NTT results were confirmed and strengthened by independent proper-motion data obtained with the 10-m Keck telescope (Ghez et al. 1998). The Keck group also reported two years later the first orbital accelerations of three stars, demonstrating that the Centre of

force was indeed centred on the radio source (Ghez et al. 2000). The NTT and Keck results proved that 2–3.3 × 10⁶ M_⊙ are concentrated within ≤ 10 milli-parsec (2000 AU) of SgrA*. This mass concentration is most likely a supermassive black hole.

NAOS/CONICA Observations

While a central black hole is the most probable configuration, the NTT/Keck data before 2002 could not exclude several alternatives, such as an extremely compact cluster of dark astrophysical objects (e.g. neutron stars, stellar black holes, or white dwarfs), or a degenerate ball of hypothetical heavy neutrinos. Even if most of the mass is in a black hole, the hole may be surrounded by a halo of heavy stellar remnants or heavy particles, or may even not be a single object. To address these questions, it is necessary to determine the gravitational potential closer to SgrA*, and with greater precision than was previously possible. The resolution of an 8-m-class telescope is required. It is desirable to replace the statistical method of deducing the mass distribution from averaging velocities of many stars by the more precise technique of determining masses from individual stellar orbits. There are also a number of other intriguing issues that could not be addressed by the comparatively shallow NTT/Keck observations. If SgrA* is indeed a massive black hole there should be a cusp of low mass stars centred on it. It would also be important to explore other theoretical predictions characteristic of the black hole environment, such as stellar collisions and disruptions, or gravitational lensing. These goals call for much more sensitive measurements than have been achievable with speckle techniques. Adaptive optics (AO) imaging with good Strehl ratios is required. It is of great interest to better understand the evolution of the nuclear star cluster itself. Given the existing evidence for hot, massive stars in the central parsec (e.g. Genzel et al. 1996) one would like to understand how they have come into being in the very dense central environment. Finally it is highly desirable to detect the infrared counterpart of SgrA* itself. Infrared flux, spectral energy distribution and polarization provide important constraints on the poorly understood properties of black hole accretion flows.

The ideal instrument for tackling all these basic questions is the new AO imager/spectrometer NAOS/CONICA. NAOS/CONICA was mounted on UT4 (Yepun) in late 2001, and first observations became possible in early/mid 2002 during the commissioning and science verification phases of the in-

strument. Compared to the AO imagers at the Keck and Gemini telescopes, NAOS/CONICA has two unique advantages. First, the Galactic Centre passes through zenith, compared to a minimum airmass of 1.5 at Mauna Kea. Second, NAOS/CONICA has an infrared wavefront sensor. This permits wave front correction on the bright red supergiant IRS7 located 5.5" north of SgrA*. All other instruments have to lock on a relatively faint visible star at a distance of about 20". Furthermore, the 1K² CONICA detector gives a field of view as large as 30", resulting in a major improvement in the astrometric analysis of the infrared data (see below). After discussion and consultation with the ESO Director General, it was decided, therefore, to immediately carry out a first series of imaging observations of the Galactic Centre with the new instrument, as part of a collaboration of the two instrument teams and the ESO/Paranal staff. Beyond the scientific results, it also turned out that the Galactic Centre was an optimal target for verifying and optimizing the technical performance of NAOS/CONICA. The 2002 NAOS/CONICA observations immediately gave us the best Galactic Centre images ever taken, and led to a major breakthrough in our knowledge of the central parsec. The data are publicly available in the ESO archive. We give here a first account of what we have learned (see also Schödel et al. 2002, 2003, Ott et al. 2003, Genzel et al. 2003, Reid et al. 2003).

Image Analysis and Astrometry

The observations were carried out during commissioning and science verification with NAOS/CONICA between March and August 2002. Data were taken in H-band, (1.65 μ m), K_s-band (2.16 μ m) and L'-band (3.76 μ m) with the 13 and 26 milli-arcsec (mas) pixel scales, with seeing varying between 0.5 and 1.3". For H and K we used the infrared wavefront sensor of NAOS to close the loop on the bright supergiant IRS 7 ~5.5" north of SgrA*. At L' we closed the AO loop on a V ~ 14 star ~20" to the north-east of SgrA* (at the time of the observations the dichroic allowing the simultaneous use of the infrared wavefront sensor and the L/M-bands was not available). The individual images were flat-fielded, sky-subtracted and corrected for dead/bad pixels. The final frames were co-added with a simple shift-and-add (SSA) algorithm. In Figure 1 we show the K_s-band SSA image (left inset), as well as an H/K_s/L'-colour composite, SSA image (right inset) obtained as part of the science verification run in August 2002. These are the best images of the 2002 season, with Strehl ratios > 50% at K_s and 33% at H. With in-

We assume here that the Galactic Centre is 8 kpc from the Sun. At that distance 1 arcsecond corresponds to 0.038 pc, or 1.2 × 10¹⁷ cm.

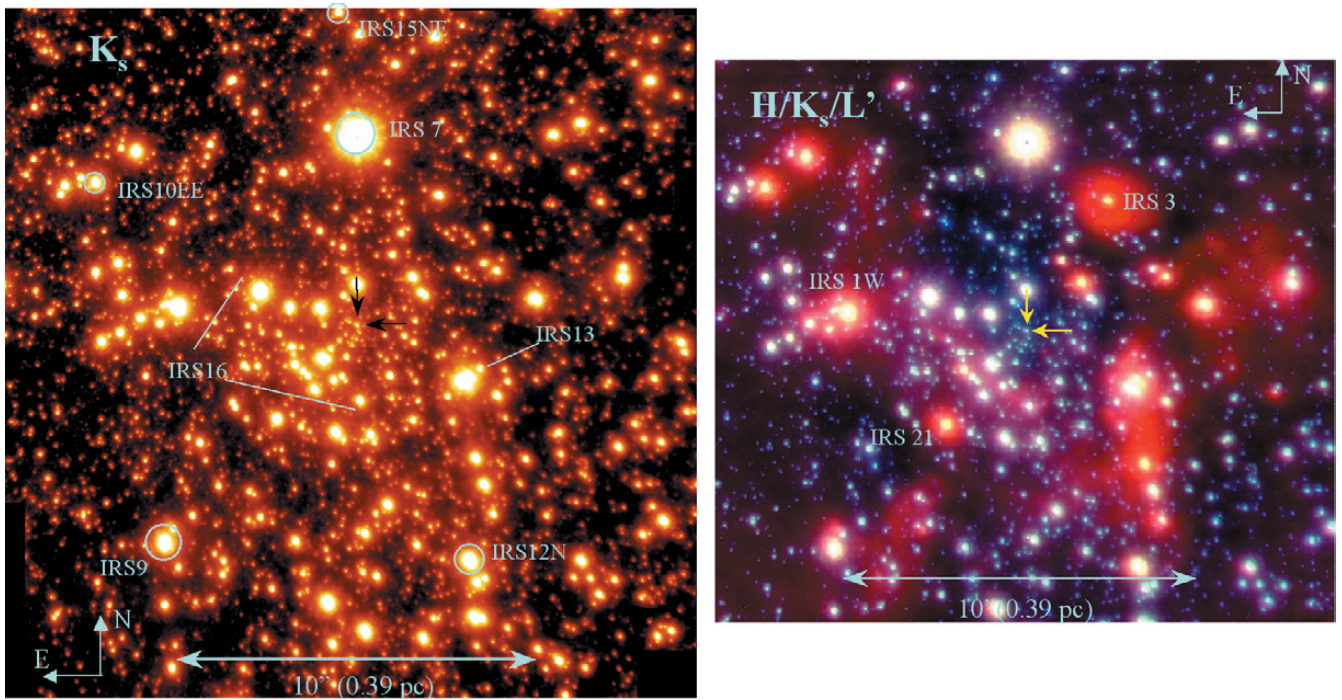


Figure 1: Left: K_s -band NAOS/CONICA shift-and-add image of the Galactic centre taken in August 2002 (55 mas FWHM resolution, Strehl ratio $>50\%$: from Schödel et al. 2002, Genzel et al. 2003). East is to the left, and north is up. The brightest star, IRS7 (6.7 mag) was used as infrared AO guiding star. The five encircled stars are also radio SiO masers and have been used for establishing the astrometry (Reid et al. 2003). The IRS16 and IRS13 complexes of emission line stars are marked. The two arrows denote the position of SgrA*. Right: H/ K_s /L' three-colour composite of the central $\sim 20''$. Several bright, dusty L-band excess stars are marked. The two arrows denote the position of SgrA*.

tegration times of about 20 minutes in each band, the data reach to $H/K_s \sim 20$ and $L' \sim 14$, ~ 3 magnitudes deeper than any Galactic Centre image taken before. The dynamic range of the images is about 13 magnitudes but bright stars are saturated in the deepest images. The final diffraction limited resolution was 40, 55 and 95 milli-arcseconds (mas) in the H, K_s and L' -bands (FWHM). The images in Figure 1 demonstrate the complexity of the dense stellar environment in the central parsec. Bright blue supergiants (in the IRS16 and IRS13 complexes), as well as red supergiants (IRS 7) and asymptotic giant branch stars (IRS12N, 10EE and 15NE) dominate the H- and K_s -images. At L' there is an additional group of dusty sources (IRS1, 3, 21). Extended L' emission comes from hot dust in the gaseous ‘mini-spiral’ streamers comprising the most prominent features of the SgrA West Hill region. The immediate vicinity of SgrA* lacks bright stars and dust. There is a concentration of moderately bright ($K_s \sim 14$) blue stars centred on the radio source (the ‘SgrA* cluster’). The faintest sources recognizable on the images are equivalent to $\sim 2 M_\odot$ A5/F0 main-sequence stars.

It is a highly challenging undertaking to extract photometry, source counts, stellar density distribution and astrometry in such an extremely dense, high dynamic range stellar field, and faced with the complex and time variable, point spread function (PSF) delivered by

adaptive optics. Our experience from a decade of SHARP data analysis is that the best method for disentangling sources, reducing the influence of the seeing halos of the numerous bright stars and determining fluxes and accurate relative positions is to first deconvolve the images with one or several, well-known methods (CLEAN, linear/Wiener filtering, Lucy/Richardson), prior to number counts and photometric analysis. The purpose of the deconvolution is not to enhance resolution, but to remove (‘CLEAN’) from the images the effects of the AO PSF. For this purpose a mean PSF is extracted from several isolated and moderately bright stars across the field. In the case of Lucy and ‘CLEAN’ the final ‘ δ -function’ images are re-convolved with a Gaussian of the original diffraction limited FWHM resolution. The agreement of sources identified with the different image analysis techniques is generally very good but naturally deteriorates within $\sim 0.5''$ of the brightest stars (and in particular those which are saturated on our images). In these regions, graininess of the seeing halo, ringing and effects of the saturated central pixels make source identification of stars four or more magnitudes fainter than the bright star unreliable. We then identified point sources and carried out photometry with the FIND procedure from the IDL Astrolib library. We took the conservative approach of including only those sources that were present on both the Lucy/Richardson and Wiener

deconvolved images, and also both in H and K_s . The final source lists comprise between 3200 and 4000 stars, depending on the FIND extraction parameters. To improve the reliability of the photometry, we applied different photometric algorithms and, where possible, averaged results from independent data sets. The final relative photometric errors are ≤ 0.1 mag below $H = 19$, $K_s = 18$ and $L' = 13$, but probably twice that for fainter stars. The absolute photometry is uncertain to 0.15 mag in H and K_s , and 0.3 mag at L' . The PSF shape can vary significantly across a field as large as that shown in Figure 1, which spans a significant fraction of the isoplanatic angle ($\sim 20''$ in radius). Remarkably the anisoplanaticity is relatively small for the data shown in Figure 1, indicating that the seeing at the time of the observations was probably dominated by the surface layers. We have also found no significant impact of the anisoplanaticity on the relative positions, at least within the central $10''$ and to a precision of ~ 5 mas (1/10 of the diffraction limited beam, Reid et al. 2003).

We determined incompleteness corrections for our images with the well-known technique of first inserting and then again recovering artificial stars randomly across the entire field. Completeness maps were created by dividing smoothed maps containing the recovered artificial sources by smoothed maps with the initially added artificial stars. The maps thus designate the

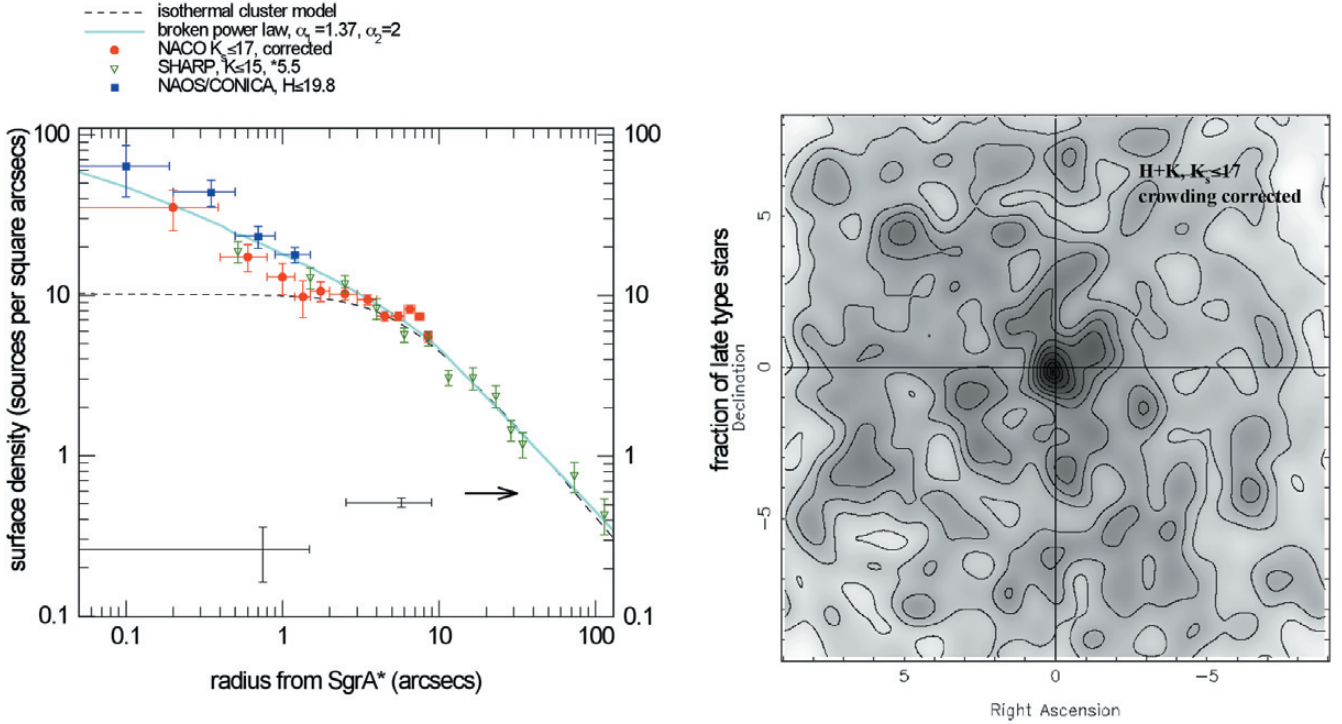


Figure 2: Surface density distribution of stars (from Genzel et al. 2003). Left: Surface density of stars as a function of projected radius from SgrA*. Red filled circles are NAOS/CONICA counts (incompleteness corrected) of sources with $K_s \leq 17$. Filled blue squares denote direct H-band NAOS/CONICA counts in the central region. Downward-pointing filled green triangles denote scaled SHARP $K \leq 15$ star counts. The short-long dash curve is the model of an isothermal sphere of core radius 0.34 pc fitting the outer SHARP counts. The blue continuous curve is the broken power-law ($\alpha = 2$ beyond $10''$ and $\alpha = 1.37$ within $10''$). Open blue circles at the bottom of the figure denote the fraction of late type stars of the total $K \leq 15$ sample with proper motions and Gemini CO narrow-band indices. All vertical error bars are $\pm 1\sigma$, and include the statistical and incompleteness correction error. Horizontal bars denote the width of the annulus. Right: Two-dimensional map of the smoothed surface density of NAOS/CONICA incompleteness corrected source counts. Contours are 10, 20,.....90, 95, 99 and 99.9% of the peak surface density. The maximum of the stellar density is at (RA, Dec) = (0.09", -0.15") relative to SgrA*, with an uncertainty of $\pm 0.2''$.

probability of recovering a source with a given magnitude at a given position. The average completeness of our K_s -images is 79%, 63% and 33% at $K_s = 17, 18$ and 19 , respectively. However, the completeness varies strongly with position, and can be very low near the brightest stars (e.g. in the IRS16 complex). All final source counts and faint star density distributions were corrected for these incompleteness effects.

An important improvement of the new NAOS/CONICA images is the accurate registration of the infrared images, in which the stars are observed, on the astrometric radio images, in which SgrA* is observed. For this purpose we aligned our NAOS/CONICA images with an astrometric grid using all 7 SiO maser sources in the field of view whose positions are known through interferometric radio measurements with the VLA and the VLBA with accuracies of a few mas (Reid et al. 2003, circled in Fig. 1). The SiO masers originate in the central 10 AU (~ 1 mas) of the circumstellar envelopes of bright red giants and supergiants, which are also present on the infrared images. We were able to improve the radio-to-infrared relative registration by a factor of 3 to ± 10 mas from the larger number of stars with SiO masers in the CONICA

images compared our earlier SHARP/NTT images. In our earlier work we had only used two SiO sources for the astrometric registration. That only allowed solving for centre position, rotation angle and a single pixel scale of the infrared images. Our new analysis allows solving, in addition, for second-order imaging terms. The nonlinear terms are negligible for NAOS/CONICA, but are significant for the SHARP data. Once the concurrent infrared and radio frames were aligned at their common observed epoch, we used the mean positions of more than a hundred stars to bring all other observed epochs into alignment by minimizing the residual astrometric errors. We were thus able to compute stellar positions (as offsets from SgrA* in right ascension and declination) with an accuracy of ± 10 mas for all epochs between 1992 and 2002. From our 10-year, SHARP-NAOS/CONICA dataset we are able to derive proper motions for about 1000 stars in the central $10''$ (Ott et al. 2003). In addition near-IR spectra are available for several hundred stars (Genzel et al. 1996, 2000, Ott et al. 2003). Finally we were able to determine individual stellar orbits (or orbital parameters) for 6 stars in the SgrA* cluster (Schödel et al. 2002, 2003, Ghez et al. 2000, 2003, Eckart et al. 2002).

Properties of the Nuclear Star Cluster: Cusp and Young, Massive Stars

The images and spectra show that the nuclear star cluster in the central parsec is highly dynamic and rapidly evolving, contrary to expectations. In particular, there appear to be many massive stars that must have formed recently. We summarize here these new results and refer to Genzel et al. (2003) for a more detailed account.

Figure 2 (left) is a plot of the stellar surface density distribution for faint stars as a function of p , the projected separation from SgrA*. The $K \leq 15$ star counts for $p(\text{SgrA}^*) \geq$ a few arcseconds can be reasonably well fit by an isothermal model of core radius 0.34 pc. However, within a few arcseconds of SgrA* the NAOS/CONICA data clearly indicate an excess of faint stars above that of the flat isothermal core whose density increases toward the centre. The two dimensional distribution (Fig. 2. (right inset)) shows that this cusp of faint stars is centred on SgrA*, within an uncertainty of $\pm 0.2''$. This is in contrast to the near-IR light distribution (Fig.1), which is centred on the bright stars in the IRS16 complex. From a broken power-law analysis we find that the stellar density increases proportion-

al to $R^{-1.37 \pm 0.15}$ within $\sim 10''$ of SgrA*. The stellar density reaches about $10^8 M_{\odot} \text{pc}^{-3}$ within $\sim 0.5''$ of the radio source. SgrA* thus is at the centre of the distribution of the faint stars. At first glance this result appears to be in very good agreement with theoretical expectations. The models predict the existence of such a cusp with power-law slopes ranging from 0.5 to 2, depending on the cusp's formation scenario and on the importance of inelastic stellar collisions. However, these models also predict that the stellar cusp ought to be dynamically relaxed and consist mostly of old, low mass stars. This is because stars migrate toward the central black hole by two-body relaxation processes. In the Galactic Centre the relaxation time scale is about 150 Myrs for a ten solar mass star, and scales inversely proportional to mass. The relaxation time scale thus is much longer than the lifetime of such a star, unless its mass is less than about $2.5 M_{\odot}$. We will see in the following that this expectation is not borne out by the observations. The data show a population of bright, apparently young stars that is not dynamically relaxed.

The central parsec contains two dozen or so, very luminous ($10^{5.6} L_{\odot}$), blue supergiants. These 'HeI emission line stars' probably are massive ($30\text{--}100 M_{\odot}$), hot ($20,000\text{--}30,000 \text{ K}$) stars in a short-lived, post-main-sequence 'wind' phase, akin to late type (W{N,C}8/9) Wolf-Rayet stars and luminous blue variables (LBVs). They can account for most or all of the far-infrared and Lyman-continuum luminosity of the central parsec. Owing to their short lifetime, these stars must have formed in the last few Myr. Consistent with a recent formation time their proper motions are not relaxed, and are dominated by a turbulent rotation pattern, with an angular momentum opposite to that of Galactic rotation (Genzel et al. 1996, 2000). About half a dozen of these luminous stars are located in the IRS16 and IRS13 complexes.

The new proper motions now demonstrate that the somewhat fainter early type stars ($K \leq 15$) are also not relaxed, and hence must be young as well. This is shown in Figure 3. While the old, late-type stars show a well mixed distribution of projected angular momenta, the early type stars exhibit a predominance of tangential orbits, that is, orbits with a velocity vector on the sky roughly perpendicular to the projected radius vector from the centre. About 75% of all early type stars are on projected tangential orbits. In the central cusp ($p \leq 3''$) about 60% of the $K \leq 15$ early type stars are on clockwise, tangential orbits. At the same time, the fraction of $K \leq 15$, late type stars decreases from 50% at $p \geq 5''$ to $< 25\%$ at $p \leq 3''$. Un-

relaxed early-type stars thus dominate the counts of the cusp at moderately bright magnitudes. Further the K-band luminosity function (KLF) constructed from the new NAOS/CONICA data also changes toward the centre. The Galactic Centre KLF between $K_s = 8$ and 19 is well described by a power law of slope ~ 0.21 , but the $p \leq 9''$ KLF in addition exhibits a prominent excess of counts near $K_s = 16$. This bump is characteristic of old, metal rich and low mass ($0.6\text{--}3 M_{\odot}$), horizontal branch/red clump stars. This bump disappears in the central few arcseconds, indicating that the cusp lacks such old, low mass stars. Finally, speckle spectrophotometry and adaptive optics spectroscopy indicate that many of the fast moving 'SgrA* cluster' stars are early type as well, equivalent to late O, early B stars with masses of $15\text{--}20 M_{\odot}$ (Genzel et al. 1997, Gezari et al. 2002, Ghez et al. 2003).

The observations portray a fascinating, albeit complicated picture of the nuclear star cluster. The central cusp appears not to be dominated by old, low mass stars. The presence of the many un-relaxed, massive stars suggests a highly dynamic picture. For the He I emission-line stars and the other early stars in the IRS16/13 complexes there are two plausible explanations. One postulates episodic infall and compression of very dense gas clouds, followed by *in situ* formation of stars. The other is the rapid sinking toward the centre by dynamic friction of a massive young star cluster that originally formed at $5\text{--}10 \text{ pc}$ from the centre. Both mechanisms appear feasible but re-

quire very special, and somewhat unlikely conditions.

For the innermost early type stars in the SgrA*-cluster both of these scenarios fail. Instead, and owing to the very high stellar densities estimated above, continuous formation of moderately massive stars by collisions and mergers of lower mass stars appears to be the most plausible mechanism. The SgrA* cluster stars thus may be blue stragglers. The stellar collisional model is also supported by the simultaneous disappearance of the late type giants and the lower mass horizontal branch/red clump stars in the central cusp.

A Star in a 15-Year Orbit Around SgrA*

Without any doubt the most exciting aspect of the new NAOS/CONICA data has been the first determination of stellar orbits around SgrA* (Schödel et al. 2002, 2003). The initial measurements of the orbital accelerations of S1 and S2, the two stars closest to SgrA*, were consistent with bound Keplerian orbits around a 3 million solar-mass central object but still allowed a wide range of orbital parameters (Ghez et al. 2000). Specifically, possible orbital periods for S2 ranged from 15 to 500 years. When we obtained the first NAOS/CONICA images in March 2002, it immediately became obvious that S2 had moved to within 10 mas of the radio source, and was now located east of SgrA*, that is, on the opposite side when compared to its position in the preceding years (see figure on cover page, left inset). This implied that S2 was just passing

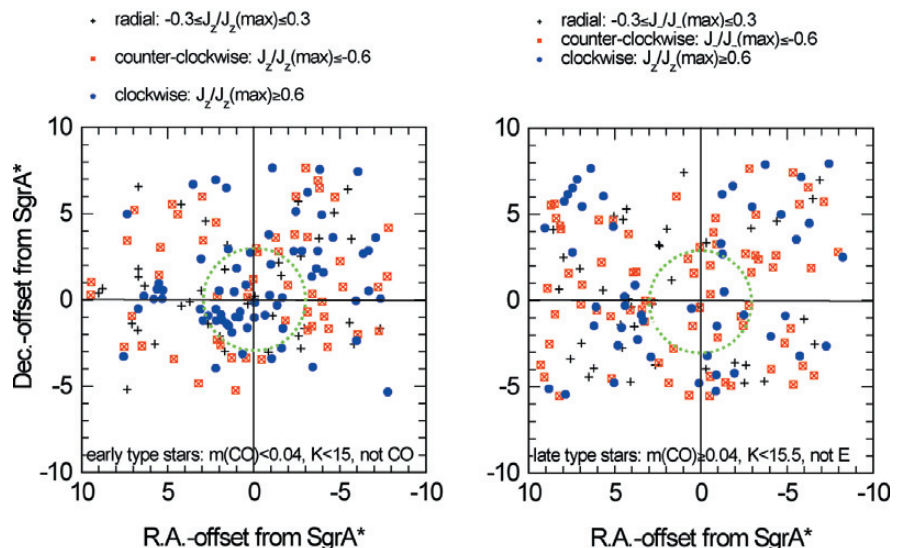


Figure 3: Spatial distribution of stars with different line-of-sight, normalized angular momenta ($J_z/J_z(\max)$), obtained from the $K \leq 15$ proper motion data set of Ott et al. (2003, see Genzel et al. 2003). Stars with mainly tangential, clockwise motions on the sky are marked as filled blue circles, stars with tangential, counter-clockwise motions are marked as crossed, red open squares, while stars with motions mostly along the projected radius vector are marked as grey crosses. Keep in mind that these are sky-projected motions. The right inset shows the distribution of spectro-photometrically identified, late type stars, while the left inset shows the same for early type stars.

through its peri-centre approach and that the S2 orbital data might probe the gravitational potential at a radius of about one light-day, 20 to 30 times further in than our earlier, statistical determinations. When more data came in, this exciting interpretation was borne out. By late May 2002 it was clear that the SHARP and NAOS/CONICA positional measurements of S2 between 1992 and 2002 sampled two thirds of a highly elliptical orbit around the astrometrically determined position of SgrA* (Reid et al. 2003).

S2 orbits the compact radio source as the planets orbit our Sun. The data shown in the right inset of Figure 4 constrain all orbital parameters with better than 10% accuracy (Schödel et al. 2002, 2003). At its peri-approach in April 2002, the star was 17 light-hours from SgrA* at which point it moved with ~ 8000 km/s. The rapid movement of the star could also be directly verified from the positional changes from month to month as more images were acquired (see Fig. 4). From the inferred

Please note that Figure 4 is shown on page 1.

orbital period of 15.2 years and its semi-major axis of 4.4 mpc, Kepler's third law implies an enclosed mass of $3.3 \times 10^6 M_{\odot}$. This value is in excellent agreement with all earlier mass measurements between ~ 15 light-days and several light-years from the centre (Fig. 5). Despite its close approach to the central mass, S2 seems to have survived this encounter without any problems. The peri-centre distance radius of S2 is 70 times greater than the distance from the black hole where the star would be disrupted by tidal forces (about 16 light-minutes for a $17 M_{\odot}$). Since tidal energy deposition falls faster than the sixth power of the ratio of tidal radius to orbital radius, tidal effects are expected to be negligible, consistent with its lack of infrared variability.

Schödel et al. (2003) have recently re-analyzed the entire 1992–2002 SHARP-NAOS/CONICA image data set. In this analysis, initial positions and fluxes of a model cluster were first fitted to the best (August 2002) NAOS/CONICA image. Subsequently, positions at other epochs were obtained by using the preceding epoch as an initial guess. By iteratively fitting and subtracting from the images first the brighter and then ever fainter stars this analysis allows tracing the positions of the fainter stars even at epochs when they move close to bright stars. Ten isolated reference stars served as anchors to align centre position and rotation angle for each epoch. By a rigorous selection of the very best imaging data and intensive image processing Schödel et al. obtained high-resolution maps of the central $1.5''$ around SgrA*

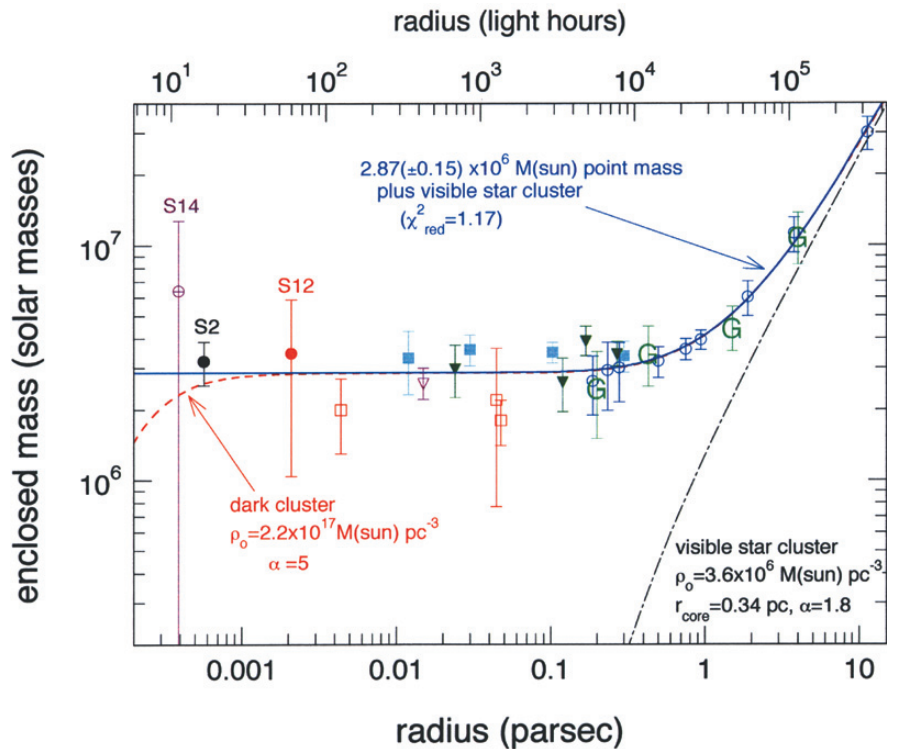


Figure 5: Derived mass distribution in the Galactic Centre (for an 8 kpc distance: Schödel et al. 2002, 2003). The filled black circle denotes the mass derived from the orbit of S2, the pink filled square the mass derived from the orbit of S12, and the filled green circle the mass derived from the orbit of S14 (Schödel et al. 2003). Error bars combine statistical (fit) and systematic/astrometry errors. Filled dark green triangles denote Leonard-Merritt projected mass estimators from a new NTT proper-motion dataset by Ott et al. (2003), separating late- and early-type stars, and correcting for the volume bias in those mass estimators by scaling with correction factors (0.9–1.1) determined from Monte Carlo modelling of theoretical clusters. An open triangle denotes the Bahcall-Tremaine mass estimate obtained from Keck proper motions (Ghez et al. 1998). Light-blue, filled rectangles are mass estimates from a parameterized Jeans-equation model, including anisotropy and differentiating between late- and early-type stars (Genzel et al. 2000). Open circles are mass estimates from a parameterized Jeans-equation model of the radial velocities of late-type stars, assuming isotropy (Genzel et al. 1996). Open red rectangles denote mass estimates from a non-parametric, maximum likelihood model, assuming isotropy and combining late- and early-type stars (Chakrabarty & Saha 2001). Black letter 'G' points denote mass estimated obtained from Doppler motions of gas (see Genzel & Townes 1987 and references therein). The black continuous curve is the overall best fit model to all data. It is a sum of a $2.9(\pm 0.15) \times 10^6 M_{\odot}$ point mass, plus a stellar cluster of central density $3.9 \times 10^6 M_{\odot}/pc^3$, core radius 0.34 pc and power-law index $\alpha = 1.8$. The grey long dash-short dash curve shows the same stellar cluster separately, but for an infinitely small core (i.e. a 'cusp'). The thick dashed curve is a sum of the visible cluster, plus a Plummer model of a hypothetical concentrated ($\alpha = 5$), very compact ($R_0 = 0.00015$ pc) dark cluster of central density $2 \times 10^{17} M_{\odot} pc^{-3}$.

down to $K \sim 16$. They find six stars in this region that show clear signs of accelerations and allow determining/constraining their orbital parameters (Fig. 6). In addition to S2, good orbital fits are also obtained for S12 and, to a lesser extent, for S14 (see below), S1 and S8. The resulting mass constraints are shown in Figure 5. They fully confirm but do not significantly improve the constraints obtained from the S2 orbit alone. The orbital periods in the central arcsecond range between 15 and a few hundred years. Most of the orbits appear to have a moderate to high eccentricity ('radial' orbits). Using the orbital accelerations of four of the six orbits in Figure 6, Schödel et al. find from a maximum-likelihood analysis that the centre of gravitational force on all orbits is at the radio position of SgrA* to with-

in the combined uncertainty of 20 mas (Fig. 6, right inset).

The Keck group very recently reported their first orbit analysis of the SgrA* cluster stars as well (Ghez, priv. comm., Ghez et al. 2003). Their results are in excellent agreement with ours, and in some cases improve the constraints significantly. Particularly exciting is the star S0-16 (S14 in our denomination, which has a very high eccentricity (0.97) and approached SgrA* in late 1999 to within about 11 light-hours (see also Fig. 6). Ghez et al. (2003) were also able to extract a radial velocity of S2 from detection of blue-shifted $Br\gamma$ absorption. This resolves the 180° inclination ambiguity of the orbit and shows that the angular momentum of S2's orbit is counter to that of Galactic rotation.

Constraints on the Nature of SgrA*

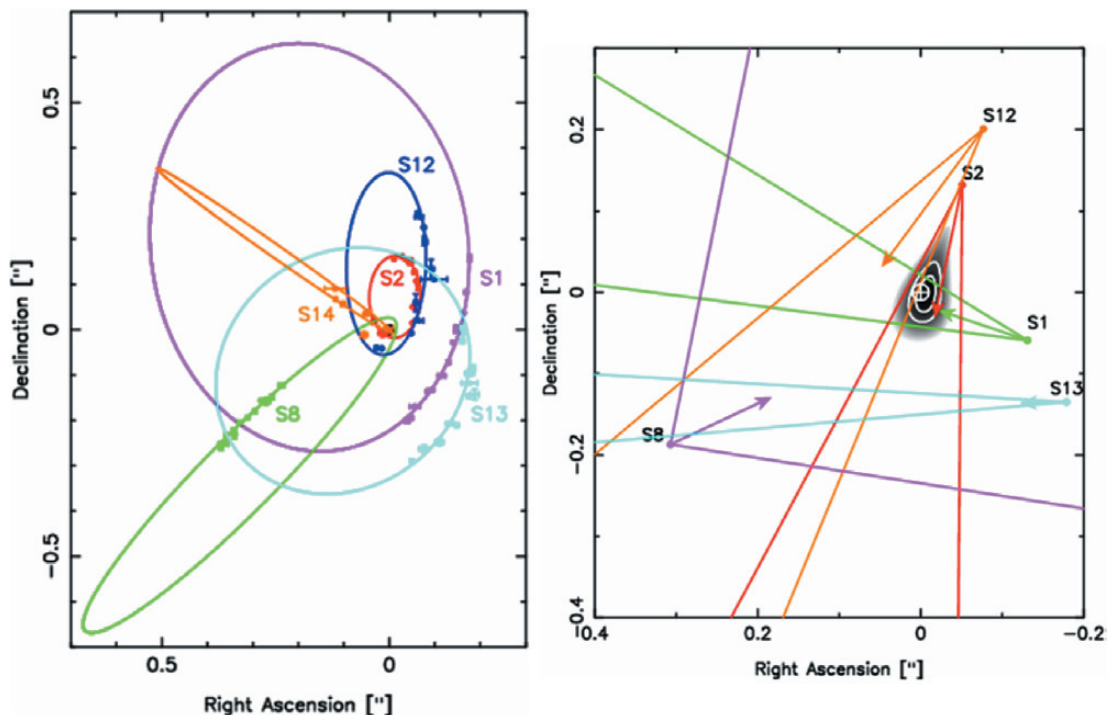
The new Galactic Centre data prove beyond any doubt that the gravitational potential resembles that of a point mass down to a scale of 10 light-hours. All available data are very well fit by the superposition of a $2.9 (\pm 0.2) \times 10^6 M_{\odot}$ point mass, plus the extended mass distribution of the visible stellar cluster. The contribution of the extended stellar cluster around SgrA* to the total mass cannot be more than a few hundred solar masses within the peri-centre distance of the orbit of S2. If the point mass is replaced by a hypothetical extended (dark cluster) mass distribution, its density must exceed $2.2 \times 10^{17} M_{\odot} \text{pc}^{-3}$, more than ten orders of magnitude greater than the density of the visible cluster at $\geq 1''$ from the centre. In addition, such a dark cluster must have a well-defined surface with a very steep density drop-off outside of it, in order to fit the flat mass distribution over three orders of magnitude in radius. If such a hypothetical dark cluster consists of low-mass stars, neutron stars, or stellar black holes, the inferred density implies a lifetime less than a few 10^5 years (Maoz 1998). This is obviously a highly improbable configuration. All stars in its vicinity are much older. Theoretical simulations of very dense, core collapsed clusters predict much shallower, near isothermal density distributions, inconsistent with the flat mass distribution. Such a dark cluster model can now be safely rejected. Our new data also robustly exclude one of two remaining, 'dark particle matter' models as alternatives to a supermassive black hole,

namely a ball of heavy ($10\text{--}17 \text{ keV}/c^2$) fermions (sterile neutrinos, gravitinos or axinos) held up by degeneracy pressure. Such a fermion ball could in principle account for the entire range of dark mass concentrations in galactic nuclei with a single physical model (Tsiklauri & Viollier 1998). Because of the finite size ($\sim 0.9''$) of a $3 \cdot 10^6 M_{\odot}$ ball of $\sim 16 \text{ keV}$ fermions, the maximum (escape) velocity is about 1700 km/s and the shortest possible orbital period for S2 in such a fermion ball model would be about 37 years, clearly inconsistent with the orbits of S2 and S14. The enclosed mass at the peri-centres of S2 and S14 would require neutrino masses of > 58 and $> 67 \text{ keV}$. Apart from the fact that the existence of a massive neutrino is not favoured by current neutrino experiments, the fermion ball model can now be safely excluded from the above constraints if the model is to explain the entire range of observed dark masses in galaxy nuclei with a single particle. The only dark particle matter explanation that cannot be ruled out by the present data is a ball of weakly interacting bosons. Such a configuration would have a radius only several times greater than the Schwarzschild radius of a black hole (Torres et al. 2000). However, it would be very hard to understand how the weakly interacting bosons first manage to reach such a high concentration (Maoz 1998), and then avoid collapsing to a black hole afterwards by baryonic accretion (Torres et al. 2000). Such accretion definitely occurs in the Galactic Centre at a rate of 10^{-7} to $10^{-5} M_{\odot} \text{yr}^{-1}$.

Figure 7 summarizes all current constraints on the size and density of the

dark mass in the Galactic Centre. In the last 15 years, gas and stellar dynamics have definitely proven the existence of a dark, non-stellar mass concentration of 3 million solar masses. Over this time period the observational constraints have pushed its size downward by 2.5 orders of magnitude, and its density upward by 9 orders of magnitude. Radio VLBI (Doeleman et al. 2001) and X-ray observations (Baganoff et al. 2001) have shown the existence of hot and relativistic gas on scales of ten Schwarzschild radii at the centre of this mass concentration. VLA/VLBA data constrain the proper motion of SgrA* in the Galactic Centre frame to be less than 20 km/s (Reid et al. 1999). Comparison of this limit to the $> 10^3 \text{ km/s}$ velocities of the stars orbiting SgrA* then implies that $> 98\%$ of the mass enclosed inside the orbit of S2 is associated with the radio source, on scales of 10 light-minutes, setting a lower limit to the density of $5 \times 10^{21} M_{\odot} \text{pc}^{-3}$ (Reid et al. 1999, Chatterjee et al. 2002). In the allowed upper left corner of parameter space there remain two possible configurations, one of which (the boson star) is purely speculative and also highly unstable. It thus seems safe to conclude that SgrA* must be a 3 million solar mass black hole, beyond any reasonable doubt. The black hole appears to be fairly 'naked' (see the constraints above on any additional extended emission surrounding it). It could in principle be a tight (< 10 light hour separation) binary black hole. However, an equal mass, binary hole would coalesce by gravitational radiation in a few hundred years. The observation of radial velocity anisotropy in

Figure 6: Stellar orbits in the SgrA*-cluster (Schödel et al. 2003). Left inset: Stellar orbits of 6 stars, obtained from an analysis of the 10-year SHARP-NACO dataset. These innermost stars are on fairly elliptical orbits, with orbital periods between 15 and a few hundred years. The right inset shows a comparison of the best maximum-likelihood distribution of the centre of gravitational force determined from the S1, S2, S12 and S8 orbits (grey scale, with 1, 2, 3 σ contours), with the nominal radio position of SgrA* (white cross with 1 σ error circle). Radio position and centre of force agree to within 20 mas.



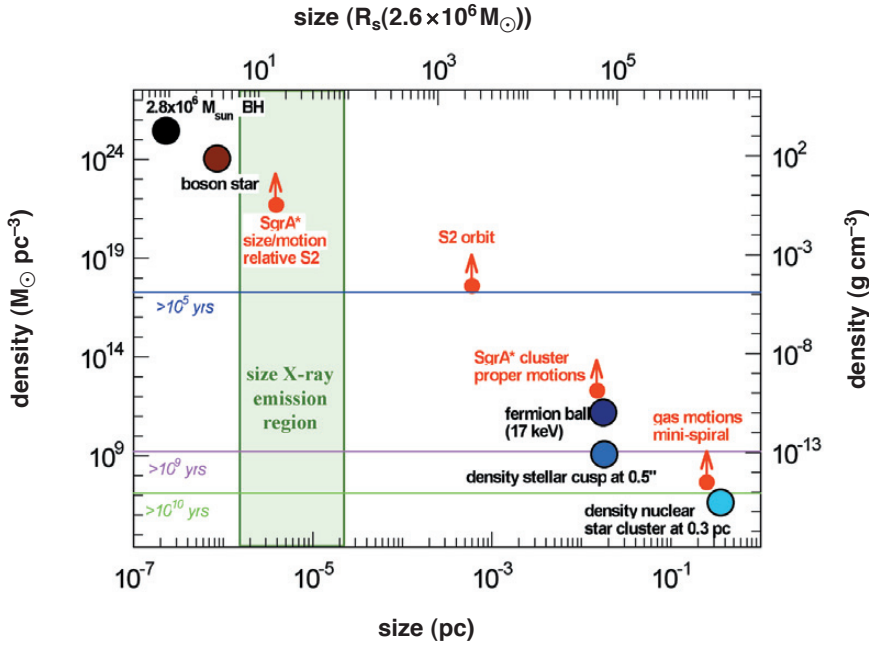


Figure 7: Constraints on the nature of the dark mass concentration in the Galactic Centre (from Schödel et al. 2003). The horizontal axis is the size (bottom in parsec, top in Schwarzschild radii), and the vertical axis density (left in solar masses per pc³, right in g cm⁻³). Red filled circles denote the various limits on the size/density of the dark mass discussed in this paper. In addition the grey shaded area marks the constraints on the size of the variable X-ray emission from Baganoff et al. (2001). Large filled circles mark the location of different physical objects, including the visible star cluster and its central cusp, the heavy neutrino, fermion ball of Tsiklauri & Viollier (1998), the boson star of Torres et al. (2000) and, in the top left, the position of a $2.8 \times 10^6 M_{\odot}$ black hole. In addition three thin horizontal lines mark the lifetimes of hypothetical dark clusters of astrophysical objects (neutron stars, white dwarfs, stellar black holes, rocks etc., Maoz 1998).

the cluster of stars closest to SgrA* (Schödel et al. 2003) appears also to favour a single black hole: A strong tangentially anisotropic velocity dispersion would be expected near a binary black hole. The Galactic Centre thus has presented us with the best astrophysical evidence we now have that the objects predicted by Einstein's and Schwarzschild's theoretical work are in fact realized in the Universe.

While the first year of NAOS/CONICA observations have led to an unexpected breakthrough in the studies of orbits, not much has been learned as yet about the emission properties of SgrA* itself. The very fact that the bright star S2 was so close in 2002 to the central source has prevented meaningful observations of its emission. The deduced upper limits to SgrA*'s flux in the H, K_s and L' bands are somewhat lower than previous observations but are broadly consistent with current low accretion CDAF, ADIOS or jet models of the source (Melia & Falcke 2001).

Outlook

The NAOS/CONICA work we have presented here is just the first step in a

new phase of near-infrared observations of the immediate surroundings of the central dark mass at the nucleus of the Milky Way. The observation of Keplerian orbits offers a clean new tool of high precision gravitational studies. Stellar orbits also allow an accurate determination of the distance to the Galactic Centre. With NAOS/CONICA we are presently able to distinguish more than 30 individual stellar sources within 0.5'' (~ 23 light-days) from SgrA*. For a number of them we hope to determine high precision orbits in the next few years. Some of them may approach the black hole within a few light-hours, with velocities approaching 10% of the speed of light and orbital time scales of less than a few years. In addition to imaging, spectroscopy will reveal the properties of the stars bound to the hole, and also give additional information on the gravitational potential and on interactions between stars. Time-resolved photometry and polarimetry will allow studies of the accretion flow and gravitational lensing effects. Another order of magnitude improvement in spatial resolution will become possible with infrared interferometry at the VLTI (once the PRIMA facility is available), the Keck interferometer

and the Large Binocular Telescope. These observations will provide a few to 10 mas (a few light-hours) resolution and offer exciting prospects for the exploration of relativistic motions at 10–100 Schwarzschild radii from the central black hole.

Acknowledgements

We are grateful to the ESO Director General, Catherine Cesarsky, and the Director of Paranal Observatory, Roberto Gilmozzi for making these observations possible. We also thank the NAOS and CONICA team members for their hard work, as well as the staff of Paranal and the Garching Data Management Division for their support of the commissioning and science verification. We are grateful to B. Schutz for a discussion of the lifetime of a hypothetical binary black hole.

References

- Baganoff, F.K., et al., 2001, *Nature*, **413**, 45.
 Chakrabarty, D. & Saha, P. 2001, *AJ*, **122**, 232.
 Chatterjee, P., Hernquist, L. & Loeb, A. 2002, *ApJ*, **572**, 371.
 Eckart, A. & Genzel, R., 1996, *Nature*, **383**, 415.
 Eckart, A., & Genzel, R., 1997, *MNRAS*, **284**, 576.
 Eckart, A., Genzel, R., Ott, T. & Schödel, R., 2002, *MNRAS*, **331**, 917.
 Genzel, R., & Townes, C.H., *ARAA*, **25**, 377.
 Genzel, R., Thatte, N., Krabbe, A., Kroker H. & Tacconi-Garman, L. E. 1996, *ApJ*, **472**, 153.
 Genzel, R., Eckart, A., Ott, T. & Eisenhauer, F. 1997, *MNRAS*, **291**, 21.
 Genzel, R., Pichon, C., Eckart, A., Gerhard, O. & Ott, T., 2000, *MNRAS*, **317**, 348.
 Genzel, R. et al. 2003, in prep.
 Gezari, S., Ghez, A. M., Becklin, E.E., Larkin, J., McLean, I.S., Morris, M. 2002, *ApJ*, in press (astro-ph/0205186).
 Ghez, A.M., Klein, B.L., Morris, M., & Becklin, E.E. 1998, *ApJ*, **509**, 678.
 Ghez, A.M., Morris, M., Becklin, E.E., Tanner, A. & Kremenek T., 2000, *Nature*, **407**, 349.
 Ghez, A. et al. 2003, in prep.
 Maoz, E., 1998, *ApJ*, 494, L181.
 Melia, F. & Falcke, H. 2001, *ARAA*, **39**, 309.
 Ott, T., Genzel, R., Eckart, A. & Schödel, R., 2003, in preparation.
 Reid, M.J., Readhead, A.C.S., Vermeulen, R.C. & Treuhaft, R., 1999, *ApJ*, **524**, 816.
 Reid, M. J., Menten, K.M., Genzel, R., Ott, T., Schödel, R. & Eckart, A. 2003, *ApJ*, in press.
 Schödel, R. et al., 2002, *Nature*, **419**, 694.
 Schödel, R., Ott, T., Genzel, R. & Eckart, A. 2003, in prep.
 Torres, D.F., Capozziello, S. & Liambase, G., 2000, *Phys. Rev. D*, **62**, id.104012.
 Tsiklauri, D. & Viollier, R.D., 1998, *ApJ*, **500**, 591.

NAOS-CONICA Performance in a Crowded Field – the Arches Cluster

A. STOLTE¹, W. BRANDNER¹, E.K. GREBEL¹, DON F. FIGER², F. EISENHAUER³,
R. LENZEN¹, Y. HARAYAMA³

¹Max-Planck-Institut für Astronomie, Heidelberg, Germany

²Space Telescope Science Institute, Baltimore, USA

³Max-Planck-Institut für Extraterrestrische Physik, Garching, Germany

1. NAOS-CONICA – Near-Infrared Camera with Adaptive Optics

NAOS-CONICA is a near-infrared imaging camera and spectrograph (CONICA) attached to an adaptive optics (AO) system (NAOS) for wavefront corrections (Lenzen et al. 1998, Rousset et al. 2000). The AO system is designed to deliver diffraction-limited observations at an 8-metre-class telescope. NAOS is equipped with two Shack-Hartmann wavefront sensors operating at visual and NIR wavelengths, respectively. Most existing AO systems feed near-infrared (NIR) cameras, but operate at visual wavelengths. In addition to the fact that the spectral energy distribution of bright stars peaks at optical wavelengths, visual detectors offer higher sensitivity and lower read-out noise than NIR detectors, thus allowing one to use fainter targets for wavefront sensing. The restriction to visual reference sources, however, excludes deeply embedded objects located in regions with active star formation or high foreground extinction such as the Galactic Centre. With wavefront sensors operating both at visual and NIR wavelengths, NAOS combines the advantages of visual, faint reference targets with the option to penetrate highly obscured regions containing bright infrared sources. NAOS-CONICA was commissioned on Yepun (UT4) in the course of Period 69. For more detailed information on NACO performance and first light, see Brandner et al. (2002) in *The Messenger* 107.

We have used the CONICA *JHK* imaging mode with the S27 camera in combination with the NAOS visual wavefront sensor for performance tests in the crowded stellar field of the dense, massive star cluster Arches. The S27 camera with a pixel scale of 27 milliarc-second (mas) and corresponding field of view (FOV) of 27" × 27" is optimized for diffraction-limited observations in the *J* to *K* band wavelength range. At 2.2 μm, the diffraction limit of an 8-m telescope is 57 mas, such that the S27 camera allows Nyquist sampling.

2. Why Arches?

The Arches cluster is one of the few starburst clusters found in the Milky

Way. With an age of only ~ 2–3 Myr it contains a rich massive stellar population with about 150 O stars located in the cluster centre (Figer et al. 1999), and several more found in the immediate vicinity. The core density has been estimated to be $3 \cdot 10^5 M_{\odot} \text{pc}^{-3}$, and the total stellar mass exceeds $10^4 M_{\odot}$ (Figer et al. 1999). The massive cluster centre contains ~ 12 Wolf-Rayet stars (Cotera et al. 1996, see also Blum et al. 2001), intertwined with an intermediate-mass main-sequence population. At the faint end, where pre-main-sequence stars would be expected, the stellar population is severely contaminated by bulge stars, as Arches is located in the central region of the Milky Way at a projected distance of only 25 pc (roughly 10 arcminutes) from the Galactic Centre (Fig. 1).

With a distance of about 8 kpc and a foreground extinction in the visual of 24 to 34 mag, Arches is a very challenging object. The high foreground extinction obscures the faint cluster population at visual wavelengths, so that NIR observations, where extinction is less severe, are necessary to detect the cluster population. Given these extreme properties, and the existence of data sets obtained with HST/NICMOS and the Gemini/ Hokupa'a AO system allowing a detailed comparison, the Arches cluster was chosen as NAOS-CONICA commissioning target to test the NACO performance on a dense, crowding-limited stellar field.

3. NAOS-CONICA Commissioning Data

Arches *H* and *K_s* images were obtained during Commissioning 3 of NAOS-CONICA in March and April 2002. 20 exposures with integration times of 1 min (2×30 s detector integration time (DIT)) each were obtained in *H*, and 15×1 min exposures in *K_s* (4×15 s DIT). As the NIR wavefront sensor was not available during Comm 3, a blue foreground giant with *V* = 16 mag (*V*–*R* ~ 1 mag) served as the reference source for the visual wavefront sensor. Although the brightest star in the Arches field, this star is already close to the limiting magnitude (~ 17 mag) of the visual wavefront sensor. As has been demonstrated on the Galactic Centre

field (Schödel et al. 2002 and Ott et al. in this issue), NIR wavefront sensing with NIR bright reference targets (*K*~10 mag) is capable of improving the performance in a highly extinguished region.

All images were taken in auto-jitter mode. The auto-jitter template allows automatic, random offsets between individual exposures to facilitate background subtraction and avoid afterglows at the position of bright sources. A set of additional exposures with short detector integration times were taken to obtain photometry of the bright cluster stars (8×1 s DIT in *H*, 8×0.5 s DIT in *K_s*). Seeing conditions varied during the Arches observations. In *H*-band, the seeing ranged from 0.45 to 0.85, while during *K*-band observations the seeing degraded from 0.8 to 1.3. On April 4, the moon was only 6° from our target, and increased background fluctuations decreased the detectability of faint sources in the cluster vicinity.

The data were reduced within IRAF, using twilight flat fields taken during Comm 3 and combined with the nacop twflat algorithm in *eclipse* (Devillard 1997). *Eclipse* is the ESO pipeline reduction package, which allows special treatment of particular instrument characteristics adapted to the available ESO instrumentation. Sky frames were created from the cluster observations themselves, which is not ideal, but was sufficient for our technical study. Starlight was excluded from these skies by rejecting the bulk of the bright pixels. As the CONICA detector has a significant fraction of time-varying hot pixels, a cosmic ray rejection routine was used to obtain a bad pixel mask. This mask was applied during the drizzling process, in which images are shifted and combined. The 7 exposures with the highest resolution were combined in *K_s* to one 7 min integrated frame, and the 14 best exposures in *H*, where seeing conditions were much more stable, could be used to obtain a 14 min *H*-band image. During the *K*-band observations, the AO performance changed with time as the seeing worsened. As crowding is the limiting factor on the Arches field, the gain in resolution by rejecting the large fraction of frames with lower quality supersedes the loss in photometric depth due to the shorter resulting total integration time on the fi-

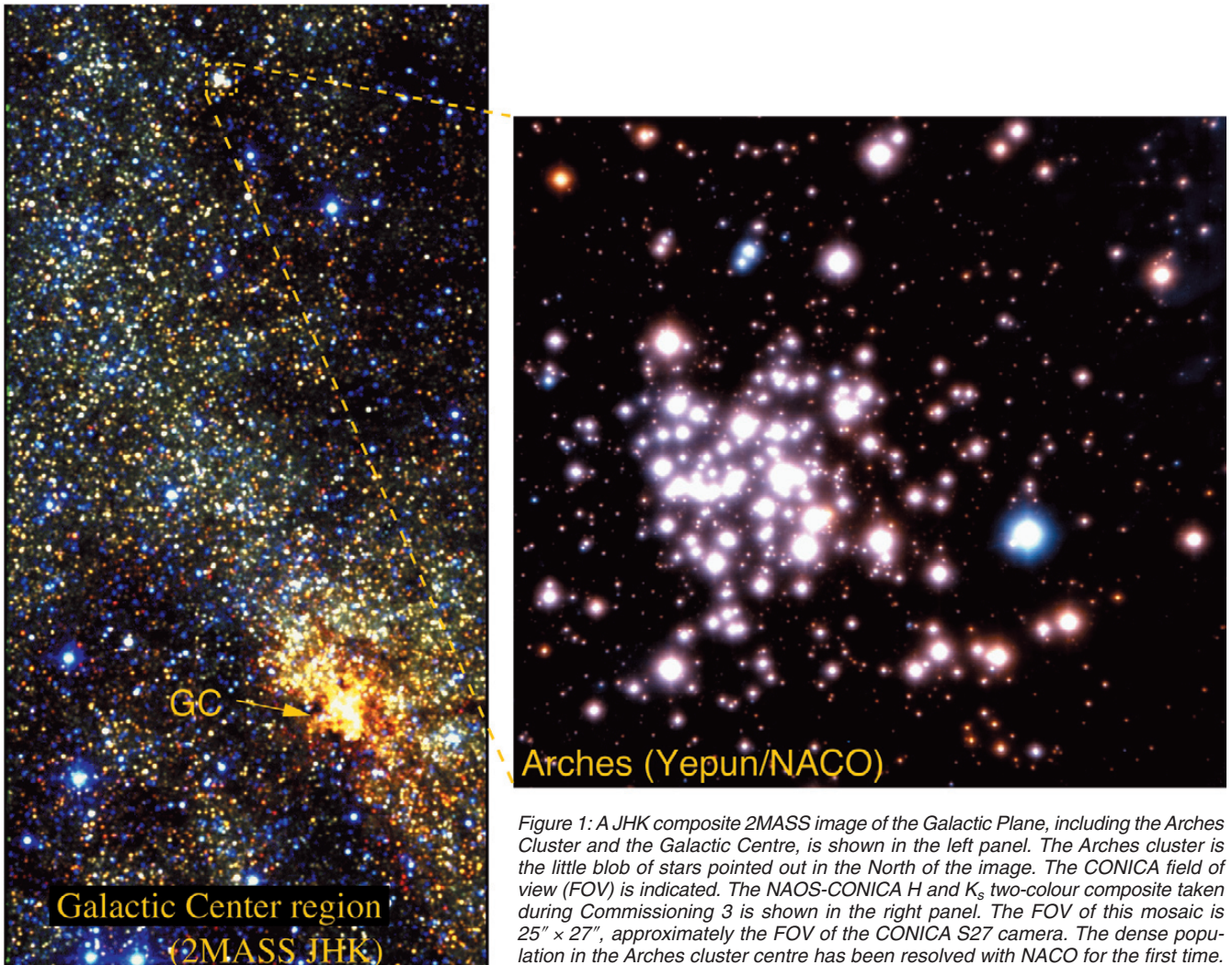


Figure 1: A JHK composite 2MASS image of the Galactic Plane, including the Arches Cluster and the Galactic Centre, is shown in the left panel. The Arches cluster is the little blob of stars pointed out in the North of the image. The CONICA field of view (FOV) is indicated. The NAOS-CONICA H and K_s two-colour composite taken during Commissioning 3 is shown in the right panel. The FOV of this mosaic is $25'' \times 27''$, approximately the FOV of the CONICA S27 camera. The dense population in the Arches cluster centre has been resolved with NACO for the first time.

nal image (see also Tessier et al. 1994). The best K -band photometry was obtained when combining only the frames where the best AO performance was achieved. The resulting images have Strehl ratios of 14% in H and 20% in K , yielding a spatial resolution of ~ 85 mas in both filters.

Standard DAOPHOT PSF fitting photometry was used to obtain the final magnitudes. A constant PSF function has been used, as isolated PSF stars are rare in the dense Arches field. A Penny function, which has a Gaussian core with elongated Lorentzian wings, yielded the best fit to the data.

The NACO data were calibrated using existing HST/NICMOS photometry of the same field (Figer et al. 1999). All calibrated data shown below are in the NICMOS photometric system. This allowed a large number of stars to be used for zero-pointing and for the study of photometric residuals over the field. We find the NACO performance to be very stable over the field. No trend of the amplitude of photometric residuals with field position is observed. Note that the measurement of anisoplanatism on the Arches field is complicated by the high stellar density and large

density gradient over small spatial scales.

4. Luminosity Functions

In Figure 2, luminosity functions (LFs) of the NACO commissioning data are compared to HST/NICMOS LFs of the same field. Arches was observed with NICMOS2 for 256 s integration time in the broadband filters F110W, F160W and F205W corresponding to J , H , and K . The NICMOS detection limits were approximately 21 mag in H (F160W), and 20 mag in K (F205W). Within a factor of 2 longer integration time in K and a factor of 3.3 in H , NACO reaches detection limits of 22 mag in H and 21 mag in K , one magnitude deeper than the NICMOS observations. Note that NICMOS does not have to fight the large NIR background from the Earth's atmosphere, but also has the much smaller collecting area of a 2.4-m mirror as opposed to Yepun's 8-m mirror.

Only objects detected in both filters are included in the NACO LF, as the requirement that objects have to be detected in both filters is a very efficient method to reject artefacts. In particular

in a very dense stellar field, background fluctuations and saturation peaks frequently cause false detections.

As sources in the Arches cluster are hidden behind ~ 30 mag of foreground extinction, reddening influences the detection of stars more severely at shorter wavelengths. Consequently, the H -band LF shown in Fig. 2 represents the photometric performance more realistically, as the K -band LF is artificially truncated by the requirement that sources have to be detected in H as well.

While the field star LF is comparable for NACO and NICMOS down to the NICMOS detection limit of $H \sim 21$ mag, NACO clearly gains a large number of sources in the cluster centre. Here, the significantly better resolution of 85 mas with VLT/NACO vs. 210 mas with HST/NICMOS allows us to resolve the cluster centre for the first time. Note that the diffraction limit of the 2.4 m HST mirror of 183 mas in H and 210 mas in K does not allow a much higher resolution with NICMOS, while better Strehl ratios may yield resolutions down to the VLT diffraction limit of 57 mas in H and 69 mas in K with NAOS-CONICA. The cluster centre LF dem-

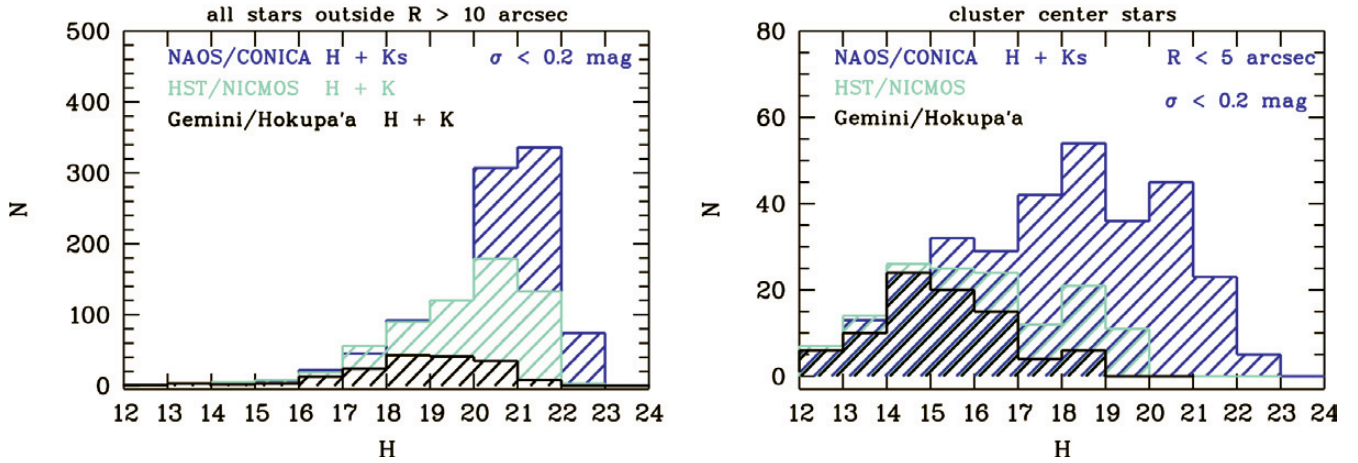


Figure 2: H -band luminosity function of the Arches cluster. The left LF contains only objects at a distance $R > 10''$ from the cluster centre, displaying the field performance in comparison to HST/NICMOS, while the right panel shows the cluster centre regions with stars within $R < 5''$. While the field performance between NACO and NICMOS is comparable until the NICMOS detection limit of $H \sim 21$ mag is approached, the cluster centre LF shows the large gain in the NACO data due to the higher spatial resolution. It is particularly intriguing that already bins fainter than $H = 15$ mag are affected. This indicates that the cluster centre population was until now never truly resolved, not even at the brighter end.

onstrates not only the deeper photometry with NACO, but also the strongly enhanced resolution, as in nearly each magnitude bin above $H = 15$ mag more stars are resolved. This affects statistically derived properties of the Arches stellar population, such as stellar density, total mass and the slope of the mass function.

5. Colour-Magnitude Diagrams

A comparison of colour-magnitude diagrams (CMDs) of the Arches cluster centre is shown in Figure 3. Here, Gemini/Hokupa'a low Strehl data (2.5% in H , 7% in K , Stolte et al. 2002), HST/NICMOS observations (Figer et al. 1999), and the new NACO observations are compared. The Gemini data cover the smallest field of view, and care was taken to select only the area in common to all data sets to allow direct comparison. The NACO and NICMOS data were selected accordingly.

While the low-Strehl Hokupa'a data show a large scatter in the main sequence due to the contamination of stellar fluxes with extended seeing halos, the NACO data show a well-confined, narrow main sequence. The NICMOS data are also very well confined, but in accordance with the results from luminosity functions the NACO main sequence appears more densely populated. Derived physical and statistical properties of the cluster population are consequently less biased by crowding losses.

The Hokupa'a data set has the highest incompleteness, being 90% complete only down to $K = 15$ mag. When the number of stars down to this magnitude limit is compared, we find 131 stars with Hokupa'a, 157 stars with NICMOS within the same field, and 169 stars with NACO. The 12 stars undetected with NICMOS are either fainter

neighbours vanishing in the PSF pattern of a bright star, or close pairs where only one component has been resolved. Figure 4 shows the comparison of resolved sources with $K < 15$ mag on a sample field in the cluster centre.

6. Mass Function

The NACO CMD was used to derive the mass function (MF) of the Arches cluster population. A 2 Myr isochrone with twice solar metallicity (see Figer et al. 1999, Stolte et al. 2002 for discus-

sion) from the Geneva set of models (Lejeune & Schaerer 2001) was used to transform K -band magnitudes into stellar masses.¹ A distance modulus of 14.52 mag and extinction of $A_V = 24$ mag, corresponding to the cluster centre, have been applied. Magnitudes

¹Note that the current best age estimate from high-resolution spectra of the bright Arches main sequence O stars is 2.5 Myr (Figer et al. 2002), but we prefer to use the 2 Myr isochrone to allow direct comparison of the NACO MF with our prior results given in Figer et al. 1999 and Stolte et al. 2002.

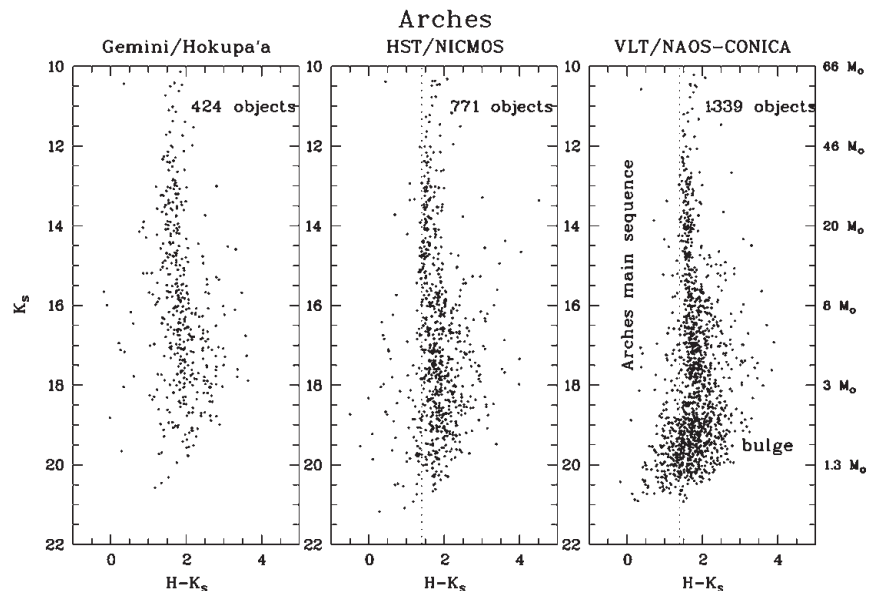


Figure 3: Arches colour-magnitude diagrams. A comparison between VLT/NAOS-CONICA, HST/NICMOS and Gemini/Hokupa'a data is shown. While the low Strehl ratio of the Hokupa'a data of only a few per cent severely limits resolving the cluster population and caused large photometric uncertainties, the moderate Strehl NAOS-CONICA observations exhibit a narrow, well-defined main sequence, reflecting the photometric quality of the data. The NICMOS data are limited by the small telescope diameter of only 2.4 m, and corresponding larger diffraction limit. In addition, the strong diffraction pattern in the NICMOS PSF hampers the detection of faint sources in the cluster centre. Despite the moderate Strehl ratio, the NACO CMD clearly displays the advantages of AO at an 8-m-class telescope. The right axis of the NACO CMD is labelled with present-day masses from a 2 Myr main sequence isochrone used to derive the mass function.

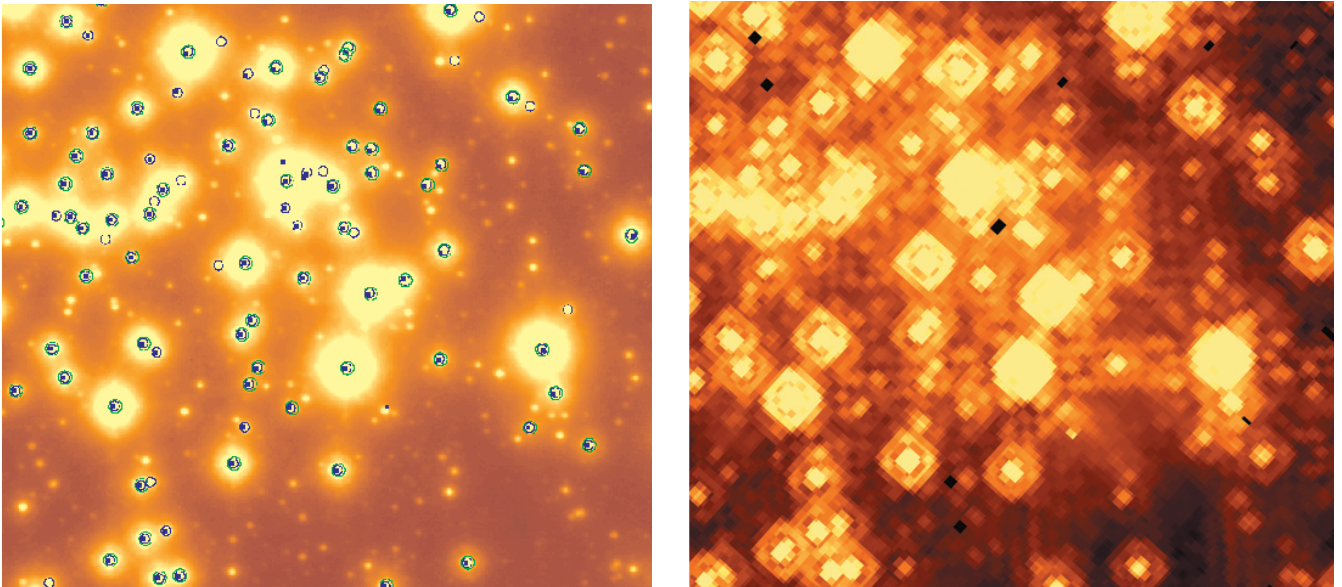


Figure 4: Sources brighter than 15 mag, the Hokupa'a 90% completeness limit, overlaid on the 7 min NACO K-band image ($9' \times 9'$ FOV, left panel). For comparison, the same area on the NICMOS K-band (F205W) image is shown in the right panel. Blue circles are NACO sources and dots are NICMOS detections in both filters. Green, larger circles are Hokupa'a sources. Several close neighbours of bright sources and equal brightness pairs are exclusively detected in the high resolution NACO data.

have been transformed to the NICMOS system using the colour equations determined by Brandner et al. 2001. A linear change in extinction is observed when moving outwards from the cluster centre. While the innermost $5''$ of the cluster population are consistent with a constant reddening of $A_V = 24.1$ mag, the extinction increases with increasing radial distance at radii $R > 5''$. The observed $H-K$ colour as well as the K -band magnitude have been corrected for this trend before transformation into stellar masses. A colour cut with $1.35 < (H-K)_{\text{corr}} < 1.77$ mag was applied to select Arches main sequence stars from the corrected CMD.

The present-day mass function for stars in the Arches cluster derived from the NACO CMD (Fig. 3) is shown in Figure 5. A power law can easily be fitted to the upper end of the MF for $M > 10 M_{\odot}$, below which the MF appears to become flat. When regarding the entire NACO field, it appears that at this point field contamination sets in, as this flat portion of the MF is very pronounced in MFs created with the above procedure at large distances from the cluster centre. Analysis of Galactic Centre fields in the vicinity of Arches is required to estimate the relative fractions of field and cluster stars in the faint regime. As the combined field of view obtained during Comm 3 does not cover sufficient area at large enough distances from the cluster to perform statistical background subtraction, the MF discussed here focuses on the massive end with $M > 10 M_{\odot}$, where field contamination is negligible.

To eliminate the dependence of binning on the derived MF slope, the starting point of the first mass bin has been shifted by $\delta \log(M/M_{\odot}) = 0.01$ at the

chosen bin width of $\Delta \log(M/M_{\odot}) = 0.1$, resulting in ten MFs with consecutive starting points. Averaging the resultant MF slopes yields an MF slope of $\Gamma = -0.91 \pm 0.15$ for the Arches main sequence, where Salpeter is $\Gamma = -1.35$ (Salpeter 1955). Although the NACO LF is more complete, this slope is identical to the slope derived from NICMOS data before (Stolte et al. 2002). This indicates that at the bright end ($K < 16$ mag, $M > 10 M_{\odot}$), all bins contributing to the LF and MF gain the same fraction of stars, such that the relative fraction of stars in each bin remains the same. Note that we only consider the massive end of the MF, up to $K = 16$ mag, such that the faint end of the LF, where the largest discrepancy to the NICMOS LF is observed, is not taken into account here, as this would require field subtraction.

This slope is slightly flatter than the average slope of $\Gamma = -1.1 \pm 0.3$ found in star forming regions in the Milky Way (Massey et al. 1995). A comparably flat slope is seen in the MF of the massive starburst cluster in NGC 3603, which has physical properties similar to Arches, although forming in a much more moderate star-forming environment in the Carina spiral arm. In NGC 3603, the MF slope is found to be $\Gamma = -0.7$ in the mass range $1 M_{\odot} < M < 30 M_{\odot}$ (Eisenhauer et al. 1998), close to the Arches MF slope. The flat slope indicates that the Arches cluster was either very efficient in forming massive stars, or that dynamical mass segregation has led to the ejection of a significant number of intermediate-mass stars. If the cluster is mass segregated (either due to primordial or due to dynamical processes), this should be particularly pronounced in the cluster centre.

The cluster centre MF is shown in Figure 5 (right). Only stars within the innermost $5''$ of the cluster centre are included. The binning width was now chosen to be $\Delta \log(M/M_{\odot}) = 0.2$ for statistical reasons. Again, only the bright end of the MF was fitted for comparison purposes. The average slope derived for the cluster centre with the same method as described above is $\Gamma = -0.6 \pm 0.2$, flatter than the slope for the entire cluster. This is consistent with massive star cluster formation scenarios, where primordial or rapid dynamical segregation causes massive stars to end up in the cluster centre, while a larger fraction of low-mass stars is found in the outskirts.

Although the entire mass range in the cluster centre appears to be consistent with a very flat MF ($\Gamma \sim 0$) down to $\log(M/M_{\odot}) \sim 0.5$, $M = 3 M_{\odot}$, where the K -band LF is more than 75% complete (derived from stars recovered in both H and K), it is currently not clear how the interplay of incompleteness correction and field contamination will alter the shape of the MF for masses below $10 M_{\odot}$. Neighbouring Galactic Centre fields and thorough incompleteness testing will be required to obtain a meaningful slope in the cluster centre down to the low-mass regime.

7. Outlook

Velocity studies of the bright cluster stars in the vicinity of Arches are necessary to draw final conclusions on the formation scenario. Stars dynamically ejected during interaction processes should obtain large velocities directed away from the cluster centre. Such a velocity study can yield new insights into the cluster dynamics as well as for-

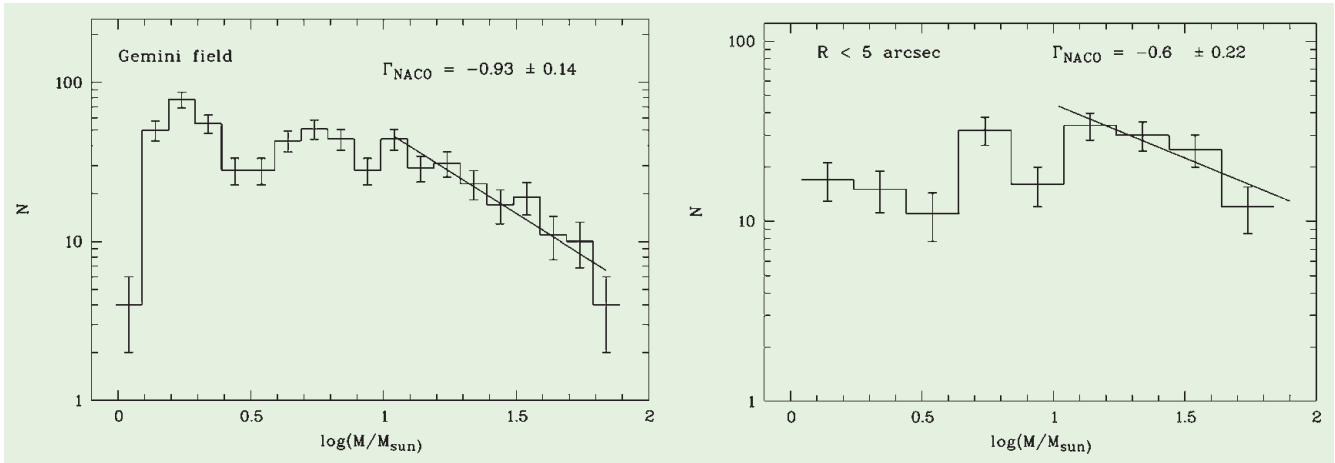


Figure 5: Mass Function of the Arches cluster. Left panel: The area within the Gemini FOV has been selected, such that the MF corresponds to the CMD displayed in Figure 3. A linear change in extinction over the field has been corrected, and a colour cut of $1.35 < H-K < 1.77$ mag has been applied to the corrected CMD to select Arches main-sequence stars. The Arches main sequence can clearly be identified down to 18.3 mag in K-band, or $2.5 M_{\odot}$ ($\log M/M_{\odot} = 0.4$), beyond which the bulge population dominates the CMD. Right panel: The mass function of Arches cluster centre stars observed with NACO. Stars within $R < 5''$ are included. A weighted least-squares fit has been performed on data points above $10 M_{\odot}$. The MF in the cluster centre appears flatter than the integrated MF, indicating mass segregation.

mer cluster membership of ejected stars. High-resolution NIR spectrographs such as CRIFES expected to go into operation in the next years have the capability to overcome the huge line of sight obscuration towards the Galactic Centre. The determination of spectral types with SINFONI/SPIFFI allows one to disentangle the cluster members from the dense background population, thereby yielding accurate estimates on the field star contamination when deriving mass functions. With these prospects in mind, spectroscopic observations may shed light on the unsolved questions of massive star formation in a dense environment.

8. Conclusions

NAOS-CONICA data of the dense stellar field in the Arches cluster centre yield significantly better spatial resolution than NICMOS on HST. About 50% more stars are resolved in the cluster centre down to the same magnitude limit. The luminosity functions reveal that each magnitude interval up to the brightest stars was affected by crowding losses before. The NACO observations of the densest cluster region with-

in $R < 5''$ are 75% complete down to $H = 19.4$ mag and $K = 17.7$ mag or $\sim 3 M_{\odot}$, while HST/NICMOS and Gemini/Hokupa'a observations were limited to ~ 10 – $20 M_{\odot}$ in the immediate cluster centre. While a lower Strehl ratio is responsible for the lower performance in the Hokupa'a data, the NICMOS resolution is limited by the smaller HST mirror and correspondingly larger diffraction limit. As we have shown, even moderate AO performance using faint visual reference sources ($V = 16$ mag) now achieves higher spatial resolution from the ground while at the same time exploiting the light collecting power and sensitivity of 8-m-class telescopes. Thus, a much more complete census of stellar populations in dense fields in our own Galaxy as well as in nearby resolved galactic systems is possible with ground-based AO instruments such as NAOS-CONICA.

References

- Blum, R. D., Schaerer, D., Pasquali, A., et al. 2001, *AJ*, **122**, 1875.
 Brandner, W., Grebel, E. K., Barbá, R. H., et al. 2001, *AJ*, **122**, 858.

- Brandner, W., Rousset, G., Lenzen, R., Hubin, N. et al. 2002, *The Messenger* No. **107**, 1.
 Cotera, A.S., Erickson, E.F., Colgan, S.W.J., Simpson, J.P., Allen, D.A., & Burton, M.G., 1996, *ApJ*, **461**, 750.
 Devillard, N. 1997, *The Messenger* No **87**, 19.
 Eisenhauer, F., Quirrenbach, A., Zinnecker, H., Genzel, R. 1998, *ApJ*, **498**, 278.
 Figer, D.F., Najarro, F., Gilmore, D., et al. 2002, *ApJ*, **581**, 258.
 Figer, D.F., Kim, S.S., Morris, M., et al. 1999, *ApJ*, **525**, 750.
 Lejeune, T., & Schaerer, D. 2001, *A&A*, **366**, 538.
 Lenzen, R., Hoffmann, R. et al. 1998, *SPIE* **3354**, 606.
 Massey, P., Johnson, K.E., Degioia-Eastwood, K. 1995, *ApJ*, **454**, 151.
 Rieke, G.H., & Lebofsky, M.J. 1985, *ApJ*, **288**, 618.
 Rousset, G., Lacombe, F. et al. 2002, *SPIE* **4007**, 72.
 Salpeter, E.E. 1955, *ApJ*, **121**, 161.
 Scalo, J.M. 1998, in *ASP Conf. Ser.*, Vol. **142**, The stellar initial mass function, 201.
 Schoedel, R., Ott, T., Genzel, R. et al. 2002, *Nature* **419**, 694.
 Stetson, P.B. 1987, *PASP*, **99**, 191.
 Stolte, A., Grebel, E.K., Brandner, W., Figer, D.F., 2002, *A&A*, **394**, 462.
 Tessier, E., Bouvier, J., Beuzit, J.-L., Brandner, W. 1994, *The Messenger* No. **78**, 35.

Early Galactic Chemical Evolution with UVES

M. PETTINI, *Institute of Astronomy, Cambridge, UK*

The UVES instrument on the ESO VLT2 telescope has now been providing high-resolution spectra of faint stars and galaxies for nearly three years. European astronomers have taken advantage of this new facility to conduct extensive and accurate studies of the first stellar generations of our Galaxy,

and to probe the chemical composition of gas in the high-redshift universe. In November of last year, a workshop on the theme "Early Galactic Chemical Evolution with UVES" was held at the ESO headquarters in Garching. Attended by more than 50 stellar and extragalactic astronomers, the work-

shop served as a focus to bring together scientists interested in the general theme of how the chemical enrichment of galaxies progressed over the cosmic ages, from the Big Bang to the present time. The meeting proved to be a valuable opportunity to exchange ideas, assess progress to date, and to chart fu-

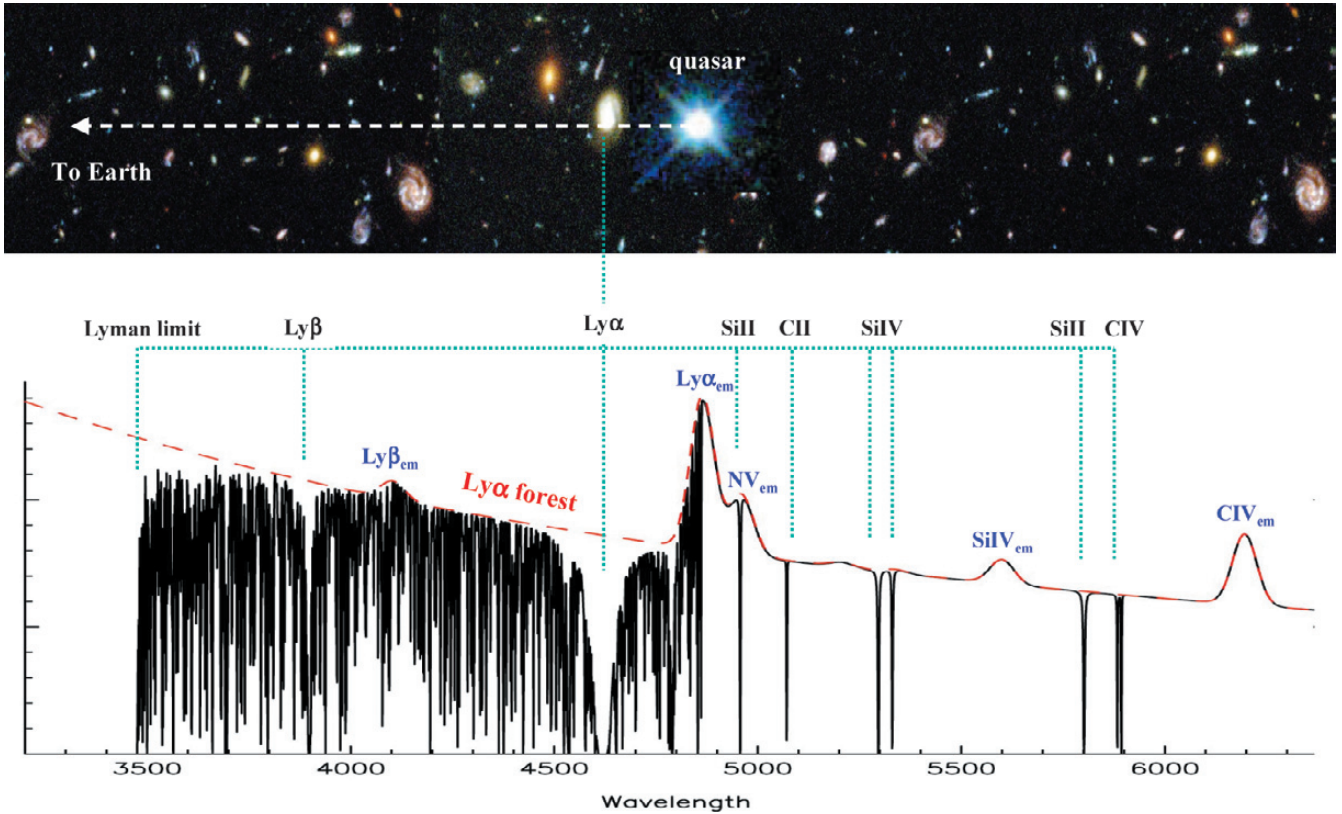


Figure 1: The technique of QSO absorption line spectroscopy is illustrated in this montage (courtesy of John Webb). QSOs are among the brightest and most distant objects known. On the long journey from its source to our telescopes on Earth, the light from a background QSO intercepts galaxies and intergalactic matter which happen to lie along the line of sight (and are therefore at lower absorption redshifts than the QSO emission redshift). Gas in these structures leaves a clear imprint in the spectrum of the QSO in the form of narrow absorption lines which carry a wealth of information on the physical properties and chemical composition of the gas producing the absorption. The strong absorption feature near 4600 Å is a damped Lyman alpha line.

ture directions of research in this field of study. In this article, I highlight some of the extragalactic aspects of the workshop, concentrating in particular on recent developments in the study of element abundances at high redshifts.

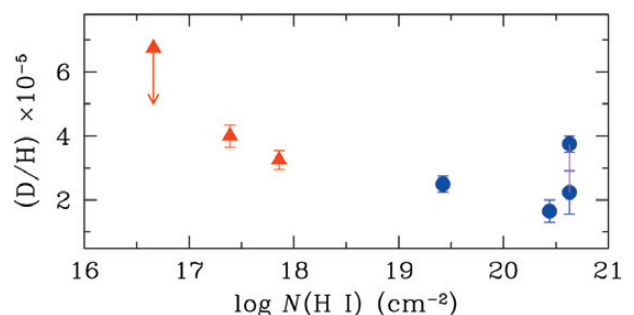
To set the scene for the non-specialists, let me just clarify a couple of points. First, to astronomers the words ‘high redshift’ are synonymous with ‘a long time ago’. With UVES on the VLT we can observe galaxies – and measure their chemical composition – at a time when the universe was only 10–20% of its present age. Second, the technique which is most widely used for detailed measurements of element abundances in these distant (both in space and time) reaches of the universe is QSO absorption-line spectroscopy, illustrated in Figure 1. The galaxies are generally not seen directly, but through the absorption they cast in the spectra of background bright sources, such as quasars (or QSOs for short).

The Primordial Abundance of Deuterium

Among the light elements created in the Big Bang, Deuterium is the one whose abundance is most sensitive to the density of baryons in the universe. Astronomers have been aware since the 1970s of the potential of QSO ab-

sorption line spectroscopy for the determination of the ratio of deuterium to hydrogen (D/H). If D could be found in distant galaxies which have experienced little star formation, the D/H ratio measured in their interstellar media should be very close to the primordial value. However, this technique has had to wait for more than twenty years to be implemented, since it requires recording the light of relatively faint sources at high spectral resolution and signal-to-noise ratio – a combination which only echelle spectrographs on 8–10-m-class telescopes can deliver. Even with current technology these are still difficult observations, and this is why the total sum of available data today consists of only five measurements (plus one upper limit), obtained with UVES on VLT2, HIRES on the Keck I telescope, and the *Hubble Space Telescope*.

Figure 2: Available measurements of the abundance of deuterium at high redshift (plotted against the neutral hydrogen column density) obtained via QSO absorption line spectroscopy of either Lyman limit (red triangles) or damped Lyman alpha (blue circles) systems. (Adapted from Pettini & Bowen 2001).



These data are reproduced in Figure 2. The mean value from the five detections is $\langle D/H \rangle = (2.6 \pm 0.2) \times 10^{-5}$ which in turn corresponds to a density of baryons $\Omega_B = 0.05$ (for a value of the Hubble constant of $65 \text{ km s}^{-1} \text{ Mpc}^{-1}$). That is, the baryons of our familiar physical world only make up 5% of the critical density of the universe. Furthermore, since the currently favoured value of the density of matter, in all its forms, is $\Omega_M = 0.3$, the primordial abundances of deuterium and other light elements are one of the strongest pieces of evidence we have for the existence of non-baryonic dark matter, which outnumbers the baryons by 5 to 1.

The value $\Omega_B = 0.05$ now seems secure since an entirely different method for its determination, which uses the power spectrum of the cosmic microwave background, has recently been

shown to give results in excellent agreement with those from primordial nucleosynthesis. Thus the problem can be considered 'solved'... or can it? There are some remaining nagging doubts as to the origin of the dispersion of the different measurements which, as can be seen from Figure 2, deviate from the mean by several times their estimated (random) errors. Is this scatter real, or just evidence for unrecognised systematic errors? Experience would tell us that the second possibility is the more likely, except that when we measure the D/H ratio in the solar neighbourhood we also find an unexplained dispersion in the data. Figure 3 is the most recent compilation of the best relevant data, all obtained with space missions. While all the measurements in the interstellar medium within 100 parsecs of the Sun are in agreement at $D/H = 1.6 \times 10^{-5}$, interstellar sightlines to more distant stars span a range of almost a factor of three. There is a general agreement that this dispersion is both real and unexplained. The puzzle arises because the ISM is well mixed over these distances and shows a high degree of uniformity in other chemical elements such as nitrogen and oxygen, so why should D be different? We know of no way of either producing deuterium nor of destroying it selectively. The scatter we see beyond 100 pc of the Sun is comparable to the total amount of astration of deuterium (its destruction through star formation) over the lifetime of the Milky Way. It therefore seems really important to establish whether such a scatter also exists in other galaxies, particularly those at high redshifts which we see as QSO absorption line systems and which give us our estimate of the primordial D/H ratio. There is thus a strong incentive to improve the statistics in Figure 2 with more measurements with UVES, once suitable background QSOs have been identified. This should be easier now than it has been in the past, thanks to the large numbers of new quasars discovered by on-going large-scale surveys of the sky.

Element Abundances in Damped Lyman Alpha Systems

This class of QSO absorbers, known as DLAs for short, are characterised by large column densities of neutral hydrogen, in excess of 2×10^{20} H atoms per square cm. The general view is that they probably represent some early stage in the evolution of the galaxies we see around us today, perhaps at a time shortly after they had condensed out of the intergalactic medium, but before they had had time to form many stars, so that most of their mass still resided in the interstellar medium. While astronomers still debate how

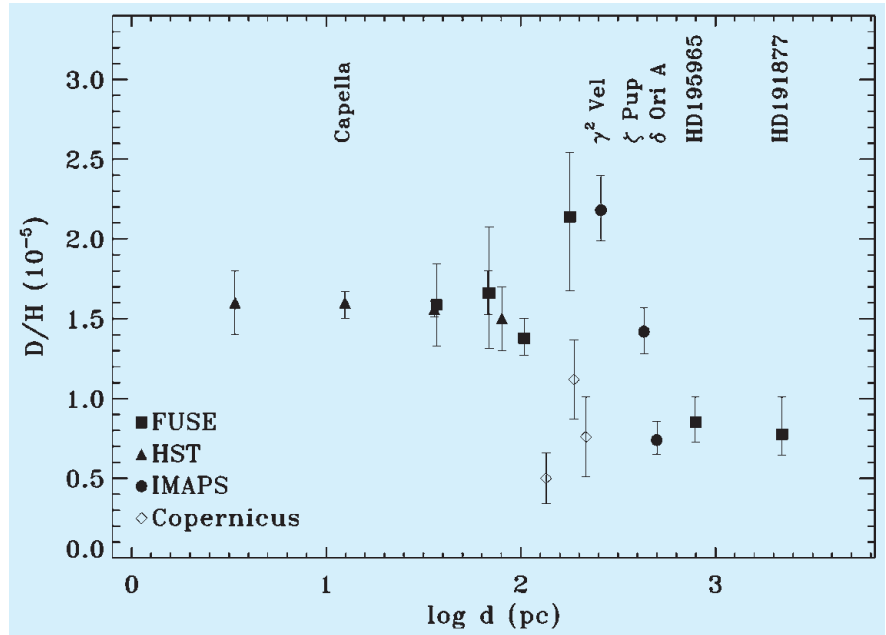


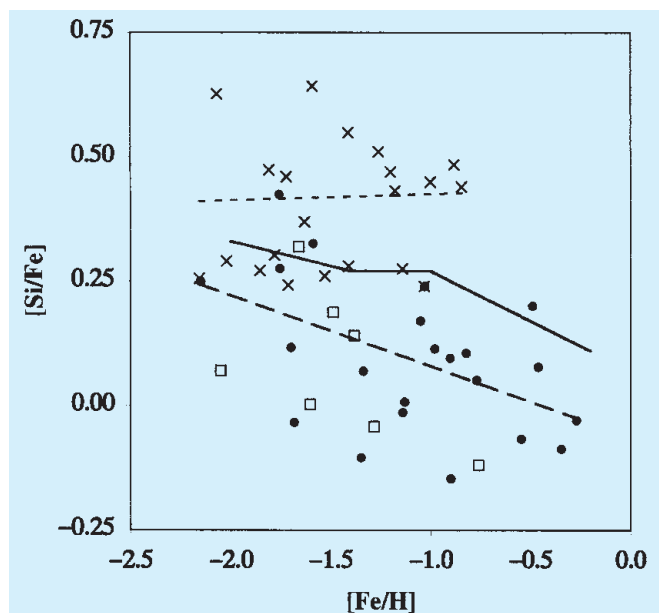
Figure 3: Compilation of available measurements of the abundance of deuterium in the Milky Way interstellar medium, all obtained with space missions as indicated in the legend, as a function of distance from the sun. (Reproduced from Hoopes et al 2003.)

DLAs are related to other populations of galaxies seen at high redshift, one thing is clear: they are our best laboratory – by far – for measuring the abundances of a wide variety of elements in the young universe. The bright background light of the quasars in which they are seen allows studies of unprecedented detail with instruments such as UVES.

If we look back to the scientific cases written in the 1980s to seek funds for the construction of large telescopes, we see that the study of element abundances in QSO absorbers such as DLAs figured very prominently. And indeed, right from its commissioning days

on the telescope, European astronomers have put UVES through its paces with observations of DLAs, capitalizing in particular on the instrument's world-beating efficiency throughout the optical spectrum, from ultraviolet to far-red wavelengths. Some European highlights in this field include: the discovery and study of some of the highest redshift DLAs, up to $z_{\text{abs}} = 4.466$ which in today's favoured cosmology corresponds to only 1.5 billion years after the Big Bang; much improved statistics on the metallicities of DLAs at redshifts greater than 3, based on the abundance of Zn; and the first comprehensive search for molecular hydrogen at

Figure 4: Relative abundances of Si and Fe in damped Lyman alpha systems. Abundances are expressed on a logarithmic scale relative to the solar composition, so that $[Fe/H] = -1$ denotes an abundance of iron relative to hydrogen equal to one tenth of the solar value. The meanings of the different symbols are given in the legend. Short- and long-dashed lines show the average trends of $[Si/Fe]$ vs $[Fe/H]$ before and after correction for the fractions of Si and Fe locked up in dust grains. The continuous line shows the mean trend for Galactic stars. (Adapted from Vladilo 2002.)



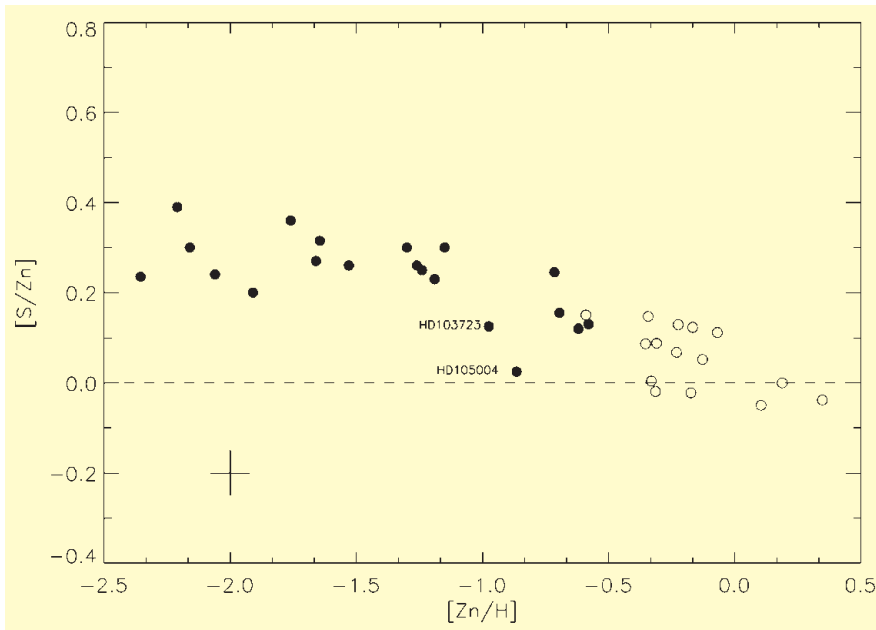


Figure 5: $[S/Zn]$ vs. $[Zn/H]$ for a sample of nearby main-sequence stars. Filled circles refer to stars with halo kinematics and open circles to disk stars. Data for the halo stars were derived from the $S\ I\ \lambda\lambda 8694.6, 9212.9, 9237.5$ and the $Zn\ I\ \lambda\lambda 4722.2, 4810.5$ lines recorded with UVES (Nissen et al. in preparation); those for the disk stars are reproduced from Chen et al. (2002). The two stars, HD103723 and HD105004, belong to a group of low $[\alpha/Fe]$ halo stars discovered by Nissen & Schuster 1997. (Figure courtesy of Poul Nissen.)

high redshift. This, the most common of astrophysical molecules, provides a wealth of data on the physical conditions in DLAs, particularly on the temperature and density of both particles and photons in the interstellar media of these early galaxies.

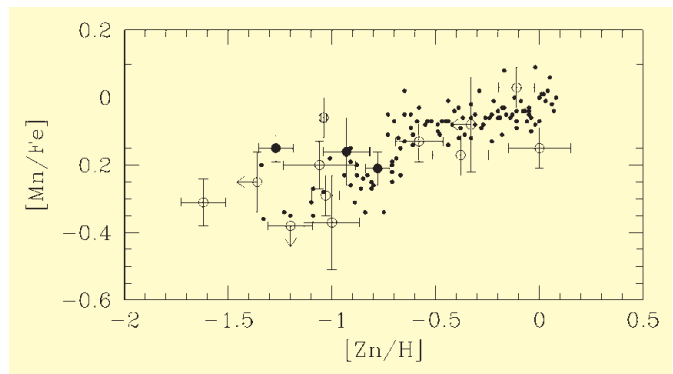
Ultimately, all of this work on DLAs complements local studies, which have focussed on old stars in the Milky Way Galaxy and on regions of ionized gas near hot stars in nearby galaxies, to address some of the same basic questions, such as the star formation histories of galaxies (How did star formation proceed in the early Galaxy and in DLAs?), and the nucleosynthetic origin of different elements (Which stars were responsible for ‘cooking’ different elements in their interiors and releasing them into the interstellar medium, making them available for subsequent generations of stars?). I shall illustrate these points with a few examples chosen from work carried out by European astronomers with UVES.

Are Oxygen and Other Alpha-Capture Elements Overabundant Relative to Iron in DLAs?

Hidden behind this mouthful of jargon lies one of the cornerstones of chemical evolution studies. Oxygen and other elements which are synthesised by the addition to oxygen of one or more alpha particles (examples are Mg, Si, S, and Ca) are thought to be produced mostly in the interiors of massive stars which explode as Type II supernovae some 10 million years after an episode of star

formation. On an astronomical time scale this is quick work. On the other hand, the major producers of Fe are thought to be Type Ia supernovae whose progenitors are stars of relatively low mass which can take up to 1 billion years (100 times longer than the oxygen producers) to explode and release the Fe into the interstellar medium. In Milky Way stars with an iron abundance of less than 1/10 solar (or $[Fe/H] < -1$ in the usual notation), oxygen and other alpha-elements are indeed relatively more abundant than iron by factors of between two and three. The usual interpretation of this well established fact is that, during its early stages of evolution, our Galaxy reached a metallicity of 1/10 of solar relatively quickly, presumably in less than one billion years, so that Fe had not yet had time to catch up with O in the interstellar medium.

Figure 6: Relative abundances of Mn and Fe in DLAs, plotted vs the abundance of Zn (taken as a proxy for Fe). In the Galactic interstellar medium, Mn and Fe are generally depleted by similar amounts so that the ratio of these two elements in DLAs is expected to be relatively insensitive to the degree of dust depletion. Small dots are data for stars in the Milky Way; open and filled circles are measurements in DLAs. (Reproduced from Dessauges-Zavadsky et al. 2002, where references to the original measurements are given.)



Do we see the same pattern in DLAs? The answer to this question is complicated by the fact that most of the elements concerned can be partly hidden from view in DLAs as they condense to form interstellar dust (this problem does not affect stellar abundance measurements, since the dust all melts away when a star is formed). After some initial debate as to whether dust is present in DLAs, most astronomers working in this field now agree that dust depletions have to be taken into account when analysing the pattern of element abundances in DLAs. When this is done, as in Figure 4, a mixed picture emerges. While some DLAs exhibit an overabundance of Si relative to Fe comparable to that seen in Milky Way stars, others – perhaps most – don’t. The conclusion seems to be that DLAs trace galaxies with different pasts; some may have formed stars on timescales similar to that of the early Milky Way, while others apparently did so more slowly, or intermittently, so that Fe could catch up with Si. It makes sense (at least to the author of this article) that DLAs should sample a wide range of galaxy types, and consequently a variety of star formation activity. Even locally, we have recently begun to learn that almost no two galaxies have similar histories in the assembly of their stellar populations, and this is reflected in their varying $[\alpha/Fe]$ ratios, as evidenced by the work presented by Kim Venn at the meeting.

Of relevance to this question are also some new stellar abundance measurements reported at the workshop by Poul Nissen and collaborators, and reproduced in Figure 5. Recently obtained UVES data show that the $[S/Zn]$ ratio does show an enhancement (relative to solar) in Galactic stars of low metallicities. This result had been expected, since S is an alpha-capture element and the abundance of Zn generally follows that of Fe to within about 0.1 dex, but it is nevertheless reassuring to see it confirmed empirically. The significance of this particular pair of elements

is that neither shows much affinity for dust, thereby circumventing the depletion corrections necessary for Si and Fe. The few available data on S and Zn in DLAs (shown with open squares in Figure 4) conform to the broad picture outlined above; without doubt many more measurements of this diagnostic pair will be attempted in the near future, now that their relative abundances in Galactic stars have been clarified.

The Case of Manganese

Mn shows an opposite trend with metallicity from that of the alpha-capture elements: its abundance relative to Fe decreases, rather than increases, with decreasing metallicity. Could this also be a reflection of the pace of past star formation? Its abundance in damped Lyman alpha systems suggests that this is *not* the case. As can be seen from Figure 6, the DLA measurements match the pattern seen in Milky Way stars even though, as we have seen, the QSO absorbers are likely to sample a variety of galaxies which formed stars at different rates. The agreement between Galactic and extragalactic data suggests that perhaps there is a metallicity dependence in the yield of Mn; in any case, the DLA measurements for manganese are providing us with clues to the chemical yields, rather than to the past history of star formation.

Low- and Intermediate-Mass Stars as the Source of Primary Nitrogen

The details of the nucleosynthesis of nitrogen have been the subject of considerable debate in recent years and this element provides perhaps the best example of how observations at high redshifts are driving models of its production in stars. Available measurements of the abundances of N and O are collected in Figure 7. Without going into too much detail, two points are noteworthy. First, DLAs occupy a region of the diagram which is sparsely sampled by local H II regions. It is much easier to find metal-poor gas at high redshift than in the present-day universe. Thus, the relative abundances of N and O in DLAs offer a clearer window on the early nucleosynthesis of these two elements than was available before the commissioning of UVES. Second, note the relatively large spread of values of the (N/O) ratio, from about -1.2 to -2.4 (on a logarithmic scale). Qualitatively, this is what was expected if the main source of N at low metallicities are intermediate-mass stars, between seven and four solar masses, which release their newly synthesised N into the interstellar medium well after the injection of O by Type II supernovae. The DLA data have provided the first empir-

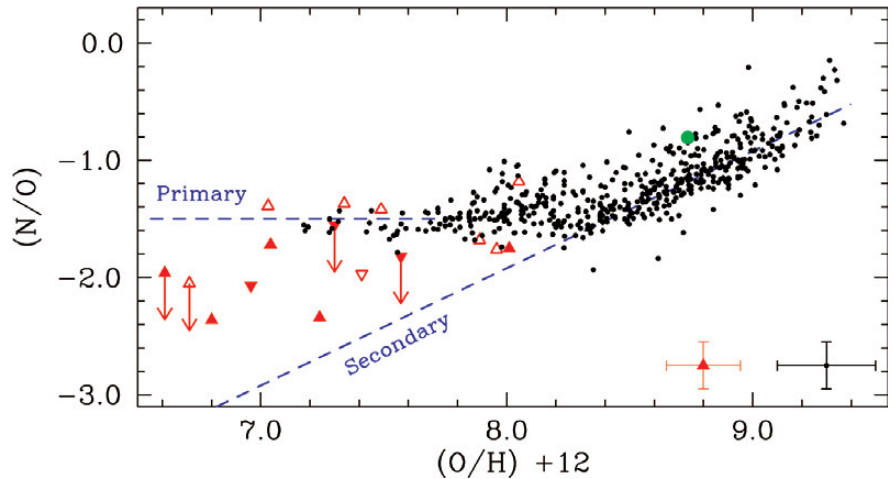


Figure 7: Logarithmic abundances of N and O in nearby H II regions (small dots) and in DLAs (open and filled triangles). Typical errors are shown in the bottom right-hand corner. Adapted from Pettini et al. (2002), where full references to the data and a more extensive discussion of this diagram can be found.

ical evidence in support of this idea of a delayed production of primary N by intermediate mass stars, an idea which had previously been based on entirely theoretical yield calculations.

Quantitatively, however, the proportion of DLAs with values of (N/O) below the level labelled 'Primary' in Figure 7 is surprisingly high, if the time delay is of the order of only 300 million years, as current models predict. Perhaps future observations with UVES will show this to be an artefact of the still limited statistics (and indeed there is by no means universal agreement between different groups as to the pattern of DLA measurements in Figure 7). However, these and similar data have already provided the impetus to theorists to examine more closely the details of the nucleosynthesis of N at low metallicities and mechanisms have been uncovered which have the potential of extending the time delay. One of the most realistic of these seems the inclusion of stellar rotation (hitherto largely ignored) into the calculations of the stellar yields. As shown by Georges Meynet and André Maeder in Geneva, rotation may allow metal-poor stars of masses lower than four solar masses to synthesize N, with the consequence that its release into the interstellar medium may be a more protracted affair, coming to completion on timescales perhaps as long as those of Type Ia supernovae. We can expect significant advances on these questions in the years ahead, both observationally and theoretically.

Concluding Remarks

I hope that this brief review has managed to convey some of the flavour of that exciting two-day meeting in Garching last November. The workshop served to highlight the major impact which UVES has had, and continues to have, on European astronomy,

not only in the depth and breadth of new results and projects which the instrument has made possible, but also in the increasing dialogue between stellar and extragalactic astronomers, and between observers and theorists, which UVES has helped to foster.

The meeting concluded with a brief outline by Sandro D'Odorico of current plans for future upgrades of UVES and, looking further ahead, for complementary instruments which will allow high-resolution spectroscopy at wavelengths from the ultraviolet to the near-infrared. This was followed by a brief user feedback session. The session was brief because generally there is a high level of satisfaction among UVES users! The merits of the data archive were highlighted, although the point was also made that the usefulness of the archive will be significantly increased when UVES pipeline reduced data are included in it. Hopefully this important development will be implemented in the near, rather than medium-term, future.

Finally, all participants expressed their sincere thanks to Francesca Primas, whose enthusiasm, generosity, and impeccable organization – always accompanied by her trademark smile – made this meeting such a resounding success.

References

- Chen, Y.Q., Nissen, P.E., Zhao, G., & Asplund, M. 2002, *A&A*, **390**, 225.
- Dessauges-Zavadsky, M., Prochaska, J.X., & D'Odorico, S., 2002, *A&A*, **391**, 801.
- Hoopes, C.G., Sembach, K.R., Hebrard, G., Moos, H.W., & Knauth, D.C. 2003, *ApJ*, in press (astro-ph/0212303).
- Nissen, P.E., & Schuster, W.J. 1997, *A&A*, **326**, 751.
- Pettini, M., & Bowen, D.V. 2001, *ApJ*, **560**, 41.
- Pettini, M., Ellison, S.L., Bergeron, J., & Petitjean, P. 2002, *A&A*, **391**, 21.
- Vladilo, G. 2002, *A&A*, **391**, 407.

The VIRMOS-VLT Deep Survey: a Progress Report

O. LE FÈVRE¹, G. VETTOLANI², D. MACCAGNI³, J.-P. PICAT⁴, B. GARILLI³, L. TRESSE¹,
C. ADAMI¹, M. ARNABOLDI¹⁰, S. ARNOUITS¹, S. BARDELLI⁵, M. BOLZONELLA³,
D. BOTTINI¹¹, G. BUZZARELLO¹⁰, S. CHARLOT⁶, G. CHINCARINI⁷, T. CONTINI⁴,
S. FOUCAUD¹, P. FRANZETTI¹¹, L. GUZZO⁷, S. GWYN¹, O. ILBERT¹, A. IOVINO⁷,
V. LE BRUN¹, M. LONGHETTI⁵, C. MARINONI¹, G. MATHEZ, A. MAZURE¹,
H. MCCRACKEN⁵, Y. MELLIER⁸, B. MENEUX¹, P. MERLUZZI¹⁰, S. PALTANI¹,
R. PELLÒ⁴, A. POLLO⁷, M. RADOVICH¹⁰, P. RIPPEPI¹⁰, D. RIZZO⁷, R. SCARAMELLA⁹,
M. SCODEGGIO³, G. ZAMORANI⁵, A. ZANICHELLI⁵, E. ZUCCA⁵

¹Laboratoire d'Astrophysique de Marseille, France; ²Istituto di Radio Astronomia, Bologna, Italy;
³Istituto di Fisica Cosmica e Tecnologie Relative, Milan, Italy; ⁴Observatoire Midi-Pyrénées, Toulouse, France;
⁵Osservatorio Astronomico di Bologna, Italy; ⁶Max Planck Institute für Astronomie, Garching, Germany;
⁷Osservatorio Astronomico di Brera, Italy; ⁸Institut d'Astrophysique de Paris, France;
⁹Osservatorio Astronomico di Roma, Italy; ¹⁰Osservatorio Astronomico di Capodimonte, Naples, Italy
¹¹Istituto di Astrofisica Spaziale e Fisica Cosmica CNR, Milano, Italy

Introduction

The VIMOS instrument has been successfully commissioned at the VLT Mephal in 2002, and is now open to the community, with a first set of observations for General Observers scheduled in Period 71. From the start, VIMOS has been designed with the goal to undertake large, deep surveys of the distant universe. VIMOS is capable of an impressive multiplexing capability: up to 1000 objects can be measured simultaneously [1], which allows to assemble large datasets of faint objects in a short time.

The VIRMOS consortium has defined the *VIRMOS-VLT Deep Survey* (VVDS), as a major programme to study the evolution of galaxies, clusters, large-scale structures, and AGNs, over more than 90% of the current age of the universe [2]. The survey aims to observe more than 100,000 objects in the distant universe $0 < z < 5$, which will allow a solid knowledge of the luminous content of the universe at early epochs, and its evolution, based on large statistical samples.

We describe here the start of the survey with the first guaranteed night observations which have been carried out in the October-December 2002 time frame. The general survey strategy,

performances, and first results are presented.

VVDS Outline

The goal of the VIRMOS deep redshift survey is to study the evolution of galaxies, AGNs, and large-scale structures, over a redshift range $0 < z < 5+$. The requirement is to be able to analyse the basic properties such as the luminosity function or spatial correlation function of the galaxy population, as a function of galaxy type or local density, in each of several time steps covering the redshift range of interest.

We are therefore planning to observe the following magnitude-limited samples:

1. "Wide" survey: more than 10^5 galaxies with redshifts measured to $I_{AB} = 22.5$ (redshift up to $z \sim 1.3$), it will be conducted in 5 fields identified in Table 1.

2. "Deep" survey: more than 4×10^4 galaxies with redshifts to $I_{AB} = 24$ (redshift up to $z \sim 5$) conducted in the 0226-04 field.

3. "Ultra deep survey": more than 10^3 galaxies with redshifts to $I_{AB} = 25$ conducted in the 0226-04 field.

The spectroscopic samples will be observed with $R \sim 210$ in a first pass. A subsample of 10,000 galaxies will then be selected for spectroscopy at a resolution $R \sim 2500-5000$ to allow the study

of the evolution of the fundamental plane, and perform a detailed analysis of the spectro-photometric properties of galaxies.

Four fields in addition to the Chandra Deep Field South are targeted during the course of the survey. Each field is $2 \times 2 \text{ deg}^2$ for the "wide" survey, and 1.3 deg^2 for the "Deep" survey. Extensive imaging has been carried out using the CFHT12K camera, the ESO 2.2-m WIF1, and the NTT-SOFI to assemble a sample of around 2 million galaxies with BVRI photometry, with smaller subsets having in addition U and/or K' photometry [3].

The complete photometric survey gives access to a volume of the universe which is equivalent to the 2DF redshift survey, although at a much higher mean redshift of $z \sim 1$.

First Observations

The ESO Director General has granted the VIRMOS consortium the early use of guaranteed time in the period October-December 2002, immediately following the last commissioning period in September, interleaved with periods of "Paranalization". This approach had a double advantage: to ESO because the consortium committed to technically attend to the instrument with its own

Table 1: VVDS fields

Field	Alpha (2000)	Delta (2000)	Survey area (deg ²)	Survey mode	Observed in Oct.-Dec.2002
0226-04	02h26m00.0s	-04°30'00"	1.3 (Deep) 4 (Wide)	Wide, Deep, Ultra-deep	20 deep pointings, 9188 slits
CDFS	03h32m28.0s	-27°48'30"	0.1 (Deep)	Deep, IFU, early community release	5 deep pointings, 1 deep IFU pointing, 2109 slits
1003+01	10h03m39.0s	+01°54'39"	4 (Wide)	Wide	7 pointings, 2595 slits
1400+05	14h00m00.0s	+05°00'00"	4 (Wide)	Wide	
2217+00	22h17m50.4s	+00°24'27"	4 (Wide)	Wide	17 pointings, 6849 slits

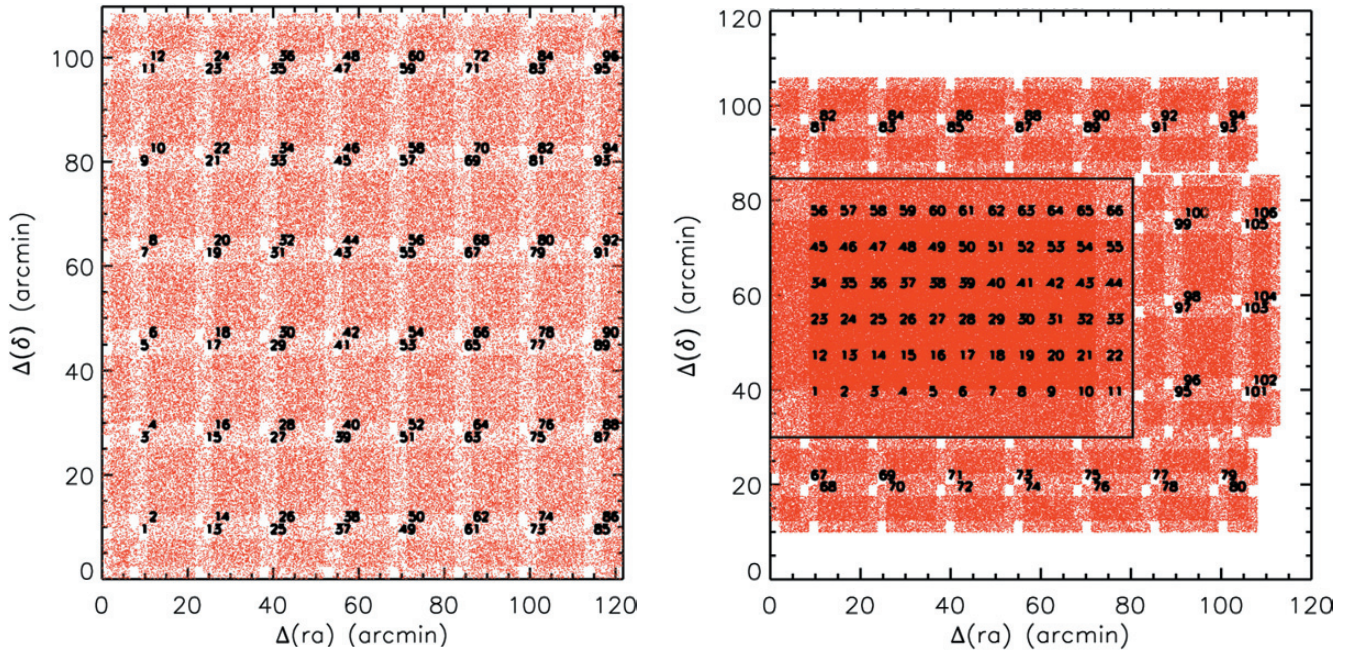


Figure 1: The distribution of the 96 VIMOS pointings for the VVDS-Wide fields (left) and 66 VVDS-Deep pointings (central area, right) and 40 VVDS-Wide pointings in the 0226-04 area. Each pointing of 4 quadrants is labelled and the area covered is shaded in red, with a density increasing at each passage. Targets are selected only in the shaded areas. The spatial selection function for the VVDS-Wide is easy to model and correct for. Carefully selected offset patterns allow to cover an area of 1.3 deg^2 in the 0226-04 Deep area with a smooth spatial selection function totalling 4 passes of VIMOS.

support staff to solve pending problems which may have occurred, therefore making the instrument more reliable; and to the consortium because of the ability of an early start of the VVDS.

Two observing periods have been allocated to the consortium: 29 October – 11 November (14 nights) and 27 November – 11 December (15 nights). The first observing run was blessed with excellent weather, only 2 nights were lost due to high-level clouds, while during the second period strong north winds prevented us from observing dur-

ing 8 nights. In total, the equivalent of 19 dark short summer nights benefited from clear weather and nominal Paranal seeing. While some of the consortium observers had their first time ever on the instrument during this time, the training was smooth and quick. The team made its utmost to ensure that the instrument was ready for each night of observation. As anticipated, we had to face some technical problems, related in particular to the occasional failure of a mask or grism insertion, these were addressed during the day with the con-

sortium technical staff. Less than one night was lost to instrument problems in these first observing runs.

The preparation of masks for the nights of observations has been challenging but smooth, especially during consecutive long periods of nice weather, when up to 6 sets of 4 masks with more than 500 slits in each set had to be manufactured during the day with the Mask Manufacturing Machine [4]. The observing time has been balanced between long integration on the deep survey, and short integration on the

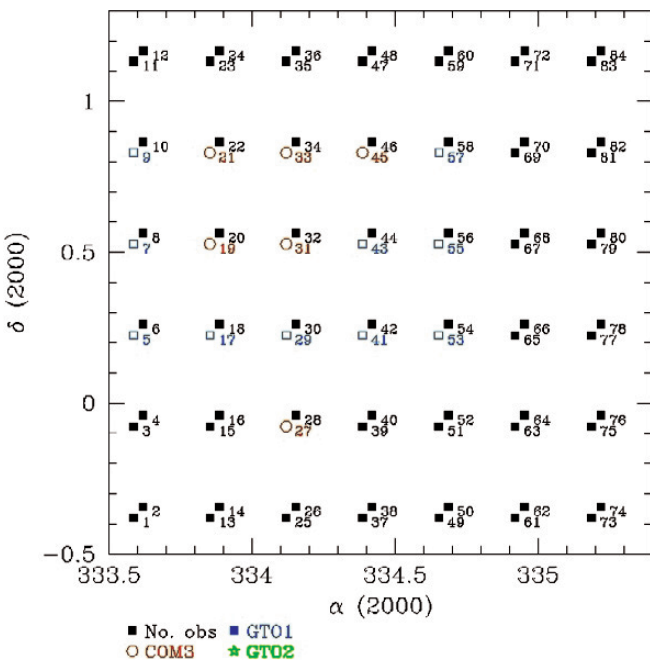


Figure 2: Pointings observed in the 1003+01 VVDS-Wide in the fall 2002.

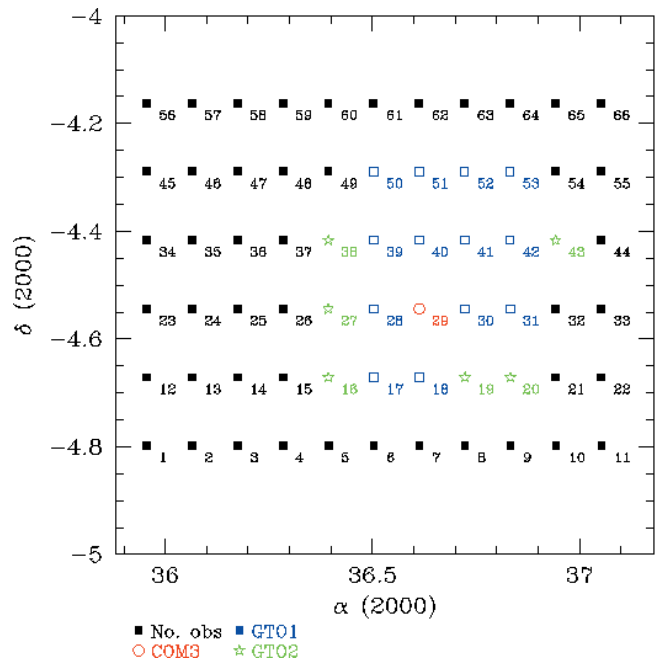


Figure 3: Pointings observed in the 0226-04 VVDS-Deep in the fall 2002.

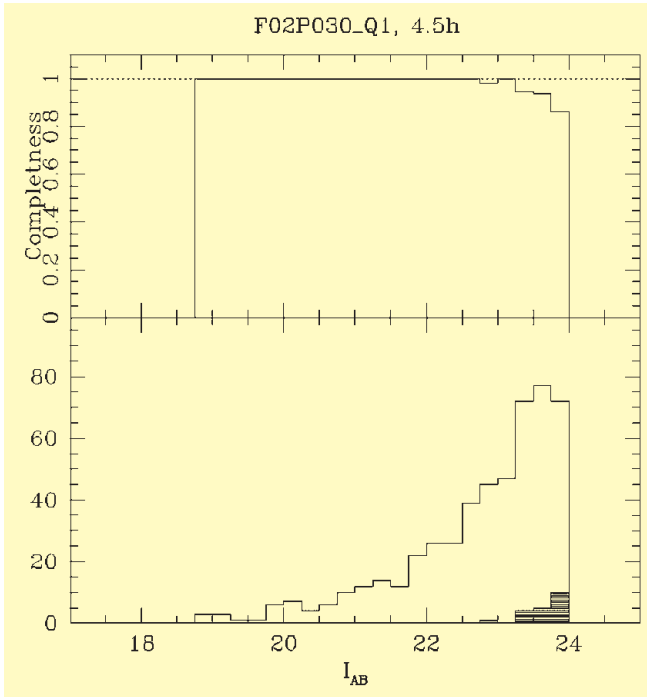


Figure 4: Completeness measurement vs. magnitude in the quadrant 1 of the F02P030-Deep pointing, defined as the ratio of objects with secure redshift identification to the total number of objects observed without instrumental bias (top), and the corresponding magnitude distribution with the objects for which no redshift could be measured, indicated as the shaded histogram (bottom).

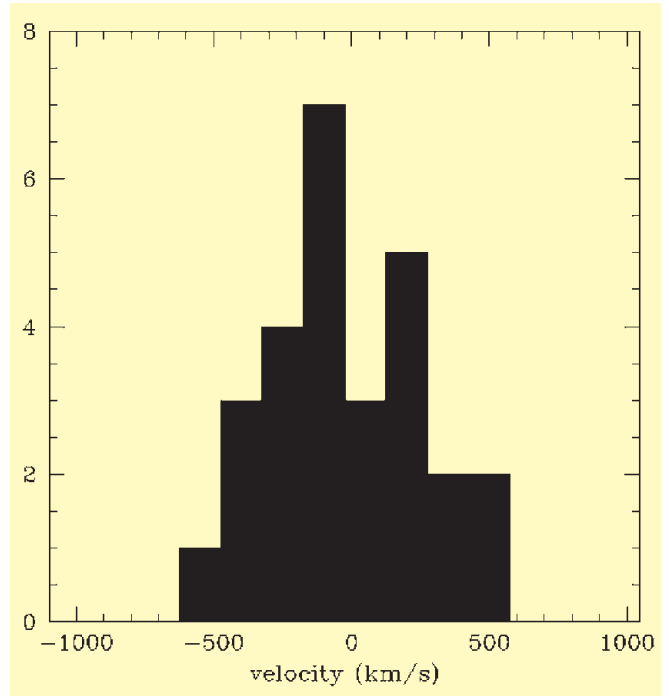


Figure 5: Velocity accuracy: comparison of redshifts measured independently on the same galaxies from two different mask datasets. The error in velocity measurement accuracy is 270 km/s rms for the LRRed grism and 1 arcsec slits.

wide survey. The strategy adopted had been tested during commissioning and is recommended for all MOS observations: because of the strong CCD fringing above 8200 Å, sequences of observations were acquired moving the objects along the slits. This allows to compute the fringing pattern in each slit,

and remove it for an improved sky and fringing correction. For the wide survey, we used an offset pattern 0, -0.7, -1.4, +0.7, +1.4 arcsec from the reference position, with 5 exposures of 9 minutes each, while for the deep survey we used an offset pattern 0, -0.8, -1.6, +0.8, +1.6 arcsec, repeating twice this pattern for

a total of 10 × 27 minutes exposure.

The VVDS has a set of carefully designed pointings (one pointing is one position of VIMOS on the sky with all four quadrants), to minimize the spatial bias applied by the non-contiguous geometry of the instrument. In the wide survey, we carry out two passes of

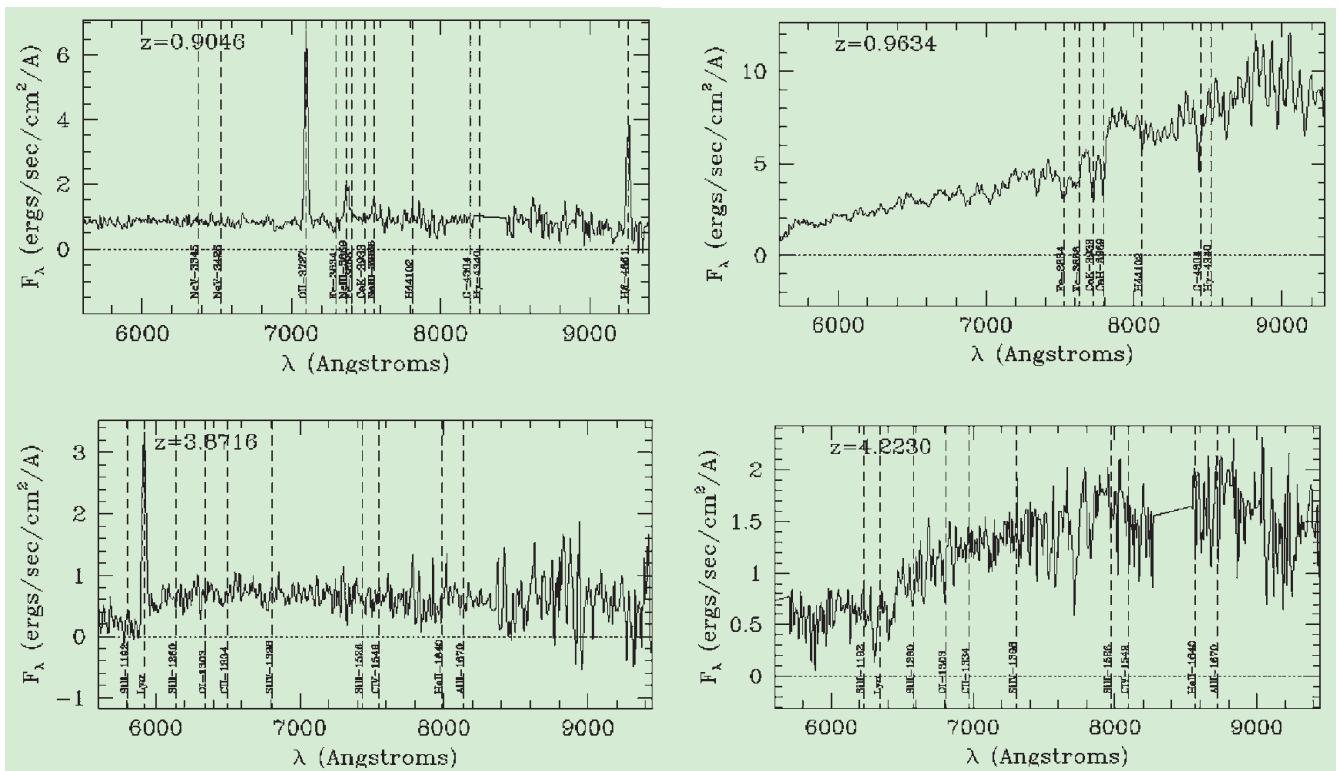


Figure 6: Sample spectra from the first VVDS observations.

VIMOS on the same sky area, offset by (2.2) arcminutes. This ensures that more than 50% of the $I_{AB} = 22.5$ objects are observed on average, with a smooth spatial sampling function which is easy to model (Fig. 1), and to correct for, e.g. for the computation of the correlation function.

For the VVDS Deep, the set of pointings allows for a continuous spatial sampling of the area, with 4 VIMOS passes at any sky location (Fig. 1).

A total of 24 wide pointings have been observed in the 2217+00 and 1003+01 fields, for a total of 9444 slits (Fig. 2), and 25 deep pointings have been observed in the 0226-04 (Fig. 1) and CDFS fields for a total of 11,297 slits.

First Results

The data processing is now in full swing, with 4 teams processing the data in parallel. Each pointing is processed twice: the automated data processing pipeline VIPGI is applied, and the product is distributed to two teams/reducer to extract the redshifts independently. A dedicated tool has been developed to automatically measure redshifts. At this time we examine spectra one by one for redshift measurements proposed by the KBRED tool. Although this process is somewhat long and tedious, it allows one person to process a set of 4 masks with ~ 500 slits in a few working days. Careful data quality assessment is made for each mask, checking the wavelength and flux calibrations.

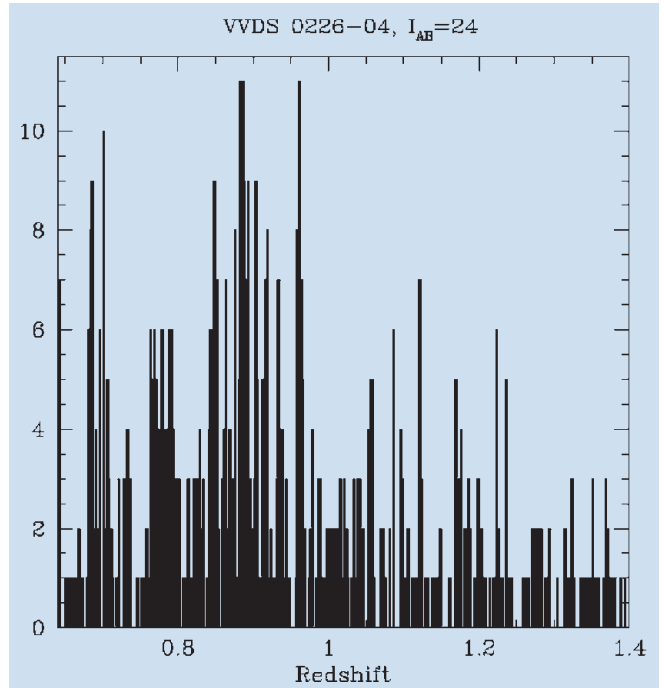
The quality of spectra is as expected. We are experiencing a completeness better than 90% of the overall sample

Figure 7: Redshift distribution of galaxies around $z \sim 1$ in the 0226-04 VVDS-Deep area. This is assembled from 3 pointings, and clearly shows dense peaks and empty regions.

for both the wide and deep surveys (Fig. 4). The velocity accuracy has been estimated from independent redshift measurements of the same galaxies in two different pointings, it is ~ 270 km/s rms as derived from a sample of 27 galaxies (Fig. 5). Examples of spectra are shown in Figure 6.

We have performed test observations for the $R \sim 2500$ follow-up observations which will be carried out on objects selected from the low-resolution survey. Spectra of $z \sim 1$ galaxies with emission lines like [OII] (Fig. 8) show that the measurement of the velocity dispersion in galaxies will be possible to a level of ~ 30 km/s.

In the VVDS-Deep pointings, we find that 10% of the objects are stars, 0.7% QSOs, since no pre-selection has been made besides the I-band limited sample. The fraction of stars is higher at about 15–20% in the VVDS-Wide. The



mean redshift is 0.55 for the VVDS-Wide and 0.8 for the VVDS-Deep. The redshift distribution for each pointing now shows the classical succession of high density peaks and low density areas (Fig. 7).

Conclusion

The VVDS survey is now proceeding with a first set of successful observations. Upon final processing of the more than 20,000 spectra acquired so far, and taking into account the fraction of stars and the completeness, the yield of secure redshift measurements should amount to $\sim 15,000$ for this first set of observations. This will allow for a first computation of the luminosity function and to map the distribution of galaxies down to $I_{AB} = 24$, from a sample free of selection effects.

The raw IFU data obtained on the Chandra Deep Field South is available on-line (<http://www.oamp.fr/virmos>), and we will make a public release of the Chandra Deep Field South MOS data (1D calibrated spectra and redshift measurements) in this same field as soon as the processing is completed.

References

- [1] Le Fèvre, O., et al., *The Messenger*, September 2002.
- [2] Le Fèvre, O., Vettolani, G., Maccagni, D., Mancini, D., Mazure, A., Mellier, Y., Picat, J.P., et al., astro-ph/0101034, ESO Astrophysics Symposia Series "Deep Fields", Cristiani, Renzini, Williams, Eds., Springer, p. 236.
- [3] Le Fèvre, O., Mellier, Y., McCracken, H.J., Arnaboldi, M., et al., 2000, A.S.P. Conf. Series, Clowes, Adamson, and Bromage Eds., vol. 232, p. 449.
- [4] Conti, G., Mattaini, E., Maccagni, D., Sant' Ambrogio, E., Bottini, D., Garilli, B., Le Fèvre, O., Saisse, M., Voët, C., et al., 2001, *PASP*, 113, 452.

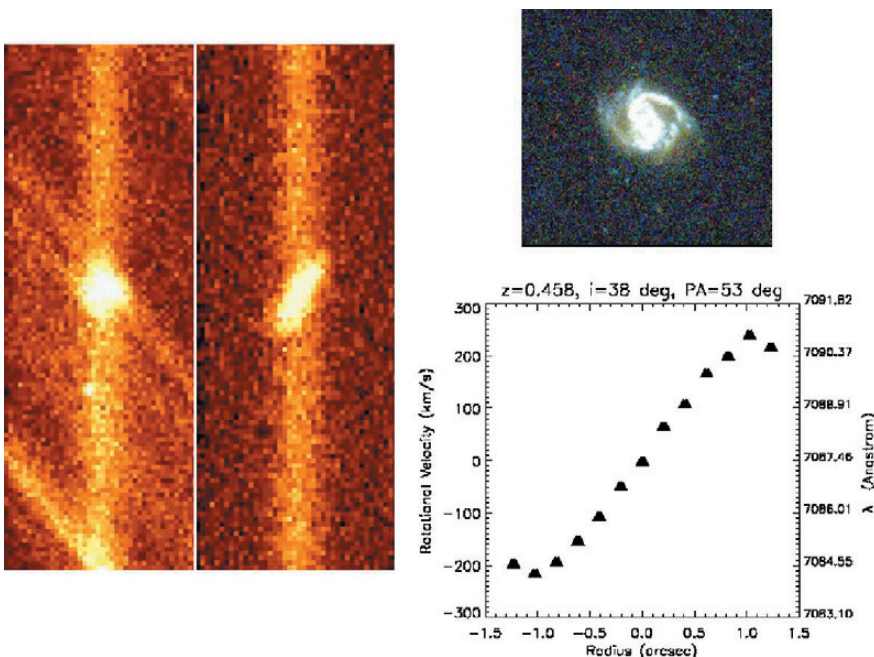


Figure 8: Velocity curve of a galaxy at $z = 0.458$ from observations in the HRRED grism ($R \sim 2500$) of the $H\beta$ line. Left: raw spectrum obtained with a slit cut by the laser machine tilted on the major axis of the galaxy, and corrected spectrum after sky subtraction and wavelength straightened. Right: velocity curve obtained after correction of the inclination angle of the galaxy. Top right: image obtained with HST/ACS (GOODS-CDFS public data).

Exploring the Icy World of the Edgeworth-Kuiper Belt – An ESO Large Programme

H. BOEHNHARDT (Max-Planck-Institut für Astronomie, Heidelberg, Germany)

*A. BARUCCI, A. DELSANTI, C. DE BERGH, A. DORESSOUNDIRAM, J. ROMON
(Observatoire de Paris, Meudon, France)*

E. DOTTO (Osservatorio Astronomico di Roma, Italy)

G. TOZZI (Osservatorio Astronomico di Arcetri, Firenze, Italy)

M. LAZZARIN, S. FOURNISIER (Osservatorio Astronomico di Padova, Italy)

*N. PEIXINHO (Observatorio Astronomico de Lisboa, Portugal, and Observatoire de Paris,
Meudon, France)*

O. HAINAUT (European Southern Observatory, Santiago de Chile)

J. DAVIES (Royal Observatory Edinburgh, Great Britain)

P. ROUSSELOT (Observatoire de Besançon, France)

L. BARRERA (Universidad Católica del Norte, Antofagasta, Chile)

K. BIRKLE (Max-Planck-Institut für Astronomie, Heidelberg, Germany)

K. MEECH (University of Hawaii, Honolulu, USA)

J. ORTIZ (Instituto de Astronomia de Andalucía, Granada, Spain)

T. SEKIGUCHI, J.-I. WATANABE (National Astronomical Observatory, Mitaka-Tokyo, Japan)

N. THOMAS (Max-Planck-Institut für Astronomie, Katlenburg-Lindau, Germany)

R. WEST (European Southern Observatory, Garching, Germany)

The Edgeworth-Kuiper Belt and the Formation of the Solar System

The first object in the Edgeworth-Kuiper Belt was observed in 1930, when Clyde Tombaugh discovered Pluto at a distance of 43 AU (1 AU = one astronomical unit, the mean distance between Earth and the Sun = 149.6 million km), i.e. beyond the orbit of Neptune. About 20 years later Edgeworth and Kuiper started to speculate about the existence of another asteroid belt at the edge of the planetary system. Another 30 years later this speculation became an hypothesis when Fernandez and Ip argued for the existence of an Ecliptic-oriented reservoir of icy bodies beyond Neptune as a source for short-period comets, the recruitment of which was difficult to explain by gravitational capturing of Oort Cloud comets through planets when approaching the inner solar system. The hypothesis became reality in 1992, when, during a search campaign for distant asteroids, Jewitt and Luu found 1992 QB₁ (now numbered: 15760) at a distance of 41 AU from the Sun.

In the meanwhile, after the detection of more than 700 objects beyond the orbit of Neptune over the past decade, a new class of solar system bodies has been discovered. These Transneptunian Objects (TNOs) are the largest members of the Edgeworth-Kuiper Belt. They have caused a complete revision of our knowledge and understanding of the outer solar system: the Edgeworth-

Kuiper Belt is believed to represent the most original remnant from the formation period of our planetary system. It was in this region where within less than 20 million years some 4.6 billion years ago, icy planetesimals formed and grew to larger bodies, nowadays observed as TNOs, Centaurs, short-period comets and some icy satellites of the major planets. Although of the same origin and most likely containing the same primordial material, these small bodies, as we observe them now, have experienced different evolution over the age of the solar system, both dynamically and physically. Nevertheless, they contain the most primordial material from the formation of the Sun and its planetary system that we can observe today.

The Global View of the Edgeworth-Kuiper Belt and its Population of Objects

The dynamical ‘zoo’ of Cubewanos, Plutinos, Centaurs and SDOs: According to current dynamical scenarios, the TNO population remained in the region of its formation, the Edgeworth-Kuiper Belt, over the age of the solar system. However, their orbits became perturbed by the presence of Neptune. The gravitational interaction with this giant planet has ‘pumped’ objects into so-called ‘excited’ (i.e. non-circular and/or inclined), but non-resonant orbits creating the dynamical class of ‘Cubewanos’ (named after the prototype object 1992 QB₁), also called clas-

sical disk objects. Other TNOs were captured in resonant orbits with Neptune forming the dynamical class of ‘Plutinos’ (named after Pluto, the most prominent representative in the 3:2 resonance orbit). Gravitational scattering at Neptune has produced the class of ‘Scattered Disk Objects (SDOs)’ in very eccentric orbits with semi-major axes between 50 and several 1000 AU. The ‘Centaurs’, presently in orbits between Neptune and Jupiter and named after half-human-half-horse demigods in Greek mythology, are also considered to be scattered TNOs, cascading towards the Sun by repeated gravitational interaction with the major planets. At the end, i.e. typically after some 10 million years in intermediate orbits, Jupiter will either capture them as short-period comets (thus, some of them even become accessible for spacecraft exploration) or will expel them into the region of the long-period Oort Cloud or even interstellar comets at the edge of the solar system. A few TNOs may get stranded as satellites around the outer gas giants (the most prominent candidate is Triton, the largest moon of Neptune).

The original formation disk, more ‘Plutos’ and TNO binaries: The drop in the number of objects with semi-major axes larger than 50 AU may indicate either a basic characteristic of the formation disk around our Sun (a ‘truncated’ disk?) or may just mark the challenge to detect the ‘cold’ and very collimated formation disk of even smaller planetesimals that escaped the gravita-

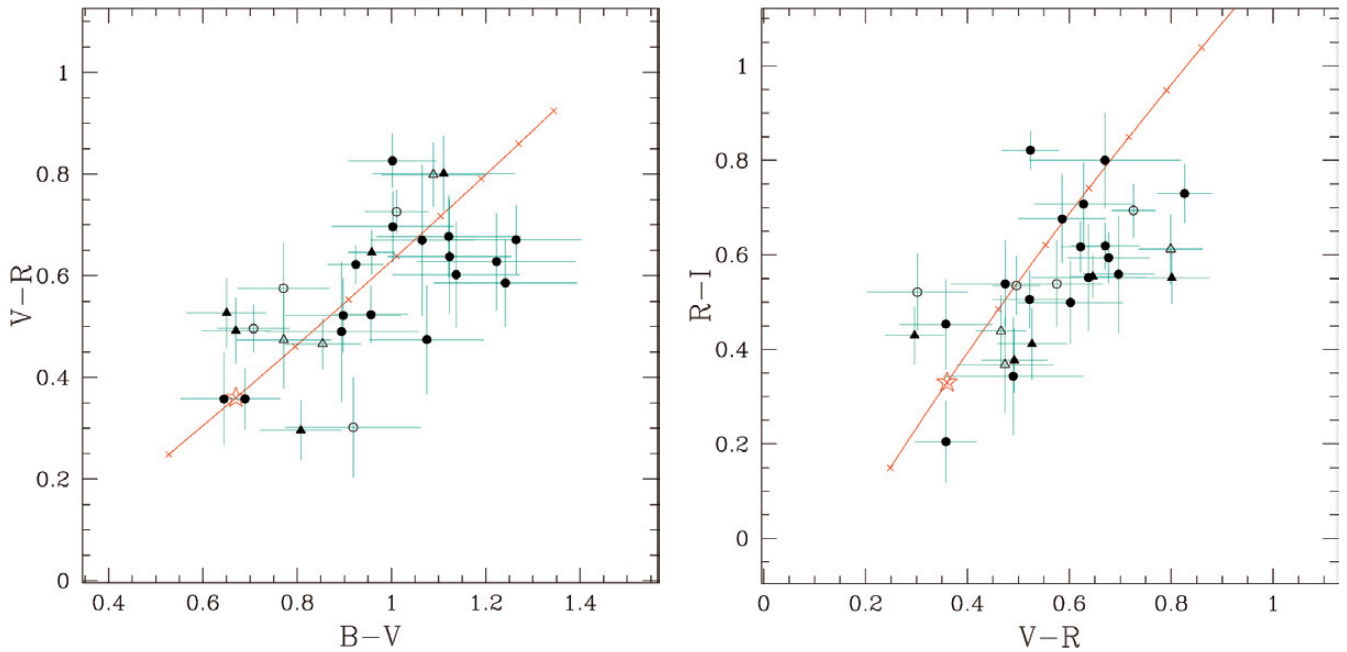


Figure 1: Colour-colour diagrams of the first 28 objects observed within the Large Programme. The two panels show the B-V versus V-R (left) and R-I versus V-R (right) colours of the objects measured. The symbols are: filled circles = Cubewanos, filled triangles = Plutinos, open circles = SDOs, open triangles = Centaurs. The colour of the Sun is indicated by the open star symbol. The lines indicate the direction of increasing reddening slopes from -10 (lower left end) to $70\%/100$ nm (upper right end) in steps of $10\%/100$ nm. The distribution of the measured objects seems to be rather uniform in the typical reddening range. The shift of the objects below the line of constant reddening in the plots involving R-I colour is due to the spectral slope change of red objects towards the near-IR end of the visible spectrum.

tional influence of the outermost planets because of their large distance from the Sun. The overall mass in the Edgeworth-Kuiper Belt seems to be very small (0.15 Earth masses) and cannot explain the existence of large TNOs like Pluto/Charon or Varuna. Instead modelling results suggest that the original formation disk in the TNO region was much heavier (10–100 Earth masses), that it should have produced more Pluto-size bodies and that most of its mass got lost by gravitational scattering at the large planets as well as by mutual collisions of TNOs and subsequent down-grinding of the colli-

sion products to micron size dust that the solar radiation pressure has removed from the Edgeworth-Kuiper Belt region. The existence of binary TNOs (about 10 objects so far) supports the idea of a serious collision environment in the belt during and possibly beyond the end of the formation period of planetesimals. Ongoing search programmes using imaging surveys and high-resolution imaging techniques at large telescopes world-wide try to solve these key questions on the Edgeworth-Kuiper Belt.

Physico-chemical properties: While the dynamical history of TNOs

and their relatives seems to be reasonably well understood, just a very vague picture of their physical properties and chemical constitution exists. The faintness of the objects (the vast majority are fainter than 23 mag) makes them difficult to observe even with the largest telescopes: the brightest representatives (about 20 mag) require easily one full observing night at an 8-m VLT unit telescope for a spectroscopic study of decent signal-to-noise.

Despite their faintness, the observed TNOs and Centaurs are only the largest members of the belt population with diameter estimates ranging be-

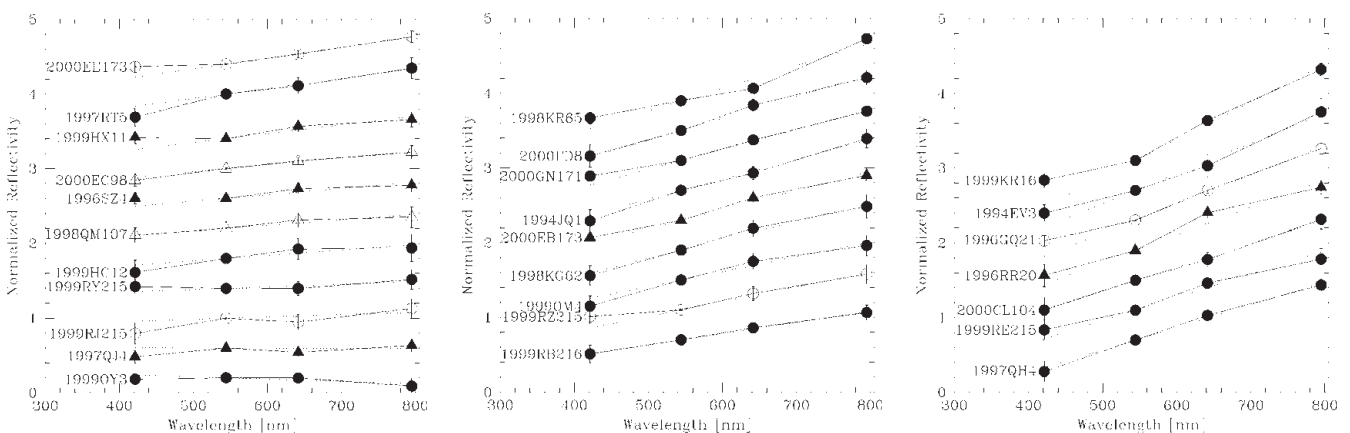


Figure 2: Photometric “reflectivity spectra” from BVRI magnitudes of TNOs and Centaurs. The three panels show the photometric “reflectivity spectra” of the first 28 objects observed with our programme. The relative reflectivity per photometric band (normalized to unity for V band) is plotted versus central wavelength of the filters used. It is a measure of the intrinsic reddening of the objects since the slope of solar spectrum is removed from the data. The broken lines indicate the numerical spectral gradient fits for the individual objects. These plots are very useful to check the consistency of the photometric data since “bad” measurements and intrinsic variability of the objects will result in noticeable deviations of the photometry from a “smooth” spectral slope in these “spectra”. If found, further investigations may be needed to clarify the nature of the scatter.

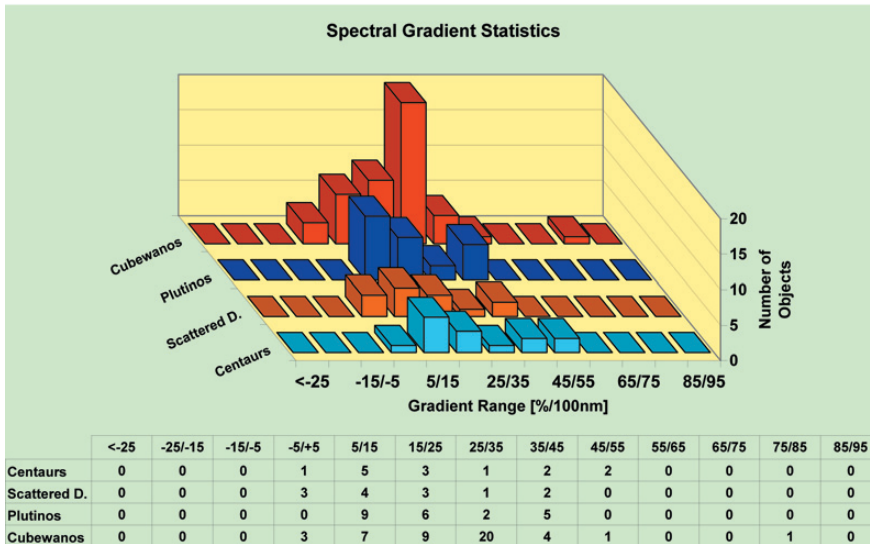


Figure 3: Spectral gradient histograms of the full sample of 96 objects in our analysis database. The histograms show the number of objects per spectral gradient interval for each dynamical class as given in the table at the bottom of the figure. The spectral gradients are calculated from the BVRI photometry of the objects.

tween 30 and 1200 km (assuming a low albedo of 4 per cent). Search programmes suggest a cumulative mass function with power exponent between 3.5 and 4. The albedo of less than 10 objects is coarsely determined: TNOs and Centaurs seem to be dark objects with albedo mostly around and below 10 per cent. Only Pluto, Charon and Chiron have high (around 50 per cent for Pluto and Charon) to moderate albedo, possibly caused by fresh ice due to intrinsic atmospheric activity (see below). The rotation period of more than 20 objects is measured with results ranging from 5 and 12 h (certainly biased since long periods are more difficult to measure). With the exception of Pluto and Charon, it is unclear whether the measured variability is due to body shape or surface reflectivity or both.

Until 2001 the taxonomic characterization of the population was based on a sample of ~ 50 TNOs and ~ 10 Centaurs, most of them observed with broadband colours in the visible wavelength range only. Nevertheless, colour-colour diagrams and reddening distributions provide a first glance of similarities and diversities in the surface taxonomy of the objects. A wide range of colours (in other words spectral gradients or 'reddenings') ranging from slightly bluer than the Sun ($\sim 5\%/100\text{nm}$) to extremely red ($\sim 50\%/100\text{nm}$) in the visible wavelength range is found in this sample. In the infrared, the photometric results indicate only minor reddening to neutral slopes of the surface reflectivity. For a finer analysis, the overall object sample contained some adverse culprits like bad number statistics for all dynamical classes, insufficient photometric accuracy of the data, incomplete wavelength coverage (7 objects had only 1 or 2 colours measured) and large differences in the results for the same objects obtained by different observers. It is thus not surprising that

different researchers arrived at different and partially contradictory conclusions, for instance a bimodal colour distribution versus a continuous one with 'outliers' in both scenarios. Through a Kolmogorov-Smirnov analysis of the sample it became clear that the identified colour populations among TNOs and Centaurs are at best to be considered as trends, but they lack clear statistical significance because of the low number of objects in the available sample.

Since formed in the outer solar nebula, TNOs and Centaurs should be made of icy and stony compounds. Except for the larger members that may have undergone constitutional modifications due to radioactive heating in their interior, and those that come closer to the Sun and thus get heated up in the surface layers, the original material remained unchanged in the body interior. Nevertheless, as outlined below, the surface layers of the bodies are all modified over the age of the solar system. N_2 and H_2O ices should be most abundant in TNOs and relatives, followed by CO , CO_2 , CH_4 and NH_3 . Signatures of N_2 , CO , H_2O , CH_4 and NH_3 ices are indeed found in spectra of Pluto/Charon. Water ice absorptions were detected in the Cubewano 1996 TO_{66} and the Centaurs 5145 Pholus and 2060 Chiron, objects that represent basically the fully colour range found in the total sample. The original 'stony' ingredients in TNOs and Centaurs should be primarily of silicate nature. Their detection, however, is extremely difficult since they may be covered completely with ice mantles. There is only one case, the Centaur 5145 Pholus, in which a very wide and close to marginal absorption feature (ranging from 0.6 to 1.6 μm) is tentatively attributed to silicates. The only other supportive argument for the presence of dust in these objects comes from the Centaur 2060 Chiron and of course their relatives, the short-period comets, i.e. through the

temporary dust coma seen around these objects.

Surface evolution scenarios: The red colour of TNOs and Centaurs is usually attributed to the effects of surface aging and darkening due to high-energy radiation and ion bombardment. Blue surface colours could be produced by major collisions through deposits of fresh icy material from the body interior or from the impactor. The estimated time scale for both types of colour resurfacing are of the order of 10 million years. The observed colour range can be modelled by computer simulations involving both effects. However, these results are unfortunately not discriminative for conclusions on the physical nature of TNO and Centaur surfaces. Resurfacing on much shorter time scales could happen due to ice re-condensation from a temporary atmosphere produced by intrinsic gas and dust activity. This process is quite efficient on Pluto and possibly Charon, but does certainly not work for all objects since crust formation may prevent the development of surface activity and/or the heat source in the bodies may not be strong enough to cause such activity.

ESO Large Programme on 'Physical Studies of TNOs and Centaurs'

Programme concept and history:

After a number of uncoordinated precursor programmes at ESO telescopes at the end of the last decade, a consortium of scientists (see the list of authors of this paper) proposed a comprehensive observing and analysis project to be performed within the framework of an ESO Large Programme: 'Physical studies of TNOs and Centaurs'. The project was accepted to be executed at Cerro Paranal and La Silla during ESO period 67 to 70, i.e. from April 2001 until March 2003. The main goal of the project is the development of a taxonomic classification scheme of these icy bodies in the outer solar system, the identification of evolutionary tracks and their relationships with dynamical classes, the exploration of the surface chemistry of the objects and its correlation with taxonomic classes. The proposed observing campaigns at the ESO Very Large Telescope (VLT) and the New Technology Telescope (NTT) comprise multi-colour broadband filter

photometry of 60–70 objects in the visible and about 25 objects in the near-IR wavelength range for the taxonomy analysis and low-dispersion spectroscopy in the visible and near-IR of about 15–20 objects each for the chemical studies. The ESO Programme Committee has allocated in total 242 hours of VLT time and 3 nights at the NTT for this Large Programme. The workhorse instruments for the proposed observations are FORS1 and ISAAC at the VLT Unit Telescopes 1 (Antu) and 3 (Melipal). Broadband photometry of some brighter targets is also conducted with SUSI2 at the La Silla NTT.

Observing modes and target selection: The majority of the photometry targets are observed in service mode (SM) at the VLT with the exceptions of brighter ones that are either imaged at the NTT or during spectroscopy runs in visitor mode (VM). Experience from previous programmes has shown that the SM targets have to be selected from amongst objects that allow safe detection in the fields of view of the instrument; in practice only objects with at least 2 observed oppositions appear to be ‘reliable’ to this respect. Less well observed targets have a high risk of being missed in the SM exposures that

typically happen about one year after the last object positions were measured. For the BVRI measurements we selected targets with V brightness of 22.5–24mag, while for JHK photometry the objects need to be brighter than 22.5mag in V. The SM targets are requested to be observed under clear to photometric dark sky conditions with seeing better than 0.8”. These constraints together with the chosen integration times guarantee a minimum signal-to-noise ratio (S/N) for the individual objects of 30–50 in BVRI and 20–40 in JHK. In terms of fulfilment of the observing requirements this part of our programme can be considered 100 per cent successful.

Observing strategies: The spectroscopy part of the programme is performed in visitor mode since the on-line detection of these slowly moving (typically 1–2”/h) faint targets in SM was considered risky and misidentifications may cause significant loss of observing time. The targets had to be selected amongst brighter objects, i.e. brighter than 22.5 mag in V for spectroscopy in the visible wavelength range and brighter than 20.5mag in V for the near-IR spectroscopy. Several of the targets had some BVRI colours measured from previous observations or other pro-

grammes. Nevertheless, quasi-simultaneous broadband photometry of the targets is taken during spectroscopy runs with the aim to verify the earlier results and – most importantly for the IR spectra – to cross-calibrate the continuum flux in the JHK bands of the objects as needed for the modelling of the spectra. Visible and near-IR spectroscopy runs are scheduled within a few days of each other in order to guarantee observations of the same object under similar phase angles. However, this scheduling usually did not allow us to correlate the rotational phase of the objects for the measurements in both wavelength ranges, mostly because for many objects the rotation parameters are not well known. The exposure times of the targets aimed for a S/N of about 3–10 per wavelength pixel element which through wavelength binning allowed improvements by a factor of 3–5. Given the faintness of the objects and the telescope/instrument capabilities, near-IR spectroscopy is the most time-consuming part of our programme even under favourable sky conditions, and typically 1 to 1½ nights of observing time are required per target. Unfortunately, the visitor mode observations so far have had an unexpectedly high ‘loss’ rate of about 25 per cent due to

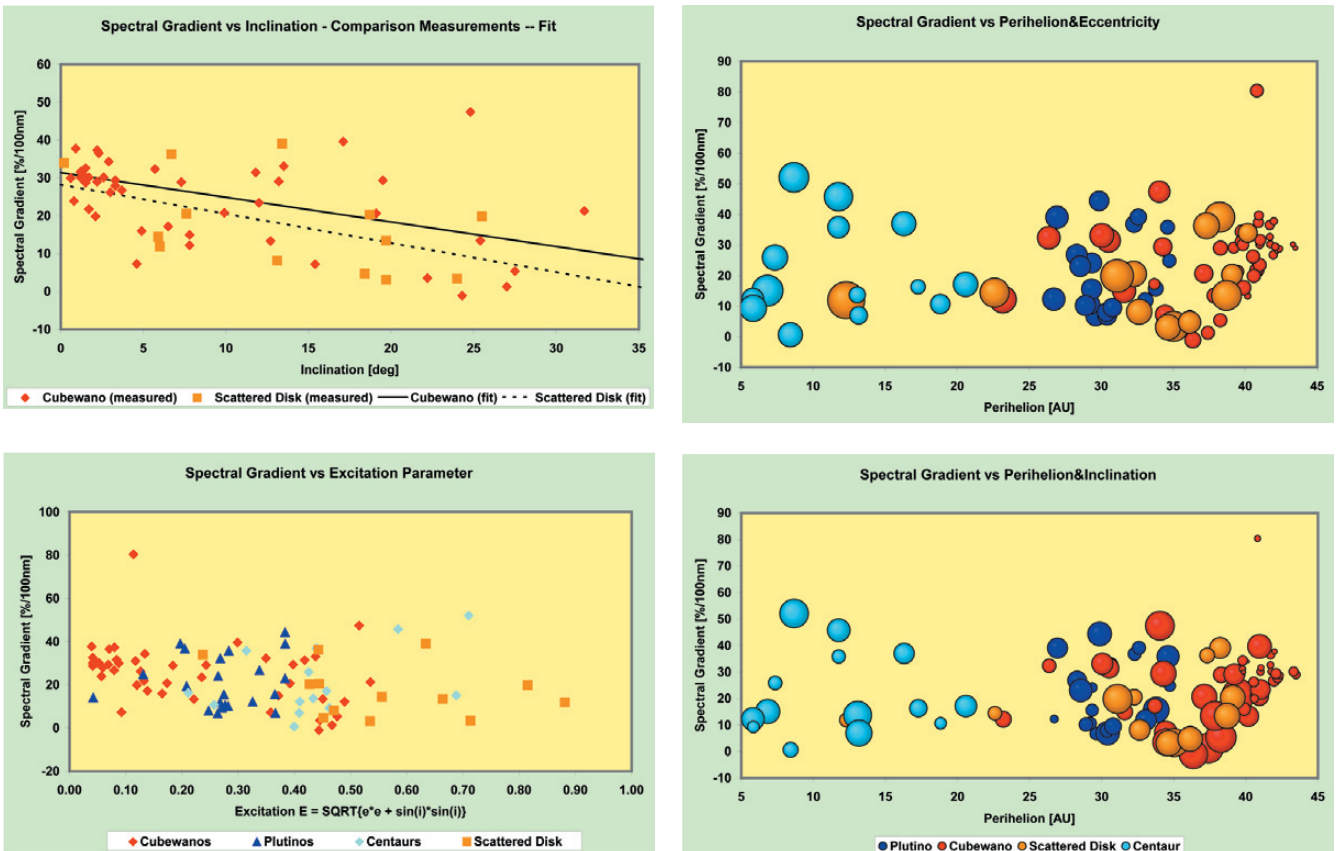


Figure 4: Spectral gradients versus orbital parameters. The plots show the measured (from BVRI photometry) spectral gradients of the objects versus orbital excitation E (lower left panel), inclination (upper left panel), and perihelion distance (upper and lower right panels). The bubble diagrams in the right panels use the orbital eccentricity (upper right) and the inclination (lower right) as size parameter of the bubbles, i.e. the smaller the bubble the lower the eccentricity and inclination, respectively. The colour coding of the dynamical classes is identical to Figure 2. The red Cubewanos beyond 41 AU mentioned in the text appear to cluster at the left end in the left panels and (as the tiny bubbles) to the right end in the right panels.

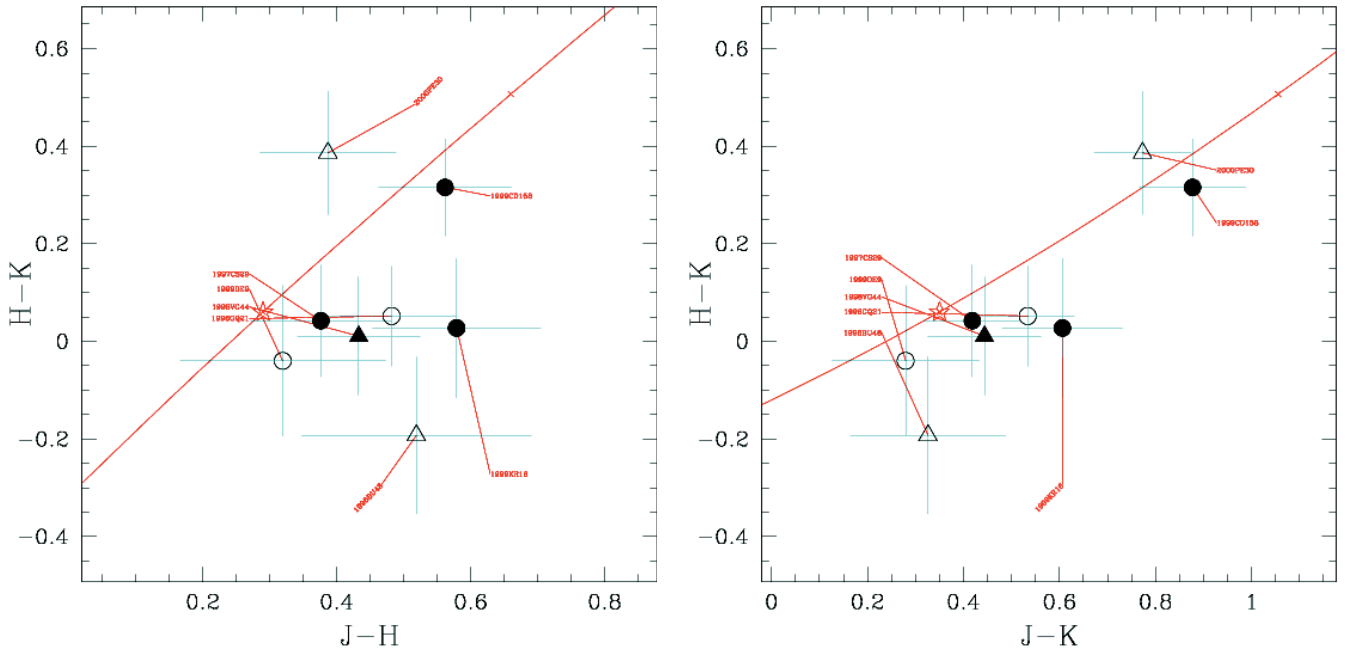


Figure 5: JHK colour-colour plots of the first 8 objects measured in the SM photometry part of our programme. $H-K$ versus $J-H$ is displayed in the left panel, the right one shows $H-K$ versus $J-K$. For explanations of symbols and lines see Figure 1. The objects are identified with small labels at the symbols.

bad sky conditions and some technical problems. Additional overheads and further time loss due to weather are caused by the need to cross-calibrate the spectra in the three near-IR wavelength regions through JHK absolute photometry. The availability of dispersive optics covering more than one near-IR band at lower spectral resolution could have resulted in additional benefits and higher efficiency for our programme.

Data reduction: The basic data reduction products of the photometry are absolute broadband filter magnitudes in BVRI and JHK, filter colours and spectral gradients. As side results astrometric positions and a search for satellites around the prime targets are performed (so far without success). The magnitude (equivalent to sizes), colour and gradient data are correlated with each other and with orbital parameters to associate and explore taxonomic classes and their colour properties through statistical methods. This exercise is applied to our database alone and to an even larger dataset merging our results with those published in the literature. The spectra are reduced to relative reflectivity units that allow us to determine spectral gradients and to identify absorption features that may be indicative for the surface chemistry. Each spectrum covering a wider wavelength range is modelled through a Hapcke reflectance modelling code to constrain and, if possible, to quantify the surface chemistry of the targets. In a final phase of the project it is planned to correlate spectral properties with the photometric taxonomy of the objects.

Status of the programme: By the end of 2002, about 90 per cent of the

observations had been conducted and about 60 per cent of the data reduction and analysis phase is performed. Table 1 shows the number of objects observed per dynamical class (Cubewano, Plutino, SDO, Centaur) and observation type (BVRI and JHK photometry, visible and near-IR spectroscopy). Up to now, the photometry worked out as planned, while the spectroscopy suffered from time losses (as explained above). Since the object selection for SM observations had to be done months in advance, some of our targets have been observed by other groups in the meanwhile, and despite all efforts, duplication of observations turned out to be unavoidable. A few targets were selected on purpose for repetition of certain types of observations in order to allow cross-checks of our results with those of other observers and to address specific unsolved questions related with the objects. The most striking constraint causing duplication is the fact that the sample of near-IR targets accessible with standard instruments at modern 8–10-m class telescopes is rather limited (~ 30 objects up to now).

Highlights from the First Results

The results outlined in this summary are obtained from data collected during the first year of this ESO Large Programme. They are described in greater detail in various papers that are already published (Barucci et al., 2002, *A&A* 392; Boehnhardt et al. 2002, *A&A* 395) or will be published soon (Dotto et al., 2003, *Icarus*, in press; Lazzarin et al. 2003, *AJ*, in press). Another three papers with results from Period 69 are in preparation for submission to scientific journals in early 2003.

BVRI colour-colour-plots and spectral gradient histograms: The database used here contains 96 objects compiled from our programme (28) and from published data. The colour-colour-plots and photometric “reflectivity spectra” of the 28 objects measured by our programme in Period 67 are displayed in Figures 1 and 2, respectively. The colour-colour plots (Fig. 1) show that the objects follow – with some scatter – the lines of constant reddening in BVR colours, but they start deviating in the transition re-

Table 1. Physical studies of TNOs and Centaurs: Number of objects observed/reduced per dynamical class (status: end 2002).

Object class	BVRI	JHK	vis.spec.	IR spec.*
Cubewanos	25/15	7/4	1/1	0/0
Plutinos	19/10	7/4	5/4	4/3
Scattered Disk	13/7	6/5	3/2	3/2
Centaurs	9/7	6/5	6/6	5/4
Total	66/39	26/18	15/13	12/9

*About 30 % of the object spectra are incomplete, i.e. JHK bands are not fully covered.

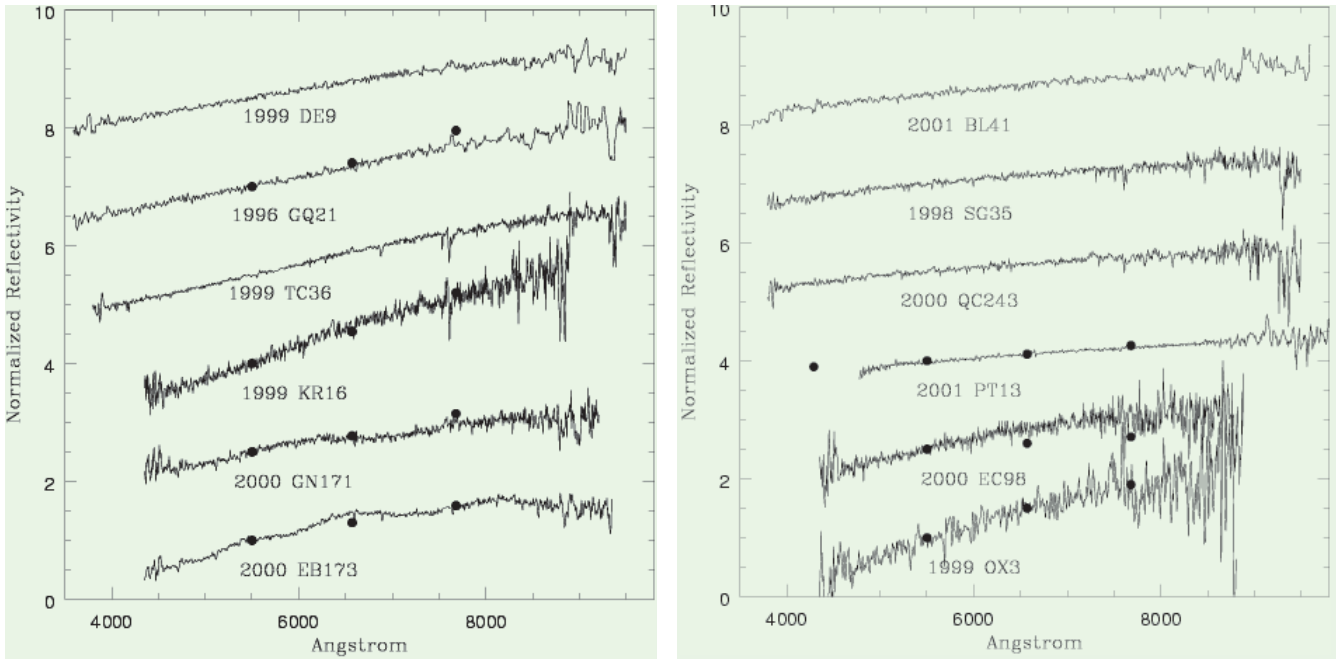


Figure 6: Visible Reflectivity spectra of TNOs and Centaurs. The spectra of TNOs are displayed in the left panel, those of Centaurs in the right one. The spectra are shifted in Y direction for clarity. The dots represent the respective results from quasi-simultaneous photometry of the objects taken during the spectroscopy runs.

gion to the near-IR. The latter is a consequence of the slope change seen in the spectra of red to very red objects beyond 750 nm. The reddening distribution seems to be continuous without a clear indication for a bi-modality as announced by other groups using smaller datasets. In the spectral gradient histogram of Figure 3 all 96 objects are used and sorted for each dynamical class in the same gradient bins of width corresponding to the averaged uncertainty of the data. With one exceptions (1994 ES₂) the spectral gradients of all objects fall between -5 and $55\%/100$ nm. Outliers in previous datasets turned out to be artefacts, most likely due to observations and data reduction (blends of background objects) or unusual object behaviour (for instance 1994 EV₃ shows rapid and large-amplitude variability that mimics unusual colours even in short-term photometric filter sequences as identified through our programme). The Cubewanos show a pronounced peak for spectral gradients between 25 and $45\%/100$ nm that is caused by a population of red objects in circular and low inclination orbits beyond 41 AU. At least for the Plutinos, and possibly also for Centaurs and SDOs, the distribution of spectral gradients in the visual wavelength region seems to be distinctly different from those of the Cubewanos.

Correlations with orbital parameters: In Figure 4 we show the measured photometric spectral gradients versus orbital excitation E , inclination and perihelion distance of the objects. The excitation parameter is defined as $E = (e^2 + \sin^2(i))^{1/2}$ with e and i as eccentricity and inclination of the orbit,

respectively. E is an estimate for the velocity of the object with respect to another one at the same distance, but in circular orbit in the Ecliptic, and it might thus be related to the collision velocity and/or the collision probability. The plots of the spectral gradients versus E and i suggest a correlation between surface colour and collision history of the objects, since the range of spectral gradients increases with increasing excitation parameter E and decreases with decreasing inclination. On the other side, the plot of the spectral gradients versus perihelion distance shows a clustering of very red Cubewanos in circular and Ecliptic orbits beyond ~ 41 AU. The peak for the Cubewanos in the spectral gradient statistics of Figure 3 is caused by exactly this group of objects. Moreover, for objects with perihelia between ~ 36 and 40 AU the width of the reddening range seems to increase the closer the object approaches the Sun. At present, these trends are not yet fully established since more objects need to be included for statistical reasons. However, if the trends can be confirmed, they would argue for different reddening scenarios, i.e. the trends with excitation and inclination for the balance between space weathering and collision resurfacing on one side and the trend with perihelion distance for the balance between space weathering and intrinsic activity on the other side. Most puzzling is the group of red Cubewanos beyond 41 AU and there is no easy explanation for their existence at present.

JHK colours: While at visible wavelengths a certain reddening range seems to be continuously populated, a

preference for neutral colours is found among the near-IR spectra of the objects – see Figure 5. Only 2 objects are definitely redder than the Sun. Whether the red objects are members of a second colour population can easily be questioned. The overall interpretation of the visible to near-IR colour range argues for only minor colour changes in the infrared part of the spectra, but for a significant and very wide absorption of variable depth for many TNOs and Centaurs in the visual wavelength range. This implies that the observed reddening in BVRI is in fact the long-wave wing of a wide absorption feature from a yet unknown chemistry that extends beyond the visible region well into the UV.

Visible spectra: The spectra of TNOs and Centaurs observed in the visible are mostly featureless and show constant (though different) slopes at wavelengths below ~ 750 nm (Fig. 6). At larger wavelength a continuous gradient change towards smaller slopes is observed in the red objects. With one exception (possibly caused by rotation effects in the photometry) the spectral gradients obtained from spectra are in good agreement with the photometric ones. It came as a surprise that wide absorption dips were found in the visible spectra of two Plutinos, 2000 EB₁₇₃ and 2000 GN₁₇₁, taken in April 2001 (see Fig. 7). The absorption features are centred around 600 and 730 nm for 2000 EB₁₇₃ and at 725 nm for 2000 GN₁₇₁. There are two very puzzling aspects with these detections: (1) The features were not confirmed with spectra taken about one year later (see Fig. 7); this would argue for a non-uni-

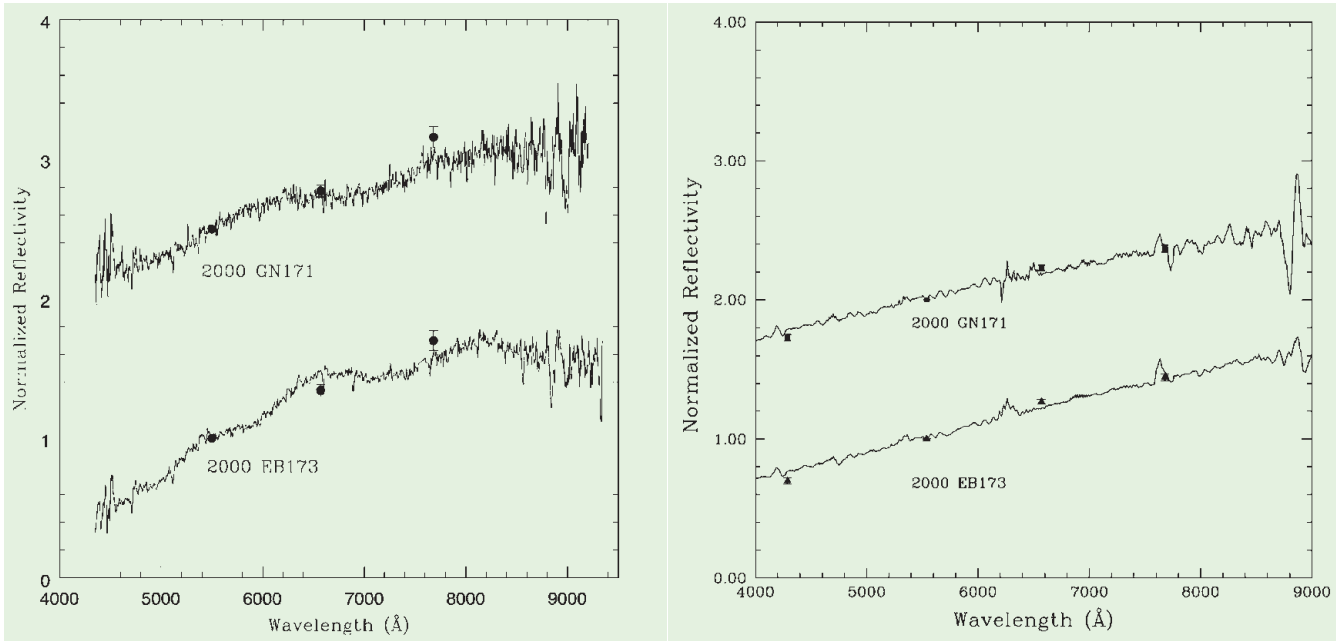


Figure 7: Two “puzzling” Plutinos: reflectivity spectra of 2000 EB₁₇₃ and 2000 GN₁₇₁. The reflectivity spectra of both objects show shallow and wide absorption features during one observing epoch (left panel), but a straight featureless slope during a second observing run about one year later (right panel). The dots and triangles in the panels indicate the corresponding ‘broadband’ reflectivity from quasi-simultaneous BVRI filter photometry of the objects.

form distribution of the absorbing material on the surface of the objects. (2) Features resembling the absorptions in these two Plutinos and identified in other solar system bodies and in lab experiments are produced by silicate material on asteroids that was exposed to long-term aqueous alteration on the surface. A similar scenario in the extremely cold and icy environment of the outer solar system obviously poses some problems. The answer to this puzzle calls for a systematic study of the objects by rotation-phase resolved spectroscopy, and, if confirmed, it will

have a great impact on our understanding of the physical nature of these bodies at the edge of the planetary system.

Near-IR spectra: We have found water ice absorption in H and K band spectra of 1 TNO and 3 Centaurs (see for instance the 2001 PT₁₃ spectrum in Figure 8). No features are seen in the spectra of other objects in our sample. For 2001 PT₁₃, a non-uniform water ice distribution on a large scale is concluded from the existence and absence of the absorption features in the spectra measured at two different epochs. The

model fits to the combined near-IR and visible spectra use a radiative transfer code with simple geographical mixtures of organics, minerals and ices. The steep slopes in the visible require the admixture of Tholins or kerogene in the model fits. Nevertheless, despite the decent match between the observed spectra and the radiative transfer model results, at present our conclusions are limited. On one hand, water ice seems to be present in

Conclusion and Outlook

these distant bodies; however, on the other hand, the identification of further surface materials as well as quantitative estimations are difficult because of the quality of the data fits and the existence of multiple model solutions for each spectrum.

The ESO Large Programme on the physical studies of TNOs and Centaurs is now approaching the end of its assigned period for the observations, and it is a little more than half way through the data reduction. The analysis of the results and model interpretation will certainly continue for another year beyond the official end of the observing programme.

With the data from this programme it has been possible to identify the first taxonomic group in the Edgeworth-Kuiper Belt, the cluster of red Cubewanos beyond 41 AU, and to get clear indications of resurfacing effects on TNOs and Centaurs. At the moment, the observed results appear to be somewhat contradictory to each other and a synoptic picture for their interpretations has not yet evolved. Water ice seems to be abundant in these objects; however, the identification of other surface ice features appears to be a difficult task. Spectra of two Plutinos may have provided the first glance of stony material, and if so, they contribute yet another puzzle with the potential to drastically change our view of these icy worlds in the outer solar system.

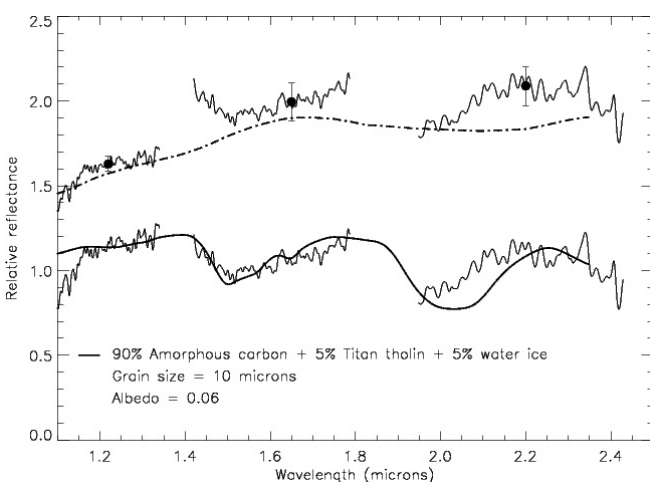


Figure 8: Near-IR spectrum of the Centaur 2001 PT₁₃. The plot shows the near-IR spectrum of the object on 10/9/2001 (upper spectrum) and on 8/10/2001 (lower spectrum). The continuous and broken lines show model fits to the observed spectra using the material mixture as indicated in the figure insert. The dots indicate the reflectivity from quasi-simultaneous broadband JHK photometry of the object.

The K20 Survey: New Light on Galaxy Formation and Evolution

A. CIMATTI¹, E. DADDI², M. MIGNOLI³, L. POZZETTI³, A. FONTANA⁴, T. BROADHURST⁵, F. POLI⁶, P. SARACCO⁷, A. RENZINI², G. ZAMORANI³, N. MENCI⁴, S. CRISTIANI⁸, S. D'ODORICO², E. GIALLONGO⁴, R. GILMOZZI², S. DI SEREGO ALIGHIERI¹, J. VERNET¹

¹INAF – Osservatorio Astrofisico di Arcetri, Italy; ²European Southern Observatory, Garching, Germany;

³INAF – Osservatorio Astronomico di Bologna, Italy; ⁴INAF – Osservatorio Astronomico di Roma, Italy;

⁵Racah Institute for Physics, The Hebrew University, Jerusalem, Israel; ⁶Dipartimento di Astronomia, Università

di Roma, Italy; ⁷INAF – Osservatorio Astronomico di Brera, Italy; ⁸INAF – Osservatorio Astronomico di Trieste, Italy

1. Introduction

Despite the recent extraordinary progress in observational cosmology and the successful convergence on a single cosmological model, the history of galaxy and structure formation and evolution remains still an open question. One of the most actively debated issues is how and when the present-day most massive galaxies (e.g. elliptical galaxies and bulges with $\mathcal{M}_{\text{stars}} > 10^{11} M_{\odot}$) built up and what type of evolution characterized their growth over the cosmic time. Addressing this question is important not only to test the different scenarios of galaxy formation, but also to understand how the general structures of the universe evolved.

There is wide consensus that galaxy formation takes place by a combination of dissipational collapse and merging of sub-units (e.g. White & Rees 1978). However, much less consensus presently exists on the main epoch (redshift) at which these events took place, and then when the bulk of the stellar mass of present-day galaxies was formed and assembled. Hierarchical merging models (HMMs) have so far favoured a rather late appearance of massive galaxies, thus only quite recently reaching their present mass, i.e., at $z < 1-1.5$ (e.g. Baugh et al. 2002). On the other hand, other scenarios and some observational evidence suggest that the bulk of star formation and galaxy assembly took place at substantial higher redshifts (see Cimatti 2003 for a recent review). Such scenarios make very different predictions depending on the formation epoch. If massive galaxies formed at $z > 2-3$ through a short-lived and intense starburst phenomenon followed by a passive and pure luminosity evolution (PLE), then old (a few Gyr) passively evolving massive systems should exist up to $z \sim 1-1.5$ with a number density identical to that observed in the local universe because their number does not change through cosmic time and the only evolution is the aging of the stellar population. On the other hand, if the most massive galaxies reach their final mass at $z < 1-1.5$, they should be

rare at $z \sim 1-1.5$, with a comoving density of $\mathcal{M}_{\text{stars}} > 10^{11} M_{\odot}$ galaxies decreasing by almost an order of magnitude from $z \sim 0$ to $z \sim 1$ (Baugh et al. 2002).

Although there is a general agreement on *cluster* ellipticals being a homogeneous population of old and passive systems formed at high redshifts (see Renzini 1999 and Peebles 2002 for recent reviews), the question of *field* spheroids is still controversial. Several observations were performed over recent years in order to test the two competing models. However, although it is established that old, passive and massive systems exist in the field out to $z \sim 1.5$, there is not yet agreement on how their number and evolutionary properties compare with the model predictions.

2. The K20 Survey

A solid and unbiased approach to investigate the evolution of massive

galaxies is to study samples of field galaxies selected in the K-band (i.e. at $2.2 \mu\text{m}$; Broadhurst et al. 1992; Kauffmann & Charlot 1998). This has two main advantages. Firstly, since the rest-frame optical and near-IR light is a good tracer of the galaxy *stellar* mass (Gavazzi et al. 1996), K-band surveys select galaxies according to their mass up to $z \sim 2$. Secondly, the similarity of the spectral shapes of different galaxy types in the rest-frame optical/near-IR makes the K-band selection free from strong biases against or in favour of particular classes of galaxies. In contrast, the selection of high- z galaxies in the observed optical bands is sensitive to the star-formation activity rather than to the stellar mass because it samples the rest-frame UV light and makes optical samples biased against old passive galaxies.

Motivated by the above open questions and by the availability of the ESO VLT telescopes, we started an ESO VLT Large Programme (dubbed “K20

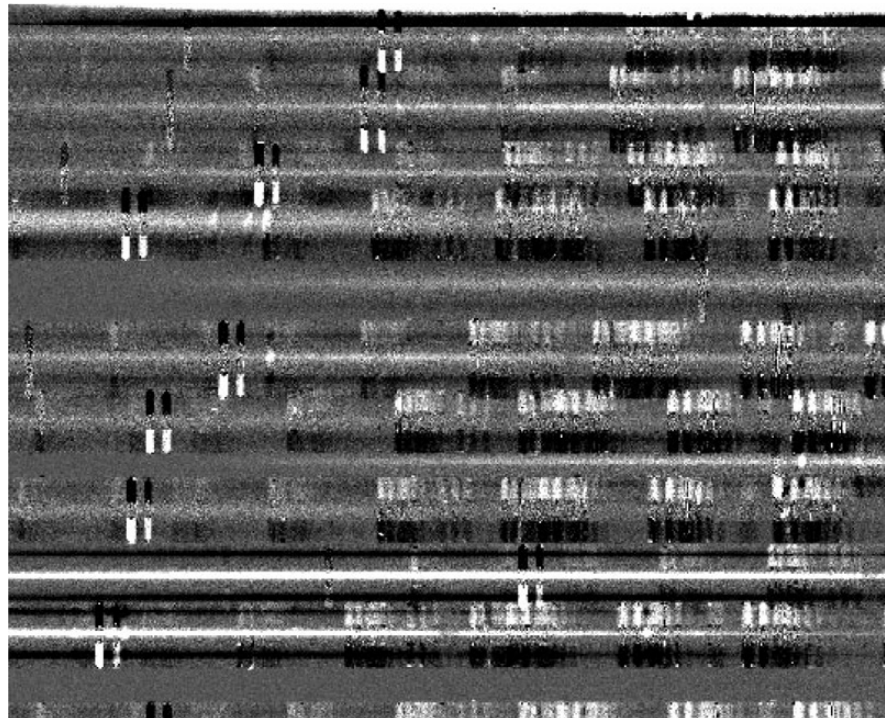


Figure 1: Zoom on two-dimensional sky-subtracted spectra of faint galaxies present in a section of one of the FORS2 MXU masks used for the “dithered” observations.

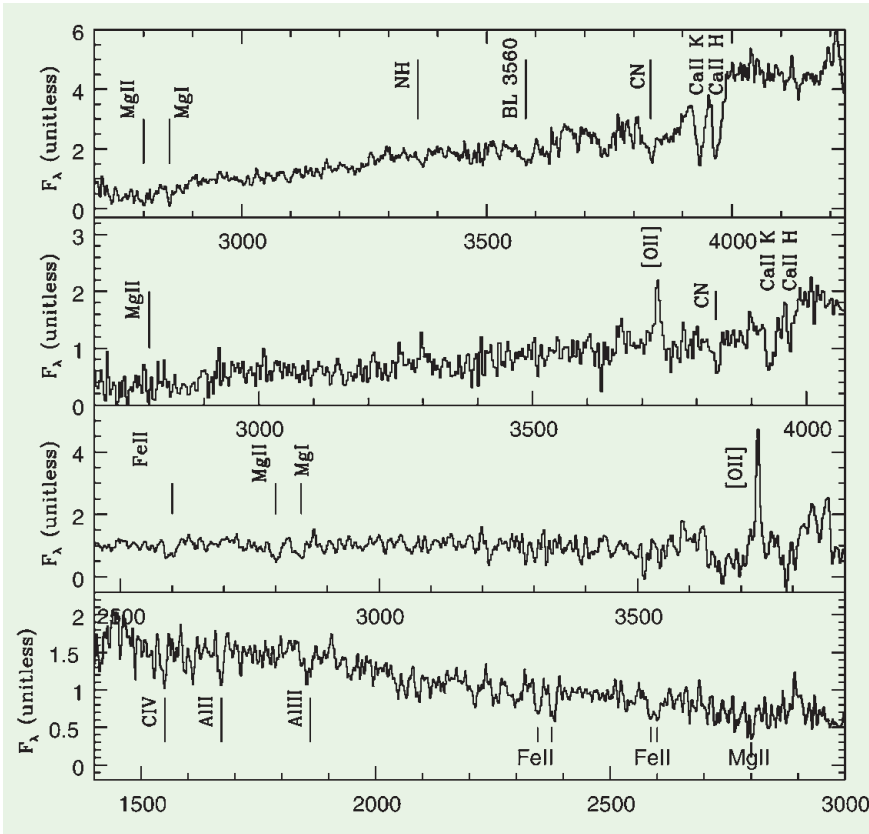


Figure 2: Examples of FORS2 spectra of high- z galaxies with the four adopted spectral classifications. From top to bottom: an early-type at $z = 1.096$ ($R = 23.0$), an early-type + $[\text{OII}]\lambda 3727$ emission at $z = 0.735$ ($R = 23$), an emission line galaxy at $z = 1.367$ ($R = 23.0$), an absorption line galaxy at $z = 1.725$ ($R = 23.5$).

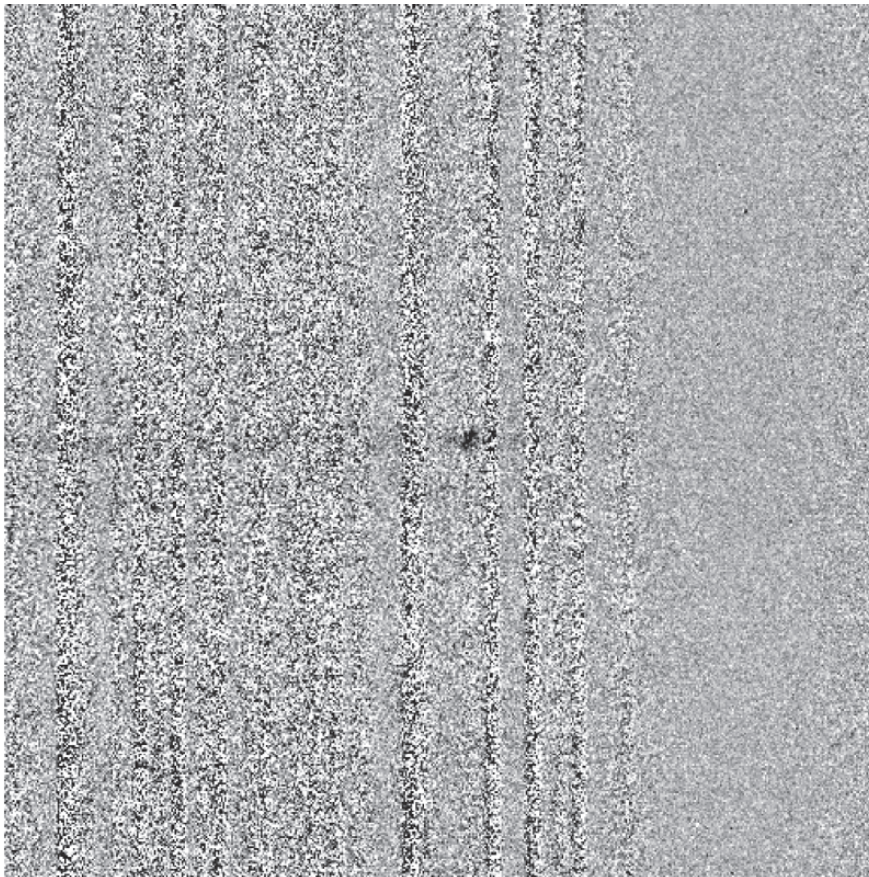


Figure 3: ISAAC two-dimensional sky-subtracted H-band low-resolution spectrum of a galaxy at $z = 1.73$ (the emission line is $H\alpha$).

survey”) based on 17 nights distributed over two years (1999–2000) (see <http://www.arcetri.astro.it/~k20/> and Cimatti et al. 2002c). The prime aim of this survey was to derive the spectroscopic redshift distribution and the spectral properties of 546 K_s -selected objects with the *only* selection criterion being $K_s < 20$ (Vega scale). Such a threshold is critical because it selects galaxies over a broad range of masses, i.e. $\mathcal{M}_{\text{stars}} > 10^{10} M_{\odot}$ and $\mathcal{M}_{\text{stars}} > 4 \times 10^{10} M_{\odot}$ for $z = 0.5$ and $z = 1$ respectively. The targets were selected from K_s -band images (ESO NTT+SOFI) of two independent fields covering a total area of 52 arcmin²: a 32.2 arcmin² sub-area of the Chandra Deep Field South (CDFs; Giacconi et al. 2001), and a 19.8 arcmin² field centred around the QSO 0055-269 at $z = 3.6$. Extensive simulations showed that the sample is photometrically highly complete to $K_s = 20.0$ and not affected by strong selection effects on the galaxy populations, with the exception of an underestimate of ~ 0.2 magnitudes for the luminous galaxies (Cimatti et al. 2002c). $H_0 = 70 \text{ km s}^{-1} \text{ Mpc}^{-1}$, $\Omega_m = 0.3$ and $\Omega_{\Lambda} = 0.7$ are adopted throughout this article.

3. The VLT Observations: Optimizing Spectroscopy for Faint Red Galaxies

The most crucial probes of massive galaxy evolution are galaxies with the very red colours expected for passively evolving systems at $z > 1$ (e.g. $R - K_s > 5$). For $K_s < 20$, such red colours imply very faint optical magnitudes ($R \sim 24\text{--}26$), close to the spectroscopic limits of 8-m-class telescopes. Moreover, the most prominent spectral features (e.g. the 4000 Å break and H&K absorptions) fall in the very red part of the observed spectra for $1 < z < 2$ ($\lambda_{\text{obs}} > 8000 \text{ Å}$), where the strong OH sky lines and the CCD fringing (very strong in FORS2 before its recent upgrade of March 2002 with new red-optimized MIT CCD mosaic) make the spectroscopy of faint $z > 1$ galaxies extremely challenging.

For such reasons, the spectroscopy was optimized to reach the highest possible signal-to-noise ratio in the red by applying the innovative technique of “dithering” the targets along the slits every 15–20 minutes between two (or more) fixed positions. Such a method (routinely used in the near-IR) has the crucial advantage of efficiently subtracting both the CCD fringing and the OH sky lines. A similar method can also be performed with the so-called “nod and shuffle” technique by nodding the telescope rapidly between targets and adjacent sky positions and recording object and sky spectra on adjacent regions of a low-noise CCD through charge shuffling. At the time of the observations, no automatic templates

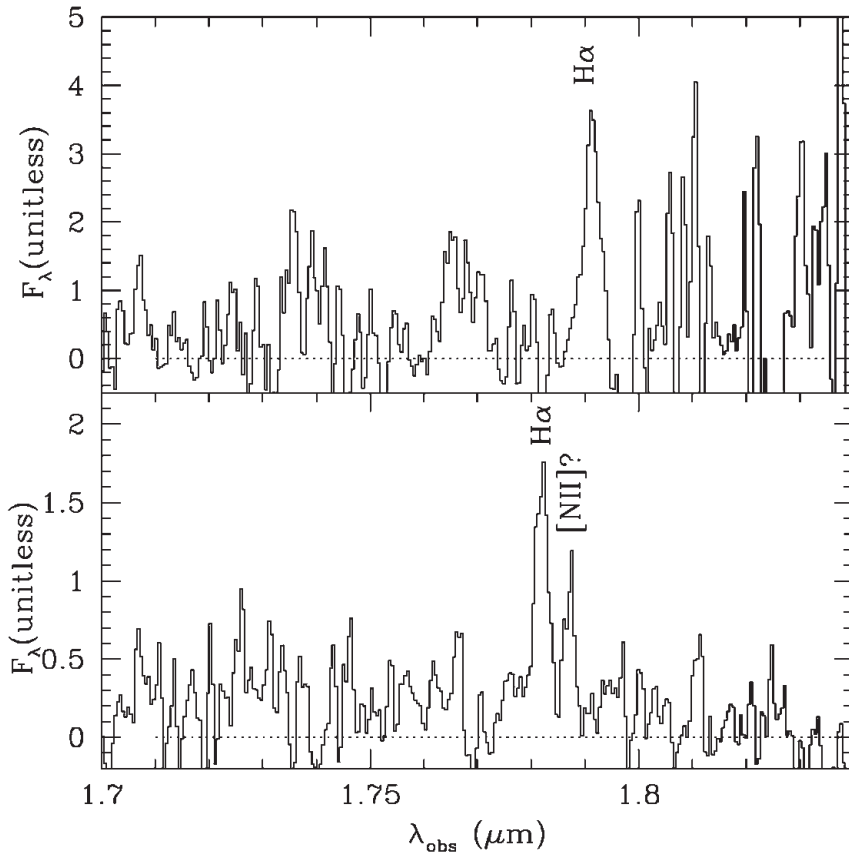


Figure 4: ISAAC H-band low resolution spectra of two emission-line galaxies with $H\alpha$ redshifted at $z = 1.729$ (top panel) and $z = 1.715$ (bottom panel).

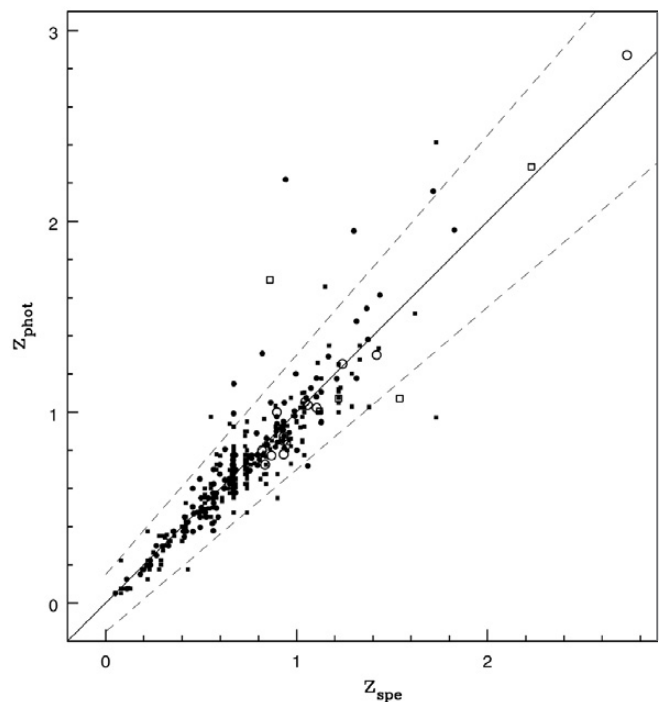
were available to perform dithered observations with FORS2, but we succeeded in applying this technique by moving the telescope “manually” from one position to another thanks to the kind help of the support astronomers. Our approach proved to be very successful in achieving high-quality spectra extended to the far red (Fig. 1) and reaching a spectroscopic redshift completeness for the high- z red galaxies much higher than in previous surveys.

Optical multi-object spectroscopy was obtained with the ESO VLT UT1 and UT2 equipped respectively with FORS1 (with the MOS mode: 19 movable slitlets) and FORS2 (with the Mask Exchange Unit, MXU, mode). The MXU mode uses laser-cut slit masks prepared by the mask manufacturing unit (MMU), and allowed us to observe up to 52 targets per mask with slit lengths of $8''$ – $15''$ (a “record” for the multiplex in the pre-VIMOS era!). The seeing and the slit widths were in the range of $0.5''$ – $2.0''$ and $0.7''$ – $1.2''$ respectively. The integration times ranged from 0.5 to 3 hours. Figure 2 shows some typical spectra.

A fraction of the sample was also observed with near-IR spectroscopy using VLT UT1 + ISAAC in low-resolution mode with a $1''$ slit, 1–3 hours integration times, 1–2 targets per slit, in order to attempt to derive the redshifts of the galaxies which were too faint for optical

spectroscopy and/or expected to be in a redshift range without strong features in the observed spectral range (e.g. $1.4 < z < 2.0$). However, the absence of a multiobject spectroscopic mode, each integration being limited to a single spectral band, and the lack of very accurate photometric redshifts at the time of the observations made it difficult to derive a substantial number of spectroscopic redshifts based on near-IR spectroscopy alone. Overall, redshifts were de-

Figure 5: The comparison between spectroscopic (x -axis) and photometric (y -axis) redshifts of the galaxies in the K20 survey. Filled circles, filled squares and open symbols indicate the 0055-269 field, the CDFS and the “lower quality” spectroscopic redshifts respectively.



rived for four galaxies at $1.3 < z < 1.9$ out of the 22 observed (Figs. 3–4).

In addition to spectroscopy, $UBVR I z J K_s$ imaging from NTT and VLT observations was also available for both fields, thus providing the possibility to estimate photometric redshifts for all the objects in the K20 sample, to optimize them through a comparison with the spectroscopic redshifts and to assign reliable photometric redshifts to the objects for which it was not possible to derive the spectroscopic redshift. The dispersion on the global sample (CDFS + 0055-269 fields) is $\sigma = 0.089$ and the average is $\langle z_{\text{spe}} - z_{\text{phot}} \rangle = 0.012$ (Fig. 5). Such an accuracy is at the level of the “state-of-the-art” photometric redshifts obtained in the *Hubble Deep Fields*. The final sample covers a redshift range of $0 < z < 2.5$ and the overall spectroscopic redshift completeness is 94%, 92%, 87% for $K_s < 19.0, 19.5, 20.0$ respectively. The overall redshift completeness (spectroscopic and photometric) is 98%.

The K20 survey represents a significant improvement with respect to previous surveys for faint K -selected galaxies (e.g. Cowie et al. 1996; Cohen et al. 1999), thanks to its high spectroscopic redshift completeness, the larger sample, the coverage of two fields (thus reducing the cosmic variance effects), and the availability of optimized photometric redshifts.

4. The Redshift Distribution: Testing Galaxy-Formation Models

The observed differential and cumulative redshift distributions for the K20 sample are presented in Fig. 6 (see Cimatti et al. 2002b), together with the

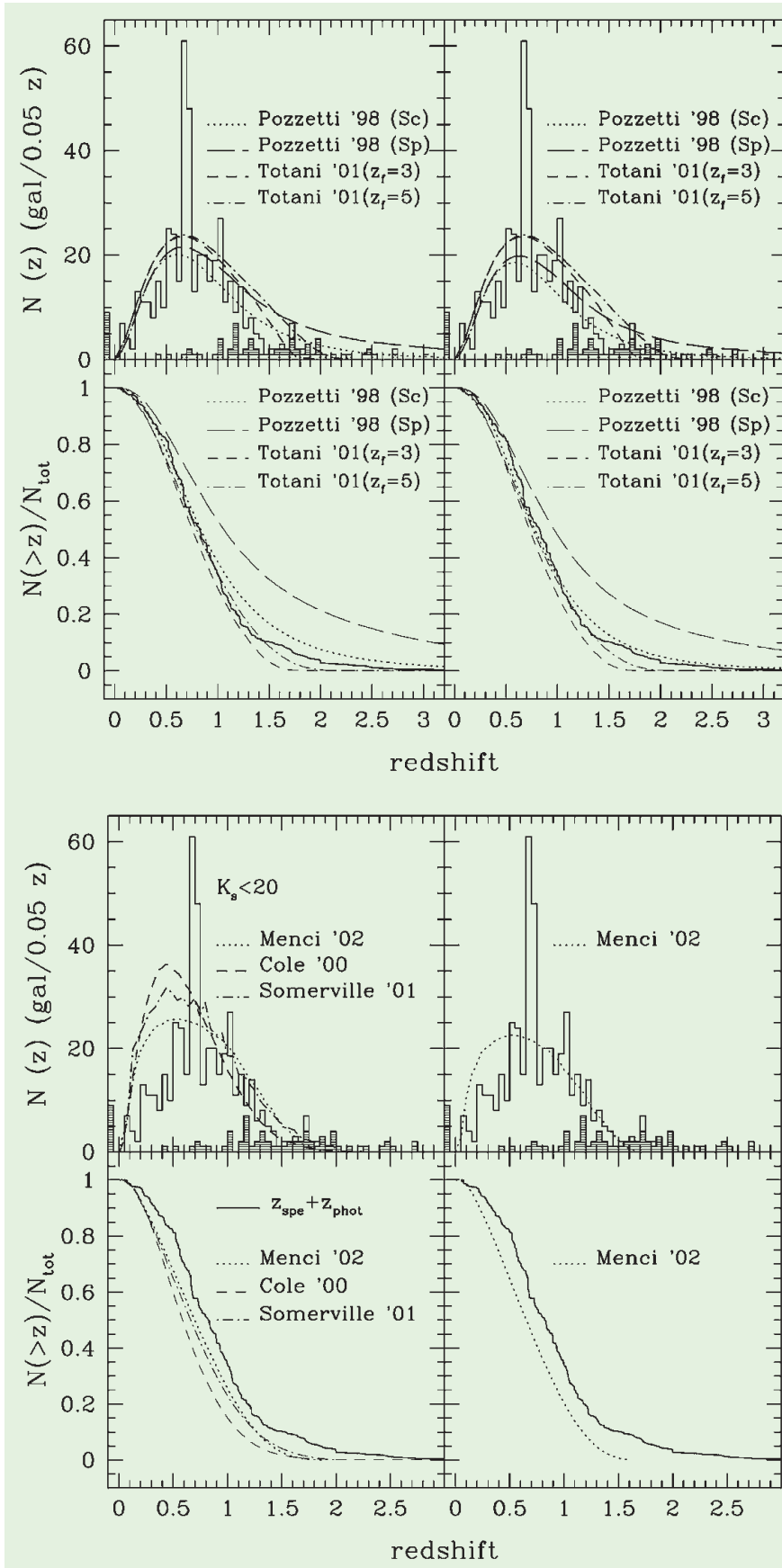


Figure 6a: Top panels: the observed differential $N(z)$ for $K_s < 20$ (histogram) compared with the PLE model predictions. Bottom panels: the observed fractional cumulative redshift distribution (continuous line) compared with the same models. The shaded histogram shows the contribution of photometric redshifts. The bin at $z < 0$ indicates the 9 objects without redshift. The left and right panels show the models without and with the inclusion of the photometric selection effects respectively. Sc and Sp indicate Scalo and Salpeter IMFs respectively. Figure 6b: Same as Fig. 6a, but compared with the HMM predictions. Right panels: the M02 model with the inclusion of the photometric selection effects.

predictions of different scenarios of galaxy formation and evolution, including hierarchical merging models (HMMs) from Menci et al. (2002, M02), Cole et al. (2000, C00), Somerville et al. (2001, S01), and pure luminosity evolution models (PLE) based on Pozzetti et al. (1996, PPLE) and Totani et al. (2001, TPLE). No best tuning of the models was attempted in this comparison, thus allowing an unbiased *blind* test with the K20 observational data. The predicted $N(z)$ from the models are normalized to the K20 survey sky area.

The observed redshift distribution can be retrieved from <http://www.arcetri.astro.it/k20>. The spike at $z \sim 0.7$ is due to two galaxy clusters (or rich groups) at $z = 0.67$ and $z = 0.73$. The median redshift of $N(z)$ is $z_{med} = 0.737$ and $z_{med} = 0.805$, respectively with and without the two clusters being included. The contribution of objects with only a photometric redshift becomes relevant only for $z > 1.5$.

Figure 6a shows fairly good agreement between the observed $N(z)$ distribution and the PLE models (with the exception of PPLE with Salpeter IMF), although such models slightly overpredict the number of galaxies at $z > 1.2$. However, if the photometric selection effects present in the K20 survey (Cimatti et al. 2002c) are taken into account, the PLE models become much closer to the observed $N(z)$ thanks to the decrease of the predicted high- z tail.

In contrast, all the HMMs underpredict the median redshift, overpredict the total number of galaxies with $K_s < 20$ by factors up to $\sim 50\%$ as well as the number of galaxies at $z < 0.5$, and underpredict the fractions of $z > 1-1.5$ galaxies by factors of 2-4 (Fig. 6b). The inclusion of the photometric selection effects (Cimatti et al. 2002c) exacerbates this discrepancy, as shown in Figure 6b (right panels) for the M02 model (the discrepancy for the C00 and S01 models becomes even larger). The deficit of high- z objects in HMMs is well illustrated by Figure 7, where the PPLE model reproduces the cumulative *number* distribution of galaxies at $1 < z < 3$ within $1-2 \sigma$, whereas the M02 model is discrepant at $\geq 3\sigma$ level (up to $> 5\sigma$ for $1.5 < z < 2.5$). This conclusion does not strongly depend on the objects with only photometric redshifts: the 7 galaxies with spectroscopic redshift $z > 1.6$ are already discrepant with the predictions by HMMs of basically no galaxies with $K_s < 20$ and $z > 1.6$.

5. The Luminosity Function and Luminosity Density Evolution

The evolution of galaxies can be investigated through the variation of their number density and luminosity (i.e. the

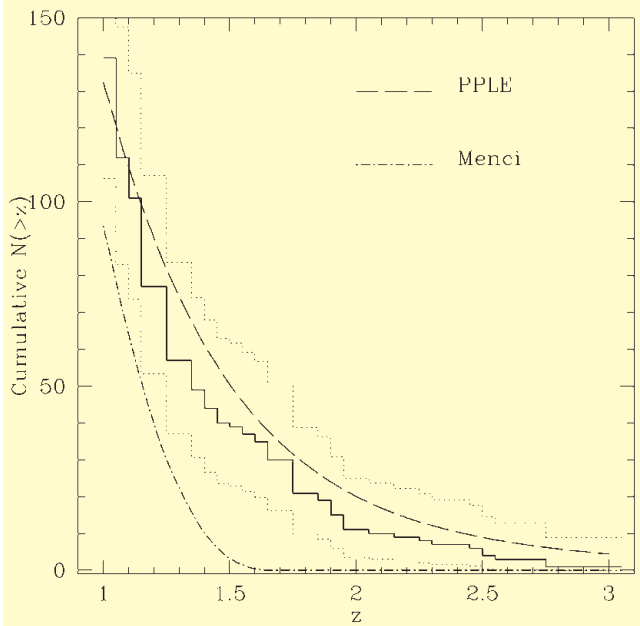
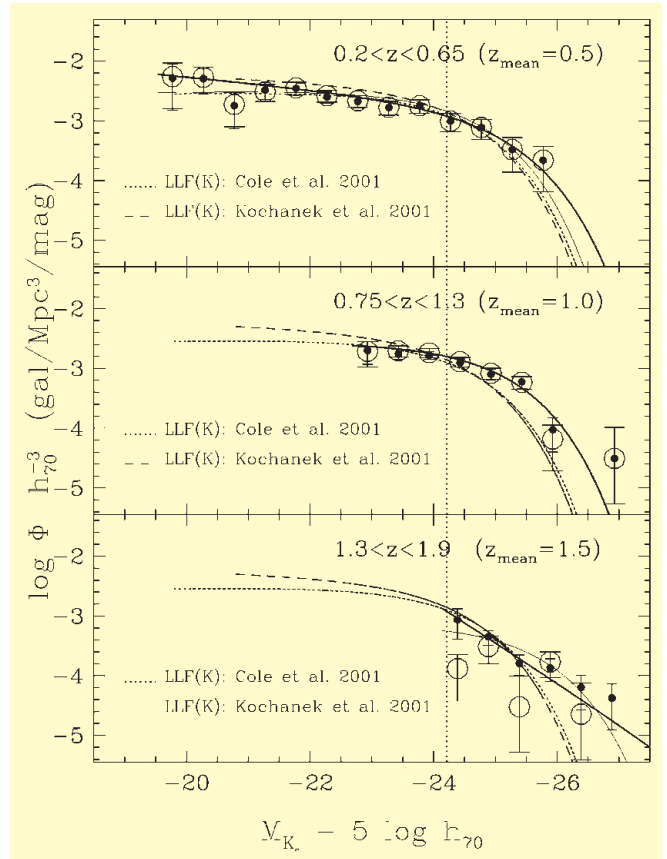


Figure 7: The observed cumulative number of galaxies between $1 < z < 3$ (continuous line) and the corresponding poissonian $\pm 3\sigma$ confidence region (dotted lines). The PPLE (Scalo IMF) and the M02 models are corrected for the photometric biases.

Figure 8: The rest-frame K_s -band Luminosity Function in three redshift bins. Solid curves: the Schechter fits. Dotted curve: the local K_s -band LF of Cole et al. (2001). Open circles: spectroscopic redshifts, filled circles: spectroscopic + photometric redshifts. ►



luminosity function, LF) over the cosmic time.

The LF of the K20 galaxies has been estimated in the rest-frame K_s -band and in three redshift bins ($z_{\text{mean}} = 0.5, 1.0, 1.5$) in order to trace its evolution (Pozzetti et al. 2003). A comparison with the local universe K_s -band LF of Cole et al. (2001) shows a mild luminosity evolution of LF(z) out to $z = 1$, i.e. the LF shifts along the X-axis as a function of z without an appreciable change in the number density (Y-axis). The brightening is approximately -0.5 magnitudes from $z = 0$ to $z = 1$ (Fig. 8).

The size and completeness of the K20 sample allowed us also to study the LF evolution by galaxy spectral or colour types, and showed that red early-type galaxies dominate the bright end of the LF already at $z \sim 1$, and that their number density shows only a small decrease from $z \sim 0$ to $z \sim 1$ (Pozzetti et al. 2003).

The PLE models describe reasonably well the shape and the evolution of the observed luminosity function up to at least $z_{\text{mean}} = 1.0$, with no evidence for a strong decline in the abundance of the most luminous systems (with $L > L^*$) (Fig. 9b). Hierarchical merging models overpredict faint sub- L^* galaxies at $0 < z < 1.3$, and underpredict the density of luminous ($M_{K_s} < -25.5 + 5 \log h_{70}$) galaxies at the bright end of the LF (Fig. 9a). A comparison between the $R - K_s$ colours and luminosity distributions of K20 galaxies with $0.75 < z < 1.3$ (a bin dominated by spectroscopic red-

shifts) to the predictions of the GIF¹ simulations (Kauffmann et al. 1999) highlights a discrepancy between the two distributions: real luminous galaxies with $M_K - 5 \log h_{70} < -24.5$ in the K20 sample have a median colour of $R - K_s \sim 5$, whereas the GIF simulated galaxies have $R - K_s \sim 4$, with a small overlap of two colour distributions (Fig. 10). This is probably due to an underestimate of $\mathcal{M}_{\text{stars}}/L$ and of the number density of massive galaxies at $z \sim 1$ by the HMMs.

An additional way to investigate galaxy evolution is to trace the integrated cosmic emission history of galaxies at different wavelengths through the study of the luminosity density ρ_λ ($\text{W Hz}^{-1} \text{Mpc}^{-3}$). Such an approach is independent of the details of galaxy evolution and depends mainly on the star-formation history of the universe. Attempts to reconstruct the cosmic evolution of ρ_λ were made previously mainly in the UV and optical bands, i.e. focusing on the star-formation history of galaxies. Our survey offered for the first time the possibility to investigate in the near-IR, thus providing new clues on the global evolution of the stellar mass density (Pozzetti et al. 2003). The results show an evolution of $\rho_\lambda(z) = \rho_\lambda(z=0)(1+z)^{0.37}$, much slower than the one derived in the UV-optical, typically $\propto (1+z)^{3-4}$. Such a slow evolution suggests that the stellar mass density should also evolve slowly at least up to $z \sim 1.3$ (see also Dickinson et al. 2003).

¹<http://www.mpa.garching.mpg.de/GIF/>

The estimate of the stellar mass function and its cosmic evolution is under way and will provide additional constraints on the evolution of massive systems (Fontana et al. 2003, in preparation).

6. Extremely Red Objects (EROs)

As discussed in previous sections, Extremely Red Objects (EROs, i.e. galaxies with $R - K > 5$) are very important because they allow us to select old passively evolving galaxies at $z > 1$. Thanks to our deep red-optimized VLT optical spectroscopy, for a fraction of EROs (70% to $K_s < 19.2$) present in the K20 sample it was possible to derive a spectroscopic redshift and a spectral classification (Cimatti et al. 2002a), thus, for the first time, allowing us to verify if the ERO population is indeed dominated by old passive galaxies. The VLT optical spectra show that two classes of galaxies at $z \sim 1$ contribute nearly equally to the ERO population: the expected old stellar systems, but also a substantial fraction of dusty star-forming galaxies (Fig. 11).

The colours and spectral properties of old EROs are consistent with ≥ 3 Gyr old passively evolving stellar populations (assuming solar metallicity and Salpeter IMF), requiring a formation redshift $z_f > 2.4$ (Fig. 12). The number density is $6.3 \pm 1.8 \times 10^{-4} \text{ h}^3 \text{Mpc}^{-3}$ for $K_s < 19.2$, consistent with the expectations of PLE models for passively evolving early-type galaxies with similar

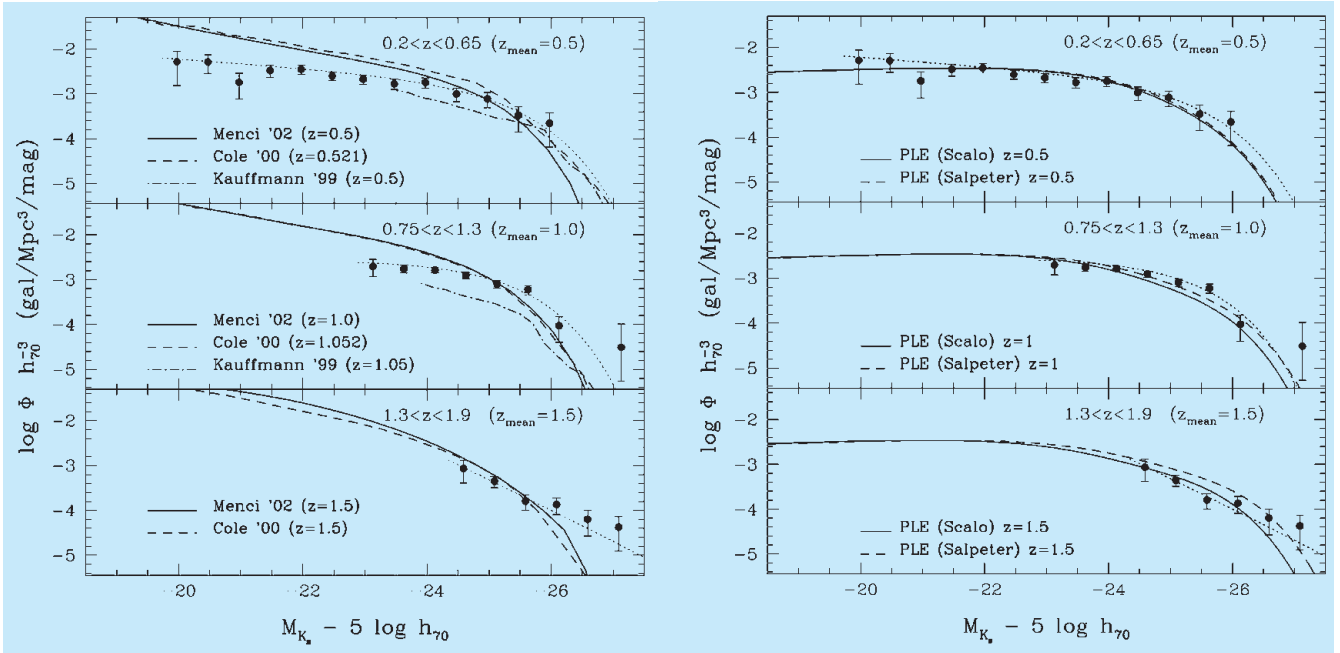


Figure 9a: The K_s -band LF compared to hierarchical merging model predictions. Figure 9b: The K_s -band LF compared to PLE model predictions.

formation redshifts (Cimatti et al. 2002a). HMMs underpredict such old red galaxies at $z \sim 1$ by factors of ~ 3 (Kauffmann et al. 1999) and ~ 5 (Cole et al. 2000).

The spectra of star-forming EROs suggest a dust reddening of $E(B - V) \sim 0.5-1$ (Fig. 12, adopting the Calzetti extinction law), implying typical star-formation rates of $50-150 M_{\odot} \text{yr}^{-1}$, and a significant contribution ($> 20-30\%$) to the cosmic star-formation density at $z \sim 1$. Such dusty star-forming systems are also underpredicted by HMMs. For instance, the GIF simulations predict a comoving density of red galaxies with $SFR > 50 M_{\odot} \text{yr}^{-1}$ that is ~ 30 times lower than the observed density of dusty EROs.

Taking advantage of the spectroscopic redshift information for the two ERO classes, we compared the relative 3D clustering in real space (Daddi et al. 2002). The comoving correlation lengths of dusty and old EROs are constrained to be $r_0 < 2.5$ and $5.5 < r_0 < 16 h^{-1} \text{Mpc}$ comoving respectively, implying that old EROs are the main source of the ERO strong angular clustering. It is important to notice that the strong clustering measured for the old EROs is in agreement with the predictions of hierarchical merging (Kauffmann et al. 1999).

7. Summary and Outlook

The high level of redshift completeness of the K20 survey and the results presented in previous sections provide new implications for a better understanding of the evolution of “mass-selected” field galaxies.

Overall, the results of the K20 survey show that galaxies selected in the

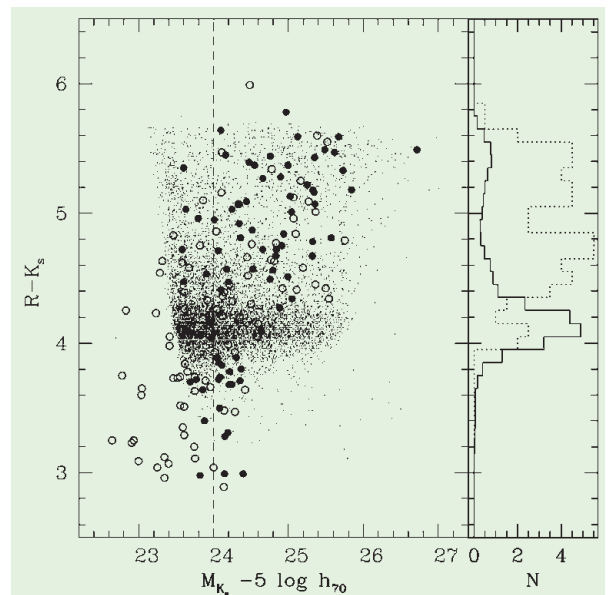
K_s -band are characterized by little evolution up to $z \sim 1$, and that the observed properties can be successfully described by a PLE scenario. In contrast, HMMs fail in reproducing the observations because they predict a sort of “delayed” scenario in which the assembly of massive galaxies occurs later than actually observed. However, it is important to stress here that the above results do not necessarily mean that the whole framework of hierarchical merging of CDM halos is under discussion. For instance, the strong clustering of old EROs and the clustering evolution of the K20 galaxies (irrespective of colours) seem to be fully consistent with the predictions of CDM models of large-scale structure evolution (Daddi et al. 2003 in preparation).

It is also important to stress that the K20 survey allows us to perform tests

which are sensitive to the evolutionary “modes” of galaxies rather than to their formation mechanism. This means that merging, as the main galaxy formation mechanism, is not ruled out by the present observations. Also, it should be noted that PLE models are not a physical alternative to the HMMs, but rather tools useful to parameterize the evolution of galaxies under three main assumptions: high formation redshift, conservation of number density through cosmic times, and passive and luminosity evolution of the stellar populations.

Thus, if we still accept the Λ CDM scenario of hierarchical merging of dark matter halos as the *basic framework* for structure and galaxy formation, the observed discrepancies highlighted by the K20 survey may be ascribed to how the baryon assembly, the star-formation

Figure 10: Left panel: $R - K_s$ colours vs. rest-frame absolute K_s magnitudes for $z = 1.05$ GIF simulated catalogue (small dots) and data (circles) at $0.75 < z < 1.3$ ($z_{\text{mean}} = 1$) (empty and filled circles refer to $z < 1$ and $z > 1$ respectively). Vertical dashed line represents approximately the completeness magnitude limit of GIF catalogue corresponding to its mass limit (see text). Right panel: Colour distribution of luminous galaxies ($M_{K_s} - 5 \log h_{70} < -24.5$) observed (dotted line) and simulated (continuous line), normalized to the same comoving volume.



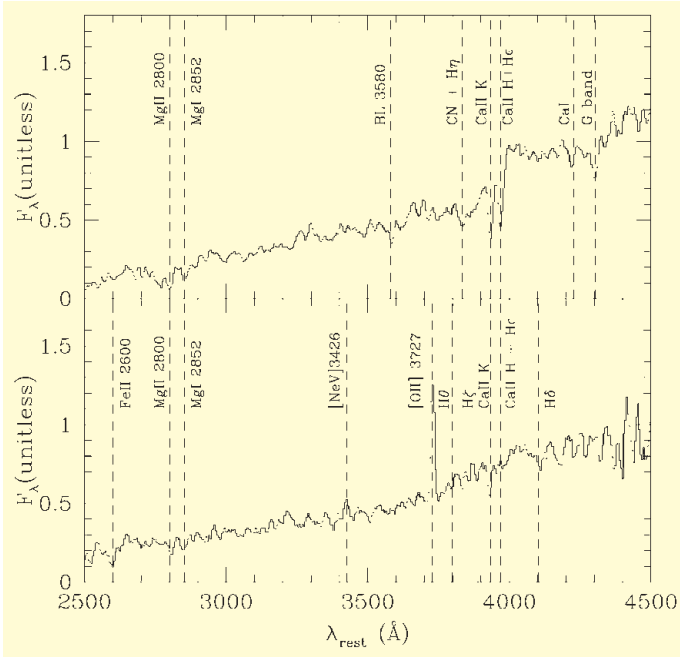


Figure 11: The average rest-frame spectra of old passively evolving (top; $z_{\text{mean}} = 1.000$) and dusty star-forming EROs (bottom; $z_{\text{mean}} = 1.096$) with $K_s \leq 20$ (Cimatti et al. 2002a).

References

- Baugh C.M. et al. 2002, in proceedings 'The Mass of Galaxies at Low and High Redshift', Venice 2001, eds. R. Bender, A. Renzini, astro-ph/0203051.
- Broadhurst, T., Ellis, R.S., & Graebrook, K. 1992, *Nature*, **355**, 55.
- Cimatti A., Daddi E., Mignoli M. et al. 2002a, *A&A*, **381**, L68.
- Cimatti A., Pozzetti L., Mignoli M., et al. 2002b, *A&A*, **391**, L1.
- Cimatti A., Mignoli M., Daddi E. et al. 2002c, *A&A*, **392**, 395.
- Cohen J.G., Blandford R., Hogg D.W. et al. 1999, *ApJ*, **512**, 30.
- Cole S., Lacey C.G., Baugh C.M. & Frenk C.S. 2000, *MNRAS*, **319**, 168.
- Cole S., Norberg P., Baugh C.M. et al. 2001, *MNRAS*, **326**, 255.
- Cowie, L.L., Songaila A., Hu E.M. & Cohen J.G. 1996, *AJ*, **112**, 839.
- Daddi E., Cimatti A., Broadhurst T. et al. 2002, *A&A*, **384**, L1.
- Dickinson M., Papovich C., Ferguson H.C., Budavari T. 2003, *ApJ*, in press, astro-ph/0212242.
- Gavazzi G., Pierini D. & Boselli A. 1996, *A&A*, **312**, 397.
- Giacconi R., Rosati P., Tozzi P. et al. 2001, *ApJ*, **551**, 624.
- Kauffmann G., Charlot S. 1998, *MNRAS*, **297**, L23.
- Kauffmann G. et al. 1999, *MNRAS*, **303**, 188.
- Menci N., Cavaliere A., Fontana A., Giallongo E. & Poli F. 2002, *ApJ*, **575**, 18.
- Peebles P.J.E. 2002, astro-ph/0201015.
- Pozzetti L. Bruzual A.G. & Zamorani, G. 1996, *MNRAS*, **281**, 953.
- Pozzetti L. et al. 2003, *A&A*, in press.
- Renzini A. 1999, in *The Formation of Galactic Bulges*, ed. C.M. Carollo, H.C. Ferguson, & R.F.G. Wyse (Cambridge: CUP), p. 9.
- Somerville R.S., Primack J.R. & Faber S.M. 2001, *MNRAS*, **320**, 504.
- Totani T., Yoshii Y., Maihara T., Iwamuro F. & Motohara K. 2001, *ApJ*, **559**, 592.
- White S.D.M., Rees M.J. 1978, *MNRAS*, **183**, 341.

processes and their feedback are treated by HMMs both within individual galaxies and in their environment. Our results suggest that HMMs should have galaxy formation in a CDM-dominated universe that closely mimics the old-fashioned monolithic collapse scenario. This requires enhanced merging and star formation in massive halos at high redshift (say, $z > 2-3$), and also suppressed star formation in low-mass halos.

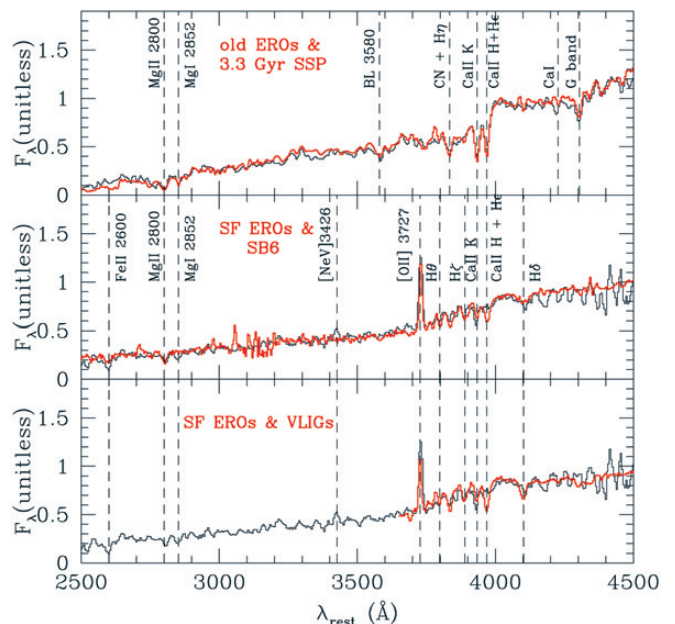
In summary, the redshift distribution of $K_s < 20$ galaxies, together with the space density, nature, and clustering properties of the ERO population, and the redshift evolution of the rest-frame near-IR luminosity function and luminosity density provide a new invaluable set of observables on the galaxy population in the $z \sim 1-2$ universe, thus bridging the properties of $z \sim 0$ galaxies with those of Lyman-break and sub-mm/mm-selected galaxies at $z \geq 2-3$. This set of observables poses a new challenge for theoretical models to properly reproduce.

The K20 survey is triggering several studies in which our team is actively involved. Ultradeep spectroscopy was obtained in November 2002 with FORS2 (MXU mode and with the new red-optimized MIT CCD mosaic) in order to derive the redshifts and the nature of the previously unidentified EROs, to increase the spectroscopic redshift completeness of the whole K20 sample, and to study (with higher resolution spectroscopy) the kinematics of $z > 1$ galaxies in order to estimate their dynamical masses. Since the sub-area of the CDFS observed in the K20 survey is also a target of the HST+ACS GOODS Treasury Programme (PI M. Giavalisco), and of the SIRTf GOODS (PI M. Dickinson) and SWIRE (PI C.

Lonsdale) Legacy Programmes, the K20 database, complemented by such additional observations, will allow us to derive new constraints on the formation and evolution of galaxies out to higher redshifts.

We thank the VLT support astronomers for their competent assistance during the observations. AC warmly thanks ESO (Garching) for the hospitality during his visits, and Jim Peebles and Mark Dickinson for useful and stimulating discussions. We also thank Piero Rosati and Mario Nonino for providing the reduced and calibrated *BVRI*/FORs1 images of the CDFS, and C. Baugh, R. Somerville and T. Totani for providing their model predictions.

Figure 12: The average spectra of EROs (black) compared to template spectra (red) of Bruzual & Charlot simple stellar population (top panel), and of dusty starbursts (Kinney et al. 1996, middle panel; Poggianti & Wu 2000, bottom panel).



Tracing the Formation and Evolution of Clusters and their Central Massive Galaxies to $z > 4$: a Progress Report

B. VENEMANS¹, G. MILEY¹, J. KURK¹, H. RÖTTGERING¹, L. PENTERICCI²

¹Leiden Observatory, Leiden, The Netherlands; ²MPIA, Heidelberg, Germany

1. Introduction: The Host Galaxies of Distant Radio Galaxies

Luminous distant radio galaxies are unique probes of the early Universe. About 15 years ago at Leiden some of us started a programme to find distant radio galaxies, study their properties and use them as probes of the early Universe. The project began as a result of the technique we developed during the late eighties to pinpoint distant radio galaxies, based on their ultra-steep radio spectra (spectral index $\alpha < -1$). Finding these objects was the subject of an ESO Key Programme in the early nineties, that discovered a substantial fraction of presently known distant radio galaxies (e.g. see *Messenger* articles Miley et al. 1992; Röttgering, Miley, & van Ojik 1996). There are now around 150 $z > 2$ radio galaxies known, the majority of which were found using this technique, the most distant of which, TN J0924–2201, has a redshift of 5.19.

During the last decade multi-wavelength studies of these high-redshift radio galaxies (HzRGs, $z > 2$) have produced strong evidence that they are massive galaxies in the process of formation, most probably the ancestors of central cluster galaxies.

Relevant results include:

- HzRGs trace the bright envelope in the infrared Hubble diagram, implying that they are amongst the *most massive* galaxies in the early Universe (e.g. De Breuck et al. 2002).

- HzRGs are usually surrounded by *giant Ly α emitting gas halos*, whose sizes (~ 100 kpc; van Ojik et al. 1997) are comparable to those of cD galaxy envelopes (for an example, see Fig. 1).

- HzRGs appear extremely clumpy on *HST* images, strikingly similar to simulations from hierarchical models of *forming* massive galaxies, e.g. brightest cluster galaxies (e.g. Fig. 2, Pentericci et al. 1998). The sizes, profiles and luminosities of the clumps are similar to those of Lyman Break Galaxies (e.g. Steidel et al. 1996).

- Long-exposure optical spectra and observations of their luminous dust emission show that HzRGs are undergoing *vigorous star formation* (e.g. Dey et al. 1997).

Further evidence that HzRGs are in cluster environments is the large measured depolarization, indicative of a dense hot gas (Carilli et al. 1997).

These properties, taken together, provided strong indirect evidence that luminous distant radio sources pinpoint forming massive galaxies at the centres of protoclusters.

2. Finding Distant Protoclusters: a Pilot Project

One of the most intriguing questions in modern astrophysics concerns the formation of structure in the early Universe (e.g. Bahcall et al. 1997). Although there are various scenarios for the development of large-scale structure, the epoch and mechanism of

the formation of galaxy clusters are still open questions. Using conventional optical and X-ray techniques, the detection of clusters with $z > 1$ is difficult. In the optical, the density contrast is low due to the contaminating foreground, while in the X-ray the detection of extended hot cluster gas is challenging because of cosmological surface brightness dimming. Because distant radio galaxies have properties expected from forming massive galaxies in protoclusters, we instigated a VLT programme to search for *direct* evidence of galaxy overdensities around them.

First, we conducted a pilot project to search for an excess of Ly α emitters around the radio galaxy PKS 1138–262 at $z = 2.2$. This radio galaxy was chosen because it is extremely clumpy, it has the largest radio rotation measure in a sample of 70 HzRGs (Pentericci et al. 2000a) and has a large (120 kpc) Ly α halo (see Fig. 1). Furthermore, the redshifted Ly α of this radio galaxy falls in one of the narrowband filters of FORS. As the first visiting observers project, narrowband and broadband images were taken in March 1999 with FORS1 on ANTU. These data resulted in a list of ~ 50 candidate Ly α emitters (Kurk et al. 2000). Subsequent multi-object spectroscopy in March and April 2000 on FORS1 revealed 15 Ly α emitters at the same distance as the radio galaxy and an additional 5 objects having continua also consistent with galaxies at redshift 2.2. All the Ly α emitters were found to have redshifts in the range 2.16 ± 0.02 , centred around the redshift of the radio galaxy, and are within a projected physical distance of 1.5 Mpc from it (Pentericci et al. 2000b). We had now confirmed that in one case there is a substantial galaxy overdensity associated with a distant luminous radio galaxy.

3. VLT Large Programme: Searching for Protoclusters to $z > 4$

The next step was to investigate whether the overdensity around 1138–

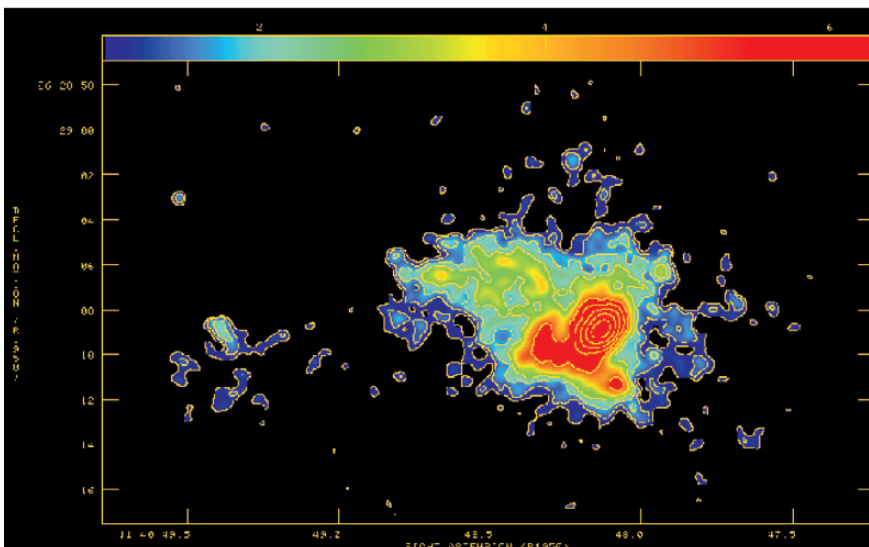


Figure 1: Ly α image of radio galaxy PKS 1138–262 at $z = 2.16$. The image is a 14,400 s exposure in a narrowband, taken with the FORS1 camera on ANTU. The size of the halo is roughly 120 kpc.

262 is typical for distant luminous radio galaxies as a class. We therefore initiated a Large Programme on the VLT to search for Ly α emitting galaxies around luminous radio galaxies at $2 < z < 4.1$. Our Large Programme was awarded 18 nights, spread over three periods, on the VLT/FORS2.

The targets for the Large Programme were selected from a list of ~ 150 radio galaxies with $z > 2$. Suitable targets satisfied the following criteria: (i) large radio luminosities ($P_{178} > 10^{26}$ W Hz $^{-1}$), (ii) luminous optical and infrared continua and (iii) redshifts suitable for Ly α imaging with the available VLT narrowband filters. This resulted in a list of objects with redshifts between $2.1 < z < 3.2$. We added one object with an even higher redshift (a radio galaxy at $z = 4.1$), for which we purchased a custom narrowband filter. This allowed us to cover a redshift range from $2 < z < 4.1$.

The strategy for finding Ly α emitters near the radio galaxy was the same as in our pilot project: each target was observed with a narrowband filter, which contained the redshifted Ly α line of the radio galaxy. The fields were also observed in broadbands, selected for having peak just redward of the Ly α line in order to measure the UV continuum. Comparison of the narrowband image with the broadband image allowed us to find objects with an excess flux in the

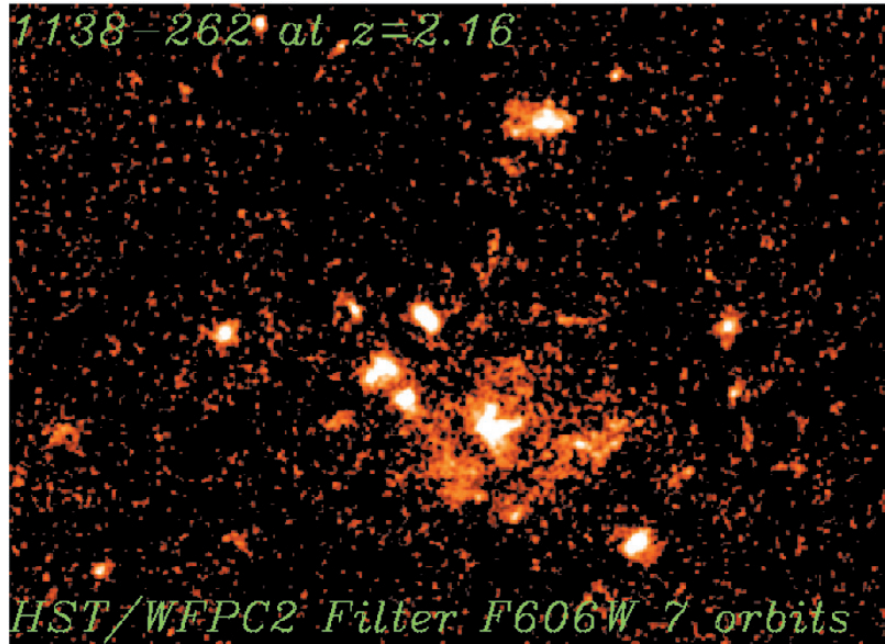


Figure 2: Seven orbit HST image of PKS 1138–262 (Pentericci et al. 1998). The image is taken through the F606W filter and shows the UV continuum.

narrowband. These excess objects were our candidate Ly α emitters. In Figure 3 an example is shown. On the left a section of a 33,300 s narrowband image is plotted of the field around the radio galaxy TN J1338–1942 at $z = 4.1$. On the right the same field is shown but this time observed in the broadband R .

The encircled objects can be easily seen in the narrowband image, but they almost disappear in the broadband image. This means that more flux falls in the narrowband than expected from the broadband “continuum” image. These objects were our primary candidates for spectroscopy.

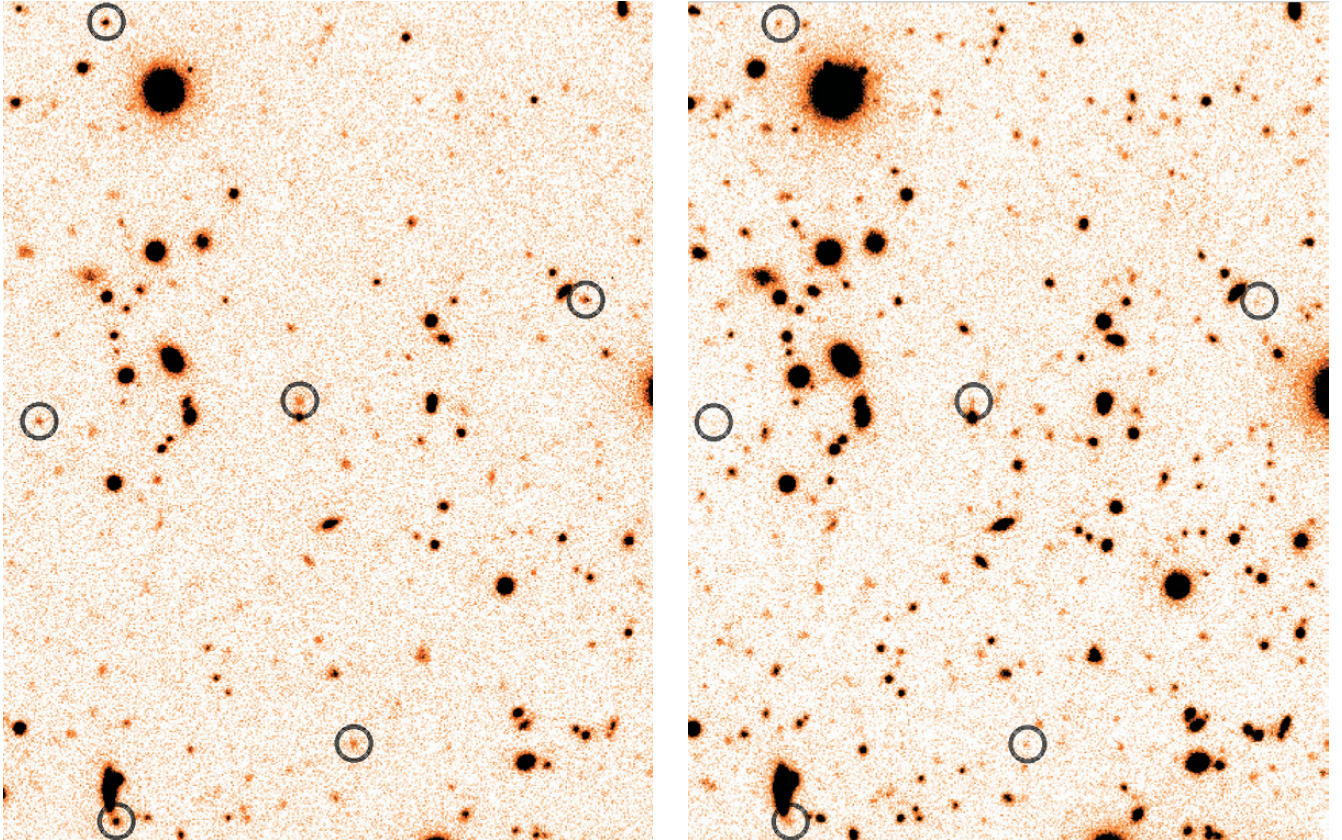


Figure 3: Narrowband and broadband image of a field near the radio galaxy TN J1338–1942 at $z = 4.1$. The narrowband filter used on the left is centred at $\lambda = 6210$ Å, which corresponds to Ly α emission at $z = 4.1$. The filter used on the right is the R filter, which measures the UV continuum at $z = 4.1$. The encircled objects all have an excess flux in the narrowband, and were our candidates for follow-up spectroscopy.

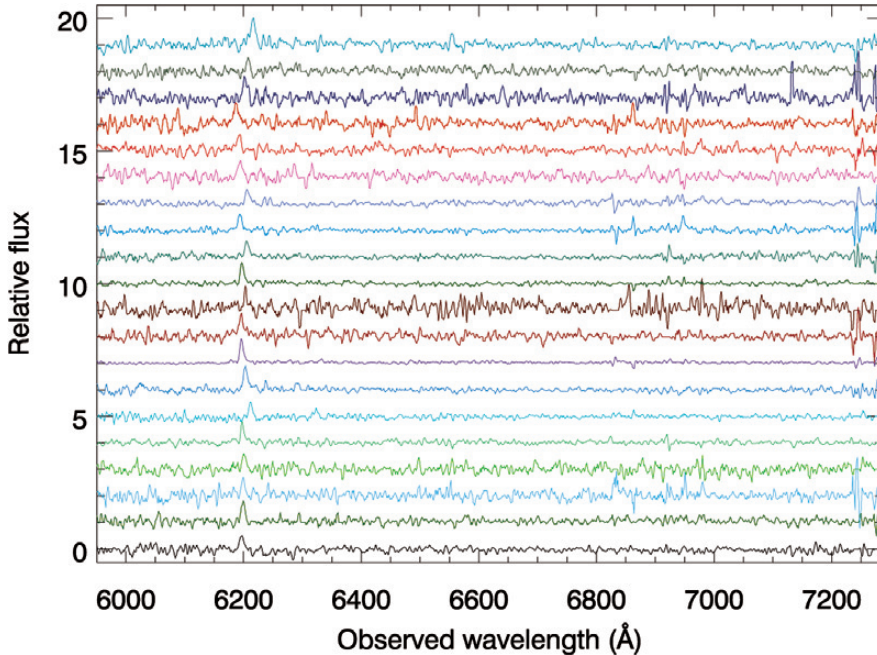


Figure 4: Spectra of 20 Ly α emitting galaxies detected around TN J1338–1942 at $z = 4.1$. All the emission line galaxies show a line near 6200 Å. Analysis of the spectra confirmed that all the lines are from Ly α at $z = 4.100 \pm 0.012$ (Venemans et al. 2002).

Follow-up spectroscopy of the brightest candidate emitters was carried out with the multiobject spectroscopy mode of the FORS2 spectrograph. The aim was to confirm whether the candidates were cluster members and to measure cluster velocity distributions. Our selection technique proved to be very successful: 70%–85% of all candidates that were observed spectroscopically showed an emission line. Our success rate for the brightest candidate emitters (with a predicted line flux greater than $1.5 \times 10^{-17} \text{ erg s}^{-1} \text{ cm}^{-2}$) exceeded 90%. In Figure 4 an example is plotted for 20 confirmed emitters at $z = 4.1$.

4. Preliminary Results

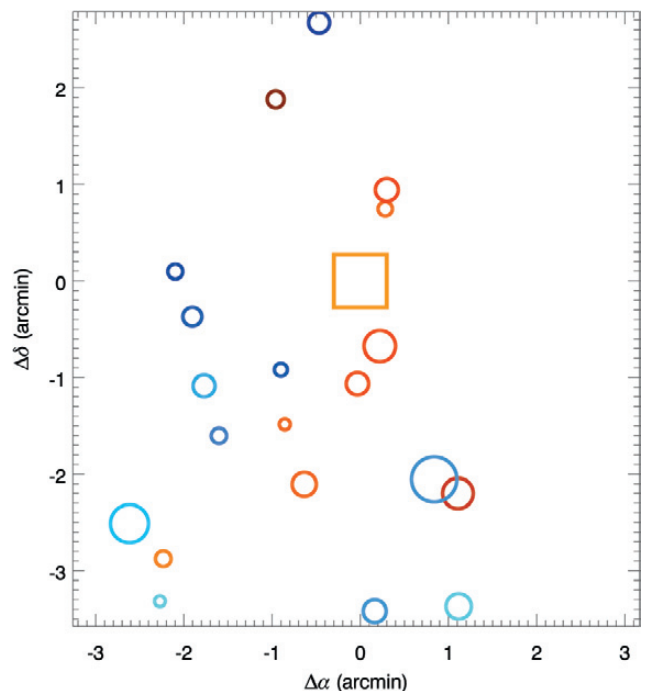
We have now carried out imaging and spectroscopy to a sufficient depth of five radio galaxy fields. A sixth target, TN J2009–3040 at $z = 3.2$, although observed for a comparable time, could not be studied to the same intrinsic depth due to the relatively high extinction.

The programme has been extremely successful. All five well-observed radio galaxies have > 20 spectroscopically confirmed Ly α and/or H α companions. In addition, despite its high extinction, TN J2009–3040 has 12 spectroscopically confirmed companions. The density of Ly α emitters found around all 6 radio galaxies can be compared with the density of emitters found in blank fields (see e.g. Cowie & Hu 1998, Rhoads et al. 2000). Taking into account the difference in volume and in depth, the overdensity of Ly α emitters in radio galaxy fields is 5–15. Furthermore, the velocity dispersions are found to be $\sim 300\text{--}1000 \text{ km s}^{-1}$, concentrated around the redshift of the

radio galaxy. This is significantly smaller than the width of the narrowband filters used in the initial imaging, providing further evidence that the groupings of galaxies are indeed associated with the radio galaxies.

The spatial distribution of the Ly α emitters is in most cases homogeneous over the field, indicating that the structure sizes generally exceed the $7 \times 7 \text{ arcmin}^2$ FORS field, which corresponds to sizes greater than $\sim 3 \times 3 \text{ Mpc}^2$. An exception is the distribution of Ly α emitters around TN J1338–1942 at $z = 4.1$, shown in Figure 5. The protocluster appears to be bound in the northwest, but

Figure 5: Distribution of the confirmed Ly α emitters (circles) at $z \sim 4.1$ on the sky. The square shows the position of radio galaxy TN J1338–1942. The size of the circles is scaled according to the Ly α flux of the object, ranging between 0.3 and $4.1 \times 10^{-17} \text{ erg s}^{-1} \text{ cm}^{-2}$. The colour of the symbols is an indication of the redshift of the object. Blue objects have a lower redshift than the median redshift of the emitters, red objects have a higher redshift. The redshifts range between 4.088 and 4.112. Note that the radio galaxy is not centred in the galaxy distribution.



the field of view is not large enough to show a boundary in the south. Note that in this field the radio galaxy is not in the centre of the protocluster.

The mass can be estimated using the volume occupied by the overdensity, the mean density of the Universe at the redshift of the protocluster, the measured galaxy overdensity and the bias parameter (Steidel et al. 1998). The computed masses are in the range $10^{14}\text{--}10^{16} M_{\odot}$, comparable with the mass of present-day rich clusters of galaxies. Taken together, the properties of the radio galaxy hosts and those of the newly-discovered structures demonstrate that luminous distant radio sources can be used to pinpoint protoclusters, the ancestors of rich clusters.

5. Conclusions

We have discovered substantial galaxy overdensities around radio galaxies at $z = 2.16, 2.86, 2.92, 3.13, 3.15$ and 4.10 .

Although preliminary, we can draw the following conclusions: (i) HzRGs are generally associated with the most massive forming galaxies at the centre of protoclusters and can be used to pinpoint such structures. (ii) Because the radio lifetimes (few $\times 10^7 \text{ yr}$) are small by the standard of cosmic evolution, there must be orders of magnitude more “dead” radio sources than living ones. When the protoclusters have evolved, the luminous radio sources are likely to be extinguished, explaining why $z < 1$ clusters do not generally harbour active luminous radio sources. (iii) The luminosity functions and lifetimes of luminous distant radio sources are consistent with such objects being associated with every pronounced veloci-

ty spike in the space density of Lyman break galaxies.

Our distant protoclusters are unique laboratories for studying the most extreme overdense regions in the early Universe and crucial locations for tracing the formation and evolution of clusters and galaxies. We are in the process of analyzing more than 100 confirmed Ly α emitting galaxies that lie within our protoclusters and in addition we are obtaining observations with other facilities, including the Advanced Camera for Surveys on the *HST* to find and study the various other populations of galaxies expected within the protoclusters. A detailed study of the morphologies and SEDs of protocluster

members between $z \sim 4$ and $z \sim 1$ will be used to trace the history of *galaxy assembly* and *star formation*.

Acknowledgements

We thank the staff at the Paranal Observatory, Chile, for their splendid support. We also wish to thank Gero Rupprecht at ESO for his guidance in the process of purchasing the narrow-band filter.

References

- Bahcall, N.A., Fan, X., & Cen, R., 1997, *ApJ* **485**, L53.
Carilli, C.L., Röttgering, H.J.A., van Ojik, R., Miley, G.K., van Breugel, W.J.M., 1997, *ApJS* **109**, 1.

- De Breuck, C. et al., 2002, *AJ* **123**, 637.
Dey, A., van Breugel, W.J.M., Vacca, W. D., & Antonucci, R., 1997, *ApJ* **490**, 698.
Kurk, J. D. et al., 2000, *A&A* **358**, L1.
Miley, G.K. et al., 1992, *The Messenger* **68**, 12.
van Ojik, R., Röttgering, H.J.A., Miley, G.K., Hunstead, R.W., 1997, *A&A* **317**, 358.
Pentericci, L. et al., 1998, *ApJ* **504**, 139.
Pentericci, L., Van Reeveen, W., Carilli, C.L., Röttgering, H.J.A., & Miley, G.K., 2000a, *A&AS* **145**, 121.
Pentericci, L. et al., 2000b, *A&A* **361**, L25.
Röttgering, H.J.A., Miley, G.K., van Ojik, R., 1996, *The Messenger* **83**, 26.
Steidel, C.C., Giavalisco, M., Pettini, M., Dickinson, M., & Adelberger, K.L., 1996, *ApJ* **462**, L17.
Steidel, C.C. et al., 1998, *ApJ* **492**, 428.
Venemans, B.P. et al., 2002, *ApJ* **569**, L11.

TELESCOPES AND INSTRUMENTATION

ESO and NSF Sign Agreement on ALMA

Green Light for World's Most Powerful Radio Observatory

(From ESO Press Release 04/03, 25 February 2003)

On February 25, 2003, the European Southern Observatory (ESO) and the US National Science Foundation (NSF) signed a historic agreement to construct and operate the world's largest and most powerful radio telescope, operating at millimetre and sub-millimetre wavelengths. The Director General of ESO, Dr. Catherine Cesarsky, and the Director of the NSF, Dr. Rita Colwell, acted for their respective organizations.

Known as the Atacama Large Millimeter Array (ALMA), the future facility will encompass sixty-four interconnected 12-metre antennae at a unique, high-altitude site at Chajnantor in the Atacama region of northern Chile.

ALMA is a joint project between Europe and North America. In Europe,

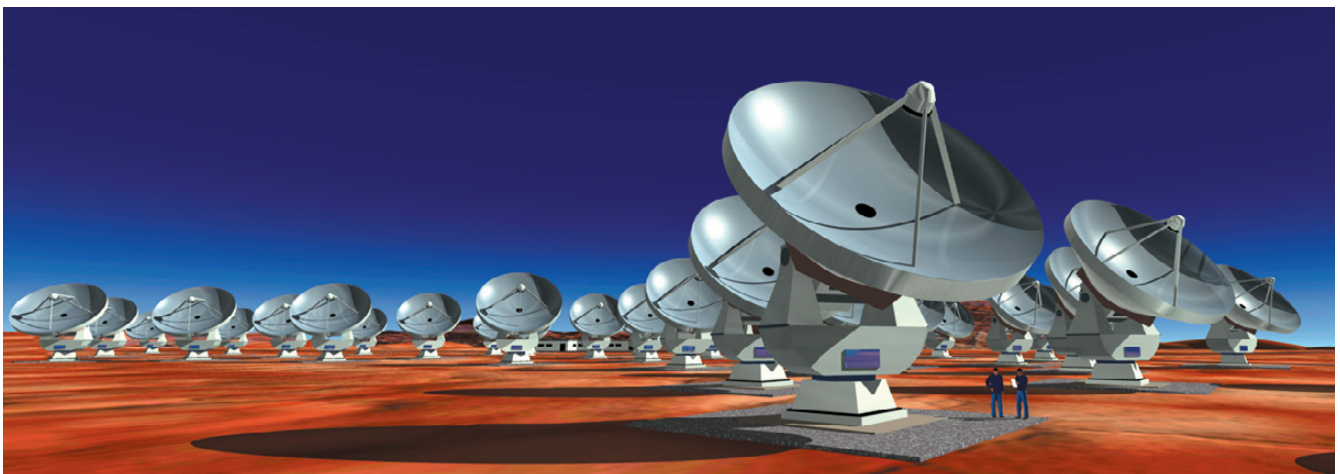
ESO is leading on behalf of its ten member countries and Spain. In North America, the NSF also acts for the National Research Council of Canada and executes the project through the National Radio Astronomy Observatory (NRAO) operated by Associated Universities, Inc. (AUI).

The conclusion of the ESO-NSF Agreement now gives the final green light for the ALMA project. The total cost of approximately 650 million Euro is shared equally between the two partners.

Dr. Cesarsky is excited: "This agreement signifies the start of a great project of contemporary astronomy and astrophysics. Representing Europe, and in collaboration with many laboratories

and institutes on this continent, we together look forward towards wonderful research projects. With ALMA we may learn how the earliest galaxies in the Universe really looked like, to mention but one of the many eagerly awaited opportunities with this marvellous facility."

"With this agreement, we usher in a new age of research in astronomy", says Dr. Colwell. "By working together in this truly global partnership, the international astronomy community will be able to ensure the research capabilities needed to meet the long-term demands of our scientific enterprise, and that we will be able to study and understand our universe in ways that have previously been beyond our vision".



Artist's view of the Atacama Large Millimeter Array (ALMA), with 64 12-m antennae.

The recent Presidential decree from Chile for AUI and the agreement signed in late 2002 between ESO and the Government of the Republic of Chile recognize the interest that the ALMA Project has for Chile, as it will deepen and strengthen the co-operation in scientific and technological matters between the parties.

A joint ALMA Board has been established which oversees the realization of the ALMA project via the management structure. This Board met for the first time on February 24–25, 2003, at NSF in Washington and witnessed this historic event.

The Atacama Large Millimeter Array (ALMA) will be one of astronomy's most powerful telescopes – providing unprecedented imaging capabilities and sensitivity in the corresponding wavelength range, many orders of magnitude greater than anything of its kind today.

ALMA will be an array of 64 antennas that will work together as one telescope to study millimetre and sub-millimetre

wavelength radiation from space. This radiation crosses the critical boundary between infrared and microwave radiation and holds the key to understanding such processes as planet and star formation, the formation of early galaxies and galaxy clusters, and the formation of organic and other molecules in space.

“ALMA will be one of astronomy's premier tools for studying the universe”, says Nobel Laureate Riccardo Giacconi, President of AUI (and former ESO Director General (1993–1999)). “The entire astronomical community is anxious to have the unprecedented power and resolution that ALMA will provide.”

The President of the ESO Council, Professor Piet van der Kruit, agrees: “ALMA heralds a break-through in sub-millimetre and millimetre astronomy, allowing some of the most penetrating studies of the Universe ever made. It is safe to predict that there will be exciting scientific surprises when ALMA enters into operation.”

Timeline for ALMA

- June 1998: Phase 1 (Research and Development)
- June 1999: European/American Memorandum of Understanding
- February 2003: Signature of the bilateral Agreement
- 2004: Tests of the Prototype System
- 2007: Initial scientific operation of a partially completed array
- 2011: End of construction of the array

Further Reading About ALMA

More information on the ALMA project can be found in earlier issues of *The Messenger* (March 1996; March 1998; December 1998; June 1999; and March 2002), and on the following web-sites:

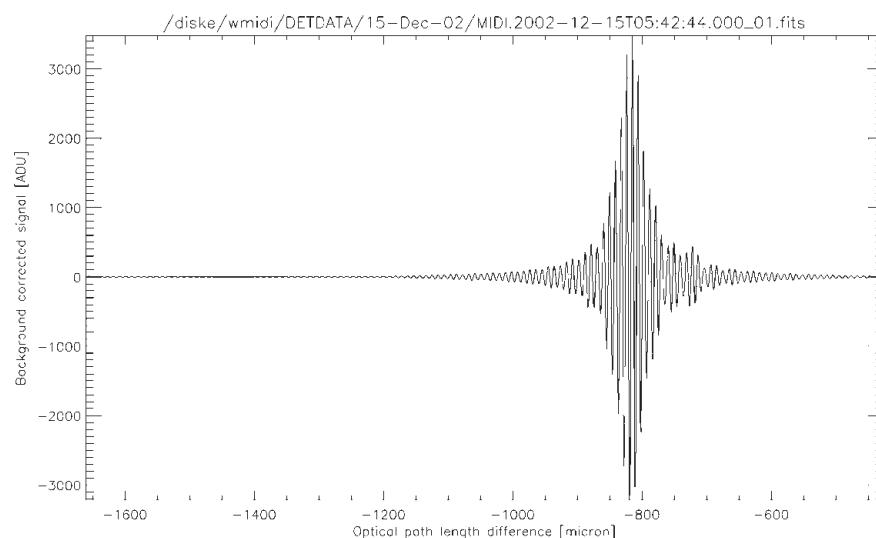
<http://www.eso.org/projects/alma/>
<http://www.alma.nrao.edu>

New Vistas Open with MIDI at the VLT Interferometer

“FIRST FRINGES” IN MID-INFRARED SPECTRAL REGION WITH TWO VLT TELESCOPES

Following several weeks of around-the-clock work, a team of astronomers and engineers from Germany, the Netherlands, France and ESO has successfully performed the first observations with the MID-Infrared interferometric instrument (MIDI), a new, extremely powerful instrument just installed in the underground laboratory of the VLT Interferometer (VLTI) at the Paranal Observatory (Chile).

In the early morning of December 15, 2002, two of the 8.2-m VLT unit telescopes (ANTU and MELIPAL) were pointed towards the southern star Epsilon Carinae and the two light beams were directed via the complex intervening optics system towards MIDI. After a few hours of tuning and optimization, strong and stable interferometric fringes were obtained, indicating that all VLTI components – from telescopes to the new instrument – were working together perfectly. Two more stars were observed before sunrise, further proving the stability of the entire system.



The upper image shows the “first fringes” of the star Epsilon Carinae, as obtained at VLTI with the new MIDI instrument at the mid-infrared wavelength of 8.7 μm .

The photograph at the bottom shows the group responsible for the MIDI installation and first tests, taken inside the VLT Control Building, right after the successful “First Fringes” in the early morning of December 15. From left to right: Front row (sitting/kneeling) Julio Navarrete, Lorena Faundez, Markus Schoeller, Andrea Richichi – Back row (standing) Francesco Paresce, Andres Pino, Nico Housen, Uwe Graser, Olivier Chesneau, Christoph Leinert, Andreas Glindemann, Walter Jaffe, Sebastien Morel, Richard Mathar, Pierre Kervella, Eric Bakker.

More details can be found in ESO press release PR 25/02 of 18 December 2002.



TIMMI2 at the 3.6-m, or The Return of MIR

V. DOUBLIER, La Silla

In October 2002, after only 12 weeks of forced retirement, TIMMI2 (Thermal Infrared Multimode Instrument) underwent a major upgrade and was successfully remounted at the Cassegrain focus of the 3.6-m telescope at La Silla.

TIMMI2 had a difficult start to 2000, when the tragic and untimely death of PI Hans-Georg Reimann overshadowed the success of the project. The instrument was first commissioned in late 2000, with TNT control software and the Wallace acquisition system. However, after almost two years of continuous operation, it became apparent that an upgrade of the control and acquisition system could improve the reliability of the instrument and reduce the operational load for the staff.

In February 2002, TIMMI2 suffered from a severe problem which took some time to locate inside the detector mount: the thermal contact of the array with the cooling support had deteriorated. Operation was resumed after three months of investigation and tests, and finally, in August 2002, the upgrade project was started at La Silla (M. Sterzik, Project Scientist; J. Valenzuela, IRACE-SW; P. Le Saux, Templates; J.-C. Guzman, ICS, OS; and U. Weilenmann, Control System and Project Leader) with active help from the IR group in Garching (H.-U. Käufel, R. Siebenmorgen, J. Stegmeier and H. Mehrگان). Thanks to the efforts of this team



Figure 1: New Control rack: tiiracq LCU on top, the Sparc and IRACE backend in the middle and the temperature and vacuum control at the bottom.

and many others, TIMMI2 is back on-sky and available to the MIR community.

Not only was the 2nd commissioning used to refurbish TIMMI2 with up-to-date electronics and software, we also took the opportunity to simplify observational procedures. Experienced MIR observers will not have a problem adjusting to the new procedures, and newcomers to the MIR community will find the instrument user-friendly. The TIMMI2 system can now be compared to those of ISAAC and NACO for 2.5–5 micron observations. For example, the exposure time set-up requires only one entry: the amount of time the user desires to spend on source. Optimum values for each set-up are defined in a configuration file – a concept developed in the first phase of TIMMI2 operations – which is read at set-up time by the Observing Software (OS). There is no more interaction between the observer and the individual parts of TIMMI2, and the data of TIMMI2 are now routinely injected into the ESO archive.

How Was This Possible?

- Above all: with great team spirit.
- The old TIMMI2 acquisition system (Wallace electronics), which handles acquisition tasks as well as clocking and biasing of the array, was replaced by the ESO IRACE system. The versatility of the IRACE system allows easy development of new timing patterns and will further increase the performance of the Raytheon array.
- The instrument control system has been refurbished with VLT standard modules and controllers for the stepper motors, enhancing functionality and increasing reliability at the same time.
- Temperature and vacuum control has been modified, allowing important system parameters to be monitored continuously and the handling of alarms.
- The system is entirely controlled by VLT SW, and communications are handled via the licence-free CCS Environment rather than RTAP. The handling of the observations is managed by “boss” which is, at high level, interfacing BOB, ICS, DCS, TCS and the OS. A series of configuration files “preset” the instrument and detector depending on the instrument mode required by the user.
- Data handling is now under the control of the DMD SW. The raw data are transferred via the data subscriber to the DHS WS which then redirects the data to an offline machine for the convenience of the user.

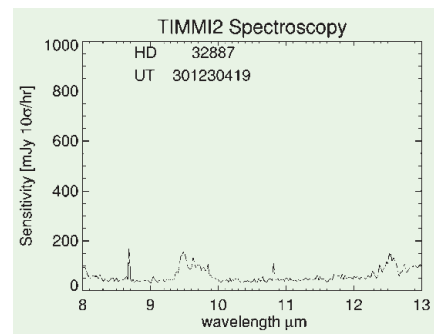


Figure 2: HD32887 8–13 μ spectrum: N band sensitivity plot shows a factor 2 better than with the Wallace acquisition system at 10 microns.

- The pipeline software has been modified to accept the new format of the raw data stored in cubes. It is available upon request. During the two commissionings of November and December 2002, the transfer of data was done directly from the instrument WS within the templates; however this dramatically increased the overheads. To keep overheads low, the transfer of data from the DHS WS is currently handled by a shell script from the pipeline machine.
- Observations preparation: “p2pp” is on the job and proved to be well accepted by the TIMMI2 community.

What did we achieve?

(1) *Imaging*: TIMMI2 shows an improvement of 40% in sensitivity in all bands, allowing us to finally offer L- and M-band observations.

A “Raster” mode (or jitter) is being implemented and tested for extended sources.

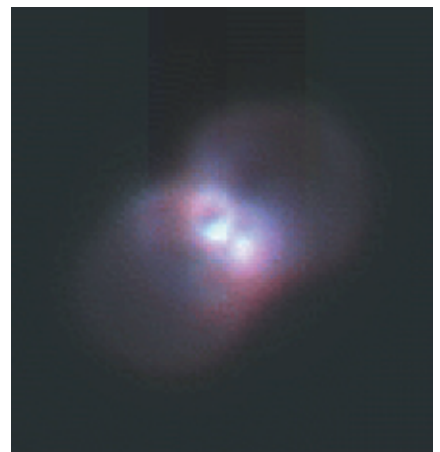


Figure 3: Eta-Carinae three-colour image: NB10.4 (Blue) Nell (Green) Q1 band (Red).

IRACE gives more freedom in programming read-out sequences. The TIMMI2 detector (Raytheon CRC774) has a rather complex architecture, and especially “long” detector integration times (exceeding 100 ms; this is long for the mid-infrared!) could only be done in very compromised form with the old system.

(2) *Spectroscopy*: The sensitivity improved by a factor of 2: 50mJy/10sigma/1hr at 10 micron.

(3) *Polarimetry*: This has been extensively tested. A new Instrument Package is available on the web and is already installed at the telescope.

Developments

In April, TIMMI2 will undergo regular maintenance. We plan to reinstall the science grade array, together with new cryo cabling and detector board.

The Lunar Occultation mode will be

implemented soon. It is not yet operational at a template level: we hope to offer it in visitor mode during Period 71, and in full operation mode for Period 72.

The possibility to chop at different PA angles is under investigation. This will be a major improvement for extended source observations.

The new, more compact control rack leaves more space in the Cassegrain cage. The implementation of a rotator function is under study.

OTHER ASTRONOMICAL NEWS

NEWS FROM SANTIAGO

International Workshop on

STRUCTURE EVOLUTION AND COSMOLOGY: NEW SYNERGY BETWEEN GROUND-BASED OBSERVATIONS, SPACE OBSERVATIONS AND THEORY

D. ALLOIN (ESO/Chile),
M. PIERRE (CEA/SAp/France) and
A. REFREGIER (CEA/SAp/France)

An international Workshop, “Structure Evolution and Cosmology: New Synergy between Ground-based Observations, Space Observations and Theory”, was organized jointly by the European Southern Observatory (ESO/Chile), the Centre National d’Etudes Spatiales (CNES/France) and the Commissariat pour l’Energie (CEA/France), at ESO/Santiago from October 28 to 31, 2002.

The ESO facilities in Santiago were hosting such a large meeting for the first time: according to the attendees it was a very successful trial and, on our side, we were very happy to share with them our renewed environment, as well as the coffee-breaks on the lawn!

A total of 144 astronomers and students attended the Workshop, which was opened by the ESO Director General, Catherine Cesarsky. After the usual welcome words given in the name of the Scientific Organizing Committee (Danielle Alloin, Marguerite Pierre and Alex Refregier), we started a half-day tutorial about Cosmology. This was an excellent way to refresh and update our ideas in the field and we recommend the superb tutorial presentations to be found on the Workshop webpage (see below)!

The unfortunate overbooking problems of some flights prevented a few of our reviewers to arrive on time for their presentation, or arrive at all! Thanks to the friendly attitude of all speakers, we did some re-shuffling of the programme and, among others, exchanged weak-lensing against strong-lensing (still lensing anyway!). This gave a touch of “impromptu” to the Workshop, creating the nice feeling that we were all involved in the Workshop organization...

A rather complete panel of topics related to Cosmology were covered: from the description of the early universe by particle physicists, to the birth and evolution of large-scale structures (simulations and observations), to various aspects of galaxy clusters, to the numerous lensing effects one encounters when probing the high-z universe... Vivid and interesting discussions followed the presentations, continued at the posters display and at the coffee-breaks/lunches. The need for a good interplay between space-based and ground-based observations (to accomplish a multi-wavelength coverage), but also with simulations and theoretical approaches, was highlighted throughout the Workshop. And this is indeed what is giving rise to the great achievements of modern astrophysics!

The dense programme of the Workshop was interrupted for half a day to visit La Sebastiana, the house of Pablo Neruda in Valparaíso: an attempt to join the dreams of the poet with our more arid research activities?

*“La luz bajo los árboles,
la luz del alto cielo.
La luz verde enramada
que fulgura en la hoja
y cae como fresca arena blanca.
Una cigarra eleva
su son de aserradero
sobre la transparencia.
Es una copa llena de agua,
el mundo.”*

Then, walking down through Valparaíso’s stairs and paths, we reached the restaurant at the top of a tower in the port, where the Workshop dinner was held, and from there we could enjoy the magnificent view to the bay and the hills of Valparaíso, all twinkling in the night. On our way back to Santiago, the bus was stopped for a while because of an excess of weight (!) and during this unexpected pause, some of our skilled theoreticians were desperately trying to see the Magellanic Clouds, in spite of an intense light background. The happy ones who went to

the Paranal visit after the Workshop, did see them, however!

The pleasant environment of the ESO facilities in Santiago, the tutorial, particularly appreciated by students and non-cosmologists and the great reviews/contributions/posters all contrib-

uted to making this Workshop a very exciting one!

The group of reviewers and the SOC decided that there is no need to print another book on Cosmology and that the interest of the meeting had been largely in discussing and meeting with

colleagues and young researchers ... Yet, most of the reviews and presentations are available on the Workshop webpage. To retrieve the information, please go to:

<http://www.eso.org/gen-fac/meetings/cosmology2002/programme.html>

International Workshop on STELLAR CANDLES FOR THE EXTRAGALACTIC DISTANCE SCALE

*D. ALLOIN (ESO/Chile) and
W. GIEREN (Concepción University, Chile)*

An international Workshop, "STELLAR CANDLES for the EXTRAGALACTIC DISTANCE SCALE", was organized jointly by the European Southern Observatory and the Astronomy Group at the University of Concepción as a member of the FONDAP/Conicyt Centre for Astrophysics launched in Chile in 2002. The Workshop received support grants from ESO, FONDAP/Conicyt, the University of Concepción and Fundación Andes.

The Workshop was hosted on the beautifully green campus of the University of Concepción, on December 9–11, 2002, under blue skies and in a pleasant atmosphere. More than 73 astronomers had registered and attended the Workshop. We are happy to acknowledge a good participation of students from various Chilean universities. After a formal opening of the Workshop by the Rector of the University, Don Sergio Lavanchy Merino, and the Dean of the Physics and Mathematics Faculty (where the Workshop was taking place), Dr. José Sanchez, a few words of welcome were given by Dr. Wolfgang Gieren, Head of the Astronomy Group in Concepción.

A fairly large number of possible stellar "candles" used for the determination of the extragalactic distance scale, were examined and discussed during the Workshop. These encompassed: Cepheids, RR Lyrae stars, blue supergiants, the red giant clump, supernovae of types Ia and II, novae, planetary nebulae, eclipsing binaries, and globular clusters. Both theoretical and observational reviews were given by top specialists on the various candles, and some recent advances were presented. Pros and cons were discussed for each candle, giving rise to lively, sometimes hot, debates.

The comparison of distances derived for a same galaxy using different indicators was extremely interesting. Obviously, the Large Magellanic Cloud is the galaxy which has been studied

through the greatest variety of distance indicators. In spite of fairly large-size variations, still to be understood, the value for the distance modulus of the LMC seems to be slowly converging: as quoted in the concluding remarks, 60 values were mentioned during the Workshop, with a mean close to 18.5 mag and uncertainty of ± 0.1 mag. The question was raised about how accurately do we actually need to measure this number, for the various astrophysical applications?

Using the same distance indicator, the Cepheids, does not always lead to similar results, even if one uses the same data set! Very puzzling was the comparison of distances derived from the same large *HST* data set on Cepheids in some 25 nearby galaxies. Two independent studies have been concluded on two different values of the Hubble constant, with a net difference of 12 km/s/Mpc, three times larger than the quoted total error-bars (± 2 km/s/Mpc) on each value. This opened a vivid and enlightening discussion about unknown systematics: it was wisely suggested that we use a current "best value" of 66 ± 6 km/s/Mpc for the Hubble constant, until the source of the discrepancy has been understood.

On the side of theory, progress in stellar atmosphere modelling of Cepheids opens the door to direct distance determinations of improved accuracy. Coupled to interferometric measurements, this is becoming a superb and promising technique to directly derive a very accurate distance to Cepheids, to distances further out than those in reach by parallax measurements.

More and more refined analyses of other indicators are currently being developed, either from a modelling or an observational point of view. Progress is being made on RR Lyrae star observations and modelling, especially on the near-infrared period–absolute magnitude–metallicity relation which is a par-

ticularly useful tool in old population systems, on the intermediate-aged clump stars for which the most recent K-band studies in the Magellanic Clouds and other Local Group galaxies seem to indicate that very accurate distance results can be expected from this method in the near-infrared domain, and on blue supergiant stars which offer the advantage of being intrinsically very luminous candles which can be used in galaxies as distant as 10–15 Mpc but are appropriate for young population systems only. The wind momentum–luminosity relation and the flux-weighted gravity–luminosity relation for these stars are very promising tools for spectroscopic distance determinations of high accuracy from these objects. The use of spectroscopic information, which gives metallicity and reddening information on the studied objects "for free", is indeed an important plus.

The use of supernovae for distance determinations was extensively discussed since these constitute privileged – and often unique – indicators at high redshift. SNIa remain the best indicators to be used so far in very distant galaxies, although not being the perfect candle – since there are slowly declining and fast declining SNIa. It has been recommended at the Workshop to study them in the H band where the slope of the luminosity versus decline-rate relation seems to be essentially flat and where reddening corrections are smaller than in optical bands. The following comment was also made: "Despite the fact that we don't understand them, they are excellent stellar candles"... In turn, SNIi are not intrinsically as bright as SNIa and are subject to more systematics, hence currently less useful as candles than SNIa. An exhaustive review on the physics of SNIa explosions was given from which the following quotation is extracted: "the red model here is the truth, the blue lines are the observations".

Novae were also explored for their current usefulness as distance indicators, although they seem to be hampered by larger systematics than other stellar candles. Planetary nebulae, presented as the “Swiss-army knives” of extragalactic astronomy, are also used to derive distances to galaxies, through their luminosity function (measured in the [OIII] emission line). The technique seems to work, in spite of a number of complicating factors, which led to the following remark: “An astrophysicist is someone who sees something working in practice and wonders whether it works on the basis of first principles”.

The luminosity function of globular clusters is another attempt at enriching our tool-box of distance indicators, which was discussed at the Workshop. And, finally, the use of eclipsing binaries as distance indicators looks very promising if more appropriate systems in Local Group galaxies can be found.

Altogether, the Workshop allowed us to discuss and compare in depths the different stellar indicators used so far in the difficult quest of astronomers for distances. The very pleasant environment of the campus, the excellence of the talks, the challenges of the field were key-elements for stimulating dis-

cussions and exchanges. Remaining controversies were “discussed” during the soccer game which closed the Workshop, although some attendees (those for which all questions had been answered) had left already! The game was won by the population II team against the population I team, with the help of a Dutch referee who is known to be a friend of old stellar populations...

The reviews of this Workshop will be published early 2003 in a volume of the Springer series Lecture Notes in Physics, while all contributions – talks and posters – will be made available on the Workshop webpage in Concepción (<http://cluster.cfm.udec.cl>).

Fellows at ESO

Since the beginning ESO has provided opportunities for young scientists to interact with the environment of an observatory. Many European astronomers spent some years as post-doctoral Fellows at ESO. The Fellowship programme has been very successful; with only very few exceptions, all former ESO Fellows are now working as astronomers in the community.

In addition to developing their scientific careers the Fellows are also asked to contribute to the work of the observatories. In Chile all Fellows are involved in operational activities at Paranal and La Silla, while in Garching they participate in instrument and software development, PR activities, ALMA related studies and surveys.

With this issue of The Messenger we start short presentations of Fellows currently at ESO. They describe in their own words what research they pursue and how they are involved in ESO activities. We will continue to present some of the young faces at ESO in the coming issues.

B. Leibundgut

Aurore Bacmann



I have been a Fellow at ESO Garching since March 2002. Before that, I had done my PhD thesis with Philippe André at CEA-Saclay near Paris, France, and spent two years

as a post-doc at the University of Jena, Germany, working in the group of Thomas Henning. My area of research is star formation, mostly the early pre-stellar stages, before stars are formed within dense cores. This stage is particularly important since it represents the initial conditions of gravitational collapse and star formation. During my PhD, I used the instrument ISOCAM aboard the ISO satellite to determine the density structure of pre-stellar cores.

After my PhD, I started studying the chemistry of these cores, chiefly molecular depletion and deuteration, with collaborators from the Bordeaux and the Grenoble Observatory in France. This has been my main subject of research here at ESO. To carry out these projects, I use mostly (sub)millimetre telescopes. Additionally I work on the structure of circumstellar matter around

Herbig Ae/Be stars, using polarimetry, and I am also interested in their chemistry.

Since I arrived at ESO, I have been involved in the development of the interferometer ALMA, working with Stéphane Guilloteau (IRAM/ESO). The main goal of this task is to look into the bandpass calibration of the system and determine the frequency response of the instrument. It is extremely motivating to be taking an active part in such a major and ambitious project, all the more that ALMA will be very relevant to the research I am doing.

Maria-Rosa Cioni



I am probably an astronomer since the autumn of 1990 when I started at the University in Bologna, though the bed sheets of my earliest days were full of

planets and stars. After graduating I moved to the Leiden Observatory in the Netherlands where I obtained the Ph.D. degree. This first highly positive experience abroad exposed me to an international and active scientific environment

that could find no better match afterwards than by coming to ESO.

I study Asymptotic Giant Branch stars, their evolution and variability properties in resolved galaxies: the Magellanic Clouds and other galaxies in the Local Group. I am actively collaborating with my former supervisor Prof. Harm Habing and our most recent paper shows the metallicity gradient in the Magellanic Clouds from the ratio of carbon- and oxygen-rich stars. My work, so far predominantly photometric, is evolving to spectroscopy using the FLAMES instrument. At the same time I follow-up from the La Palma observatory AGBs in northern Galaxies.

I am presently in the middle of my ESO fellowship and I feel proud of being among the people that work at and for the observatory and provide the resources that improve our knowledge of what is above us. I have found both in Garching and Chile, where I enjoy spending part of my time, a very friendly group of colleagues and new collaborators. I learned how to support the astronomical activities in Paranal. In particular using the UVES instrument and FLAMES in the near future.

During my free time, though there is always more work than time, I enjoy the rich social life in Munich, practise various sports and am (now) learning German.

Ivo Saviane



I arrived at ESO in April 2001, from the UCLA. I was previously a postdoc in Padova, where I also received my PhD in 1997. During that time I think I gave, with the Padova and

IAC groups, an important contribution on the question of the relative ages of Galactic globular clusters (GC). Dwarf spheroidal galaxies also attracted my attention, and with another Padova group we helped establishing the idea of extended SF histories (and discovered the old population of Leo I). I was also one of the creators of the *Virtual Planetarium* educational website, at the Padova Observatory.

I am enjoying very much the La Silla environment, which offers the possibility to interact with a multidisciplinary group of people, and to contribute to instrument development (in particular, upgrading FEROS in the near future). Moreover, the ever-increasing number of students and visitors makes ESO/Chile a good and stimulating working place.

Now I am leading a project to test the luminosity-metallicity relation of dwarf

irregular galaxies, I am extending the relative age study to the LMC clusters (where I discovered a young globular), and the dwarf galaxy group in Padova still likes to have me as a collaborator! During my stay in California I discovered that the Antennae are not so far as commonly believed (and now I have to convince the referee), and I contributed to the project "Hubble Deep Field in a GC", led by the Vancouver group. Some people think I am good at free-hand drawing, and a few of my portraits are out there on the Internet. I would be very happy if you gave me Old Blue Eyes' *The complete Reprise years!*

Petri Vaisanen



I am a second-year ESO Fellow in Chile – and I do not regret accepting this job. To support and use top-notch instruments at the VLT, to learn more about a wide range of observational astronomy, to help

visiting astronomers doing exciting science, is all very rewarding. And I still have plenty of time for my own work. In fact, operating the adaptive optics instrument NACO has given new perspectives to my interests. For the third

year of my fellowship I will join the Astronomy Department of Universidad de Chile. I can concentrate on science and develop new collaborations before starting a job-hunt again.

My main scientific focus has been extragalactic infrared work aiming at acquiring an unbiased view of the formation history of galaxies. It has taken the form of several different projects, including optical and near-IR follow-up of ISO-detected mid- and far-IR galaxies using various telescopes. I have concentrated on extremely red galaxies (EROs) and interacting and starburst systems, and recently also on obscured nuclear activity. The plan is to expand this line of research using e.g. the SIRTf. I am also involved in a "more local" project of studying star formation in galactic molecular clouds using VLT/ISAAC data.

A thing I have missed is teaching, which I had done previously in Helsinki (where I finished my PhD in 2001) and Harvard (where I worked as a SAO Pre-doctoral Fellow for 3 years). However, as part of a campaign to see my own country join ESO, I have written, with others, articles about ESO and astronomy to Finnish newspapers and magazines, given interviews, and hosted journalists visiting Paranal. Exploring the universe can be great fun – that is something I have thought since a little kid, and it is the idea I hope to get across whether talking to students or the general public.

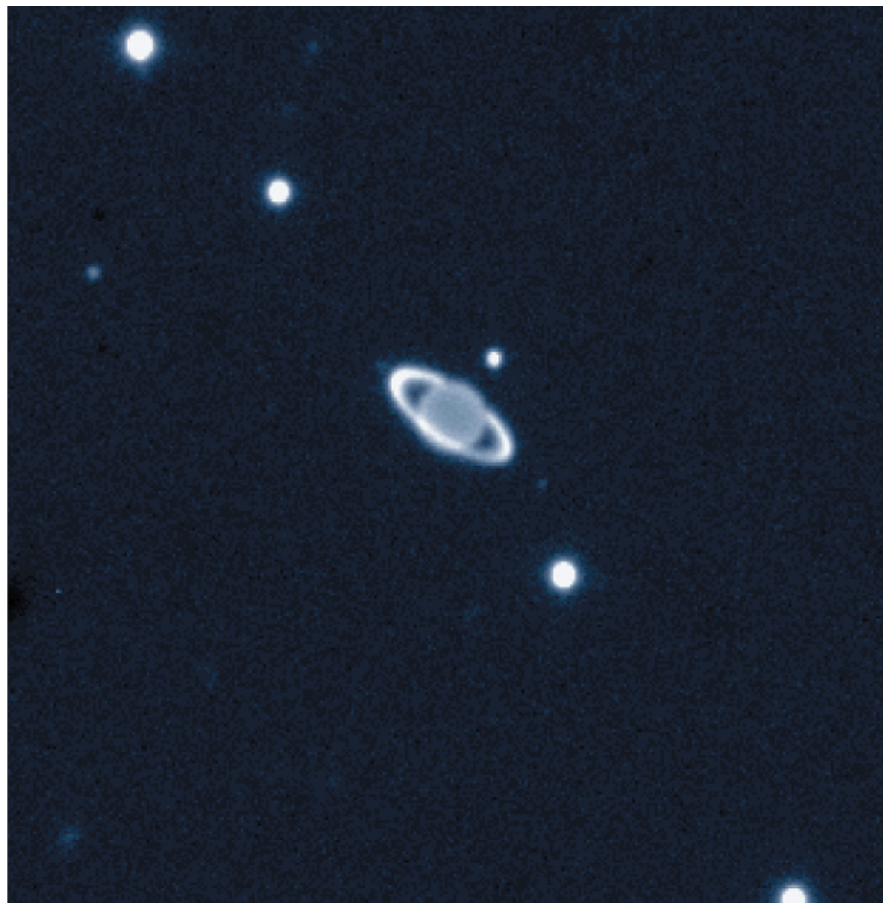
URANUS, Rings and Moons

A near-infrared view of the giant planet Uranus with its rings and some of its moons, obtained at a wavelength of 2.2 μm on November 19, 2002, with the ISAAC multi-mode instrument on the 8.2-m VLT ANTU telescope. The observing conditions were excellent, with seeing of 0.5 arcsec.

The rings of Uranus are almost undetectable from the Earth in visible light, but on this VLT near-infrared picture the contrast between the rings and the planet is strongly enhanced. At the near infrared wavelength at which this observation was made, the in-falling sunlight is almost completely absorbed by gaseous methane present in the planetary atmosphere and the disk of Uranus therefore appears unusually dark. At the same time, the icy material in the rings reflects the sunlight and appears comparatively bright.

The observers at ISAAC were Emmanuel Lellouch and Thérèse Encrenaz of the Observatoire de Paris (France) and Jean-Gabriel Cuby and Andreas Jaunsen (both ESO-Chile).

More details can be found in ESO press release PR 31/02.



ESO Workshop on Large Programmes and Public Surveys

Garching, Germany, 19–21 May 2003

An evaluation of the scientific success of the first completed Large Programmes at the VLT and public surveys should take place before the survey telescopes VST and VISTA start operating. To assess the scientific return of the Large Programmes ESO is organizing a three-day workshop in Garching.

Background

In 1996, on request of the OPC, a working group was formed to discuss the future of 'Key Programmes' in the era of the VLT. The description of Large Programmes in the Call for Proposals reflects the recommendations by the working group.

The working group further suggested that "at about the time of the start of operations of UT3 the definition of the Large Programmes and its implementations should be reconsidered".

VST operations are planned to start in 2004 and a major fraction of the time at this telescope, and later on VISTA, shall be dedicated to surveys. The workshop will address the issue on how best to deal with surveys for these telescopes.

Reason for the Workshop

ESO feels it is time to evaluate the scientific success of the first completed Large Programmes at the VLT. Since surveys in effect are Large Programmes (and many of them have been implemented as such at ESO) the relation of surveys to other forms of observational programmes should be discussed as well. This should provide an overview of the scientific return and a chance to re-assess the validity of the Large Programmes.

All Large Programmes that are either completed or near completion shall present their scientific results and the impact the project had in its field.

With the VST and VISTA on the horizon a discussion of Public Surveys at ESO is indicated as well. A special session will be devoted to discussing the handling of surveys at ESO in the future.

Scientific Organizing Committee

John Black, Gothenburg
Catherine Cesarsky, ESO
Gerry Gilmore, Cambridge
Joachim Krautter, Heidelberg
Andy Lawrence, Edinburgh
Bruno Leibundgut, ESO

Simon Lilly, Zurich
Jean-Loup Puget, Paris
Alvio Renzini, ESO
Christoffel Waelkens, Leuven
Stefan Wagner, Heidelberg

Format

The workshop will start with a presentation of every Large Programme up to Period 69. A discussion session to assess the effectiveness of the Large Programme concept is planned to follow. The extant surveys at ESO will be presented and schemes for efficient use of the survey telescopes evaluated in a separate discussion session.

Registration

Participants are asked to register for the workshop using the form available at <http://www.eso.org/surveys03>

Deadline for the registration is 1 April, 2003.

Please note that only a limited amount of participants can be accepted due to space limitations.

ESO Workshop on High-Resolution Infrared Spectroscopy in Astronomy

ESO-Headquarters, Garching near Munich, November 18-21, 2003

Infrared spectroscopy at a resolution of a few km/s offers a unique tool to study rotational-vibrational transitions of many abundant molecules as well as important atomic lines in a multitude of interesting astrophysical environments. Applications include the possible direct detection of exosolar planets, measurements of the abundances and magnetic fields of stars, studies of ISM chemistry and the kinematics of stars and gas in galactic centres.

In this workshop the latest status of the high-resolution infrared spectroscopic capabilities of the VLT (CRIRES, VISIR) and other observatories shall be presented.

For space reasons the number of participants is limited to 110.

More details, preliminary programme and registration form can be retrieved from

<http://www.eso.org/gen-fac/meetings/ekstasy2003>

or contact

ekstasy2003@eso.org for further information

FIRST ANNOUNCEMENT

ESO Workshop on Science with Adaptive Optics

ESO Headquarters, Garching near Munich, September 16–19, 2003

Over the past ten years, the concept of adaptive optics has matured from early experimental stages to a standard observing tool now available at many large optical and near-infrared telescope facilities. Indeed, adaptive optics has become an integral part of all present and future large telescope initiatives, and will be essential in exploiting the full potential of the large optical interferometers currently under construction. Adaptive optics has been identified as one of the key technologies for astronomy in the 21st century.

Adaptive optics has already delivered exciting results covering areas from solar-system astronomy (both the sun and the planetary system) over the star-forming regions in the solar neighbourhood to Local Group galaxies and objects at cosmological distances.

Recent highlights include:

- Evolution of small-scale structures on the solar surface
- Discovery of binary asteroids and asteroids moons
- High-resolution studies of circumstellar disks around young stars
- Precise mass determination of the black hole in the Galactic Centre
- Spatially resolved studies of extragalactic stellar populations

The present meeting intends to bring together users of adaptive optics from all fields of astronomy to discuss the latest scientific results obtained with diverse adaptive optics systems and to exchange ideas on how to reduce and analyse such observations.

This ESO workshop aims also at educating the general astronomical community in Europe on the unique science potential of adaptive optics for all branches of astronomy. We want to bring together researchers working in many different areas of astronomy in order to provide a comprehensive picture of the utilization of adaptive optics in astronomy. Synergy effects are expected from the comparison of different observing and data analysis strategies.

Co-chairs: Wolfgang Brandner (MPIA), Markus Kasper (ESO)

Scientific Organizing Committee:

Danielle Alloin (ESO), Laird Close (Steward Obs., Tucson, USA), Tim Davidge (Herzberg Inst., Victoria, Canada), Reinhard Genzel (MPE, Germany), Thomas Henning (MPIA, Germany), Christoph Keller (NSO Tucson, USA), Anne-Marie Lagrange (LAOG, France), Simon Morris (Durham, UK), Francois Rigaut (Gemini, USA), Daniel Rouan (Obs. de Paris, France), Hans Zinnecker (AIP, Germany)

For more details and registration, see <http://www.eso.org/aoscience03>

Symposium Secretary: Christina Stoffer

European Southern Observatory
Karl-Schwarzschild-Str. 2, D-85748 Garching bei München, Germany
FAX: +49 89 3200 6480
email: aoscience03@eso.org

PERSONNEL MOVEMENTS

International Staff

(1 January – 28 February 2003)

ARRIVALS

EUROPE

ALBERTSEN, Maja (DK), Student
ANDOLFATO, Luigi (I), VLT Software Engineer
BRAUD, Jérémy (F), Associate
FRAHM, Robert (D), VLT Software Engineer
KASPER, Markus (D), Adaptive Optics Instrument Scientist
LIMA, Jorge (P), Associate
NEVES, Antonio (P/GB), European Project Manager ALMA
NORMAN, Colin (AUS), Associate
PASQUATO, Moreno (I), ALMA Software Integrator
PERCHERON, Isabelle (F), Astronomical Data Quality Control Scientist
POPOVIC, Dan (AUS), Software Engineer
RABIEN, Sebastian (D), Associate

CHILE

CASQUILHO FARIA, Daniel (S), Student
GAVIGNAUD, Isabelle (F), Student
SBORDONE, Luca (I), Student

DEPARTURES

EUROPE

DEMARCO, Ricardo (RCH), Student
FRIEDRICH, Yawo (D), Associate
GORSKI, Krzysztof (PL), Archive Astronomer
PIERFEDERICI, Francesco (I), Paid Associate
TEIXERA, Rui (P), Trainee
VAN BOEKEL, Roy (NL), Student

CHILE

SCHÜTZ, Oliver (D), Student
SLUSE, Dominique (B), Student

Local Staff

(1 December 2002 – 31 January 2003)

JARA MARQUEZ, Maria Francisca, Personnel Assistant
MORALES CANCINO, Luis, Driver
TORREJON KOSCINA, Arturo, Telescope Instrument Operator
VEGA TELLO, Rolando, Telescope Instrument Operator

ARRIVALS

ALVAREZ BRAVO, Jose Luis, Laser Specialist
ARREDONDO HAMAME, Diego, System Administrator
CARDENAS SCHWEIGER, Cesar, Electronics Technician
GONZALEZ BURGOS, Sergio, Electronics Technician
GUERRA ESCOBAR, Carlos, Instrumentation Maintenance Technician
GUTIERREZ NIETO, Fernando, Electronics Technician
OLIVAREZ GONZALEZ, Francisco, Precision Mechanic

DEPARTURES

ACEVEDO CISTERNAS, Maria Teresa, Telescope Instrument Operator
ADRIAZOLA PUCHALT, Patricia, Purchasing Assistant
ARAYA TORO, Jorge, Telescope Instrument Operator
BARRIGA CAMPINO, Pablo, Instrumentation Engineer

ACRONYMS USED AT ESO

Confused?

Many acronyms are used in modern science, and the EPR Department of ESO (i.e. the Education and Public Relations Department of the European Southern Observatory) has from time to time received requests for translations. Clearly, it would help our friends and website-visitors to know what these acronyms really mean. We have now reacted to this need by putting a reasonably complete glossary of acronyms used at ESO on the web, at

<http://www.eso.org/outreach/epr/eso-acronyms.html>

Happy reading!

ESO Studentship Programme

The European Southern Observatory research student programme aims at providing opportunities and facilities to enhance the Ph.D. programmes of ESO member-state universities. Its goal is to bring young scientists into close contact with the instruments, activities, and people at one of the world's foremost observatories. For more information about ESO's astronomical research activities please consult <http://www.eso.org/science/>

Students in the programme work on their doctoral project under the formal supervision of their home university. They come to either Garching or Santiago for a stay of normally one or two years to conduct part of their studies under the co-supervision of an ESO staff astronomer. Candidates and their home-institute supervisors should agree on a research project together with the ESO local supervisor. A list of potential ESO supervisors and their research interest can be found at <http://www.eso.org/science/sci-pers.html#faculty> and <http://www.sc.eso.org/santiago/science/person.html>. A list of current PhD projects offered by ESO staff is available at <http://www.eso.org/science/thesis-topics/>. It is highly recommended that the applicants start their Ph.D. studies at their home institute before continuing their Ph.D. work and developing observational expertise at ESO.

In addition, the students in Chile have the opportunity to volunteer for a small amount of duties (~40 nights per year) at the La Silla Observatory. These duties are decided on a trimester by trimester basis, aiming at giving the student insight into the observatory operations and shall not interfere with the research project of the student in Santiago.

The ESO studentship programme is shared between the ESO Headquarters in Garching (Germany) and the Vitacura offices in Santiago (Chile). These positions are open to students enrolled in a Ph.D. programme in the ESO member states and, exceptionally, at a university outside the ESO member states.

Candidates will be notified of the results of the selection process in July 2003. Studentships typically begin between August and December of the year in which they are awarded. In well justified cases starting dates in the year following the application can be negotiated.

The closing date for applications is June 15, 2003.

Please apply by:
filling the form available at <http://www.eso.org/gen-fac/adm/pers/forms/studentapplifform.html>
and attaching to your application:

- a Curriculum Vitae (incl. a list of publications, if any), with a copy of the transcript of university certificate(s)/diploma(s).
- a summary of the master thesis project (if applicable) and ongoing projects indicating the title and the supervisor (maximum half a page), as well as an outline of the Ph.D. project highlighting the advantages of coming to ESO (recommended 1 page, max. 2).
- two letters of reference, one from the home(institute supervisor/advisor and one from the ESO local supervisor, and a letter from the home institution that i) guarantees the financial support for the remaining Ph.D. period after the termination of the ESO studentship, ii) indicates whether the requirements to obtain the Ph.D. degree at the home institute are already fulfilled.

All documents should be typed and in English (but no translation is required for the certificates and diplomas).

The application material has to be addressed to:

European Southern Observatory
Studentship Programme
Karl-Schwarzschild-Str.2, 85748 Garching bei München (Germany)

All material, including the recommendation letters, must reach ESO by the deadline (June 15); applications arriving after the deadline or incomplete applications will not be considered!

For further information contact Christina Stoffer (cstoffer@eso.org).

SUBJECT INDEX

ORGANIZATIONAL MATTERS

Catherine Cesarsky: United Kingdom Becomes Tenth Member of ESO **108**, 1
 Catherine Cesarsky: ESO Turns 40 **109**, 1

SPEECHES TO MARK THE ACCESSION OF THE UK TO ESO

Lord Sainsbury, UK Science Minister **109**, 2
 Dr. Arno Freytag, President of the ESO Council **109**, 3
 Dr. Catherine Cesarsky, ESO Director General **109**, 3
 Gerry Gilmore: ESO and the UK. Why Does the UK Need More Astronomy? **109**, 4

ESO Turns 40. Perspectives from the Directors General, Past and Present: Adriaan Blaauw: Reflections on ESO, 1957–2002 **109**, 7

Lodewijk Woltjer **109**, 9

Harry van der Laan: From SEST to ALMA, from NTT to OWL: Of Vision, Dreams and Realities **109**, 10

Riccardo Giacconi **109**, 11

Catherine Cesarsky **109**, 11

Some Snippets of History **109**, 12

TELESCOPES AND INSTRUMENTATION

W. Brandner, G. Rousset, R. Lenzen, N. Hubin, F. Lacombe, R. Hofmann, A. Moorwood, A.-M. Lagrange, E. Gendron, M. Hartung, P. Puget, N. Ageorges, P. Bierichel, H. Bouy, J. Charton, G. Dumont, T. Fusco, Y. Jung, M. Lehnert, J.-L. Lizon, G. Monnet, D. Mouillet, C. Moutou, D. Rabaud, C. Röhrle, S. Skole, J. Spyromilio, C. Storz, L. Tacconi-Garman, G. Zins: NAOS+CONICA at YEPUN: First VLT Optics System Sees First Light **107**, 1

R. Kurz, S. Guilloteau, P. Shaver: The Atacama Large Millimeter Array **107**, 7

L. Germany: News from the 2p2 Team **107**, 13

G. Monnet: Status of VLT 2nd Generation Instrumentation **108**, 2

R. Hanuschik and D. Silva: VLT Quality Control and Trending Services **108**, 4

Recent NAOS-CONICA Images **108**, 9

L. Germany: News from La Silla **108**, 10

L.-Å. Nyman, P. Schilke and R.S. Booth: The Atacama Pathfinder Experiment **109**, 18

O. Le Fevre, D. Mancini, M. Saïsse, S. Brau-Nogué, O. Caputi, L. Castinel, S. D'Odo-rico, B. Garilli, M. Kissler, C. Lucuix, G. Mancini, A. Pauget, G. Sciarretta, M. Scoddeggio, L. Tresse, D. Maccagni, J.-P. Picat, G. Vettolani: VIMOS Commissioning on VLT-Melipal **109**, 21

L. Germany: 2.2-m Team **109**, 27

L. Pasquini et al.: Installation and Commissioning of FLAMES, the VLT Multifibre Facility **110**, 1

F. Pepe, M. Mayor, G. Rupprecht: HARPS: ESO's Coming Planet Searcher. Chasing

Exoplanets with the La Silla 3.6-m Telescope **110**, 9

K. Kuijken et al.: OmegaCAM: the 16k × 16k CCD Camera for the VLT Survey Telescope **110**, 15

A. Glindemann: The VLTI – 20 Months after First Fringes **110**, 18

B. Koehler, C. Flebus, P. Dierickx, M. Dimmler, M. Duchateau, P. Duhoux, G. Ehrenfeld, E. Gabriel, P. Gloesener, V. Heinz, R. Karban, M. Kraus, J.M. Moresmau, N. Ninane, O. Pirnay, E. Quertemont, J. Strasser, K. Wirenstrand: The Auxiliary Telescopes for the VLTI: a Status Report **110**, 21

Roberto Gilmozzi and Jason Spyromilio: Paranal Observatory – 2002 **110**, 28

O. Hainaut: News from La Silla: Science Operations Department **110**, 30
 Two unusual views of La Silla **110**, 31

CHILEAN ASTRONOMY

L. Bronfman: A Panorama of Chilean Astronomy **107**, 14

A. Reisenegger, H. Quintana, D. Proust, E. Slezak: Dynamics and Mass of the Shapley Supercluster, the Largest Bound Structure in the Local Universe **107**, 18

REPORTS FROM OBSERVERS

D. Baade, T. Rivinius, S. Štefl: To Be or Not to Be and a 50-cm Post-Mortem Eulogy **107**, 24

F. Courbin, G. Letawe, P. Magain, L. Wisotzki, P. Jablonka, D. Alloin, K. Jahnke, B. Kuhlbrodt, G. Meylan, D. Minniti: Spectroscopy of Quasar Host Galaxies at the VLT: Stellar Populations and Dynamics Down to the Central Kiloparsec **107**, 28

J. Sollerman and V. Flyckt: The Crab Pulsar and its Environment **107**, 32

L. Vanzi, F. Mannucci, R. Maiolino, M. Della Valle: SOFI Discovers a Dust Enshrouded Supernova **107**, 35

G. Rupprecht: A Deep Look at an Active Galaxy **107**, 38

Coming Home at Paranal. Unique "Residencia" Opens at the VLT Observatory **107**, 39

G. Hasinger, J. Bergeron, V. Mainieri, P. Rosati, G. Szokoly and the CDFS Team: Understanding the sources of the X-ray background: VLT identifications in the *Chandra/XMM-Newton* Deep Field South **108**, 11

Carne Gallart, Robert Zinn, Frederic Pont, Eduardo Hardy, Gianni Marconi, Roberto Buonanno: Using color-magnitude diagrams and spectroscopy to derive star formation histories: VLT observations of Fornax **108**, 16

Thomas Rivinius, Dietrich Baade, Stanislav Štefl, Monika Maintz, Richard Townsend: The ups and downs of a stellar surface: Nonradial pulsation modelling of rapid rotators **108**, 20

L. Pentericci, H.W. Rix, X. Fan, M. Strauss: The VLT and the most distant quasars **108**, 24

Daniel Harbeck, Eva K. Grebel, Graeme H. Smith: Evidence for external enrichment processes in the globular cluster 47 Tuc? **108**, 26

M. McCaughrean, H. Zinnecker, M. Andersen, G. Meeus, N. Lodieu: Standing on the Shoulders of a Giant: ISAAC, Antu, and Star Formation **109**, 28

L. Kaper, A. Castro-Tirado, A. Fruchter, J. Greiner, J. Hjorth, E. Pian, M. Andersen, K. Beuermann, M. Boer, I. Burud, A. Jaunsen, B. Jensen, J.M. Castro-Ceron, S. Ellison, F. Frontera, J. Fynbo, N. Gehrels, J. Gorosabel, J. Heise, F. Hessman, K. Hurley, S. Klose, C. Kouveliotou, N. Masetti, P. Möller, E. Palazzi, H. Pedersen, L. Piro, K. Reinsch, J. Rhoads, E. Rol, I. Salamanca, N. Tanvir, P.M. Vreeswijk, R.A.M.J. Wijers, T. Wiklund, A. Zeh, E.P.J. van den Heuvel: Gamma-Ray Bursts: the Most Powerful Cosmic Explosions **109**, 37

R.E. Mennickent, C. Tappert, M. Diaz: Cataclysmic Variables: Gladiators in the Arena **109**, 41

L. Wang, D. Baade, P. Höflich, J.C. Wheeler: Supernova Polarimetry with the VLT: Lessons from Asymmetry **109**, 47

N.C. Santos, M. Mayor, D. Queloz, S. Udry: Extra-Solar Planets **110**, 32

I. Labbé, M. Franx, E. Daddi, G. Rudnick, P.G. van Dokkum, A. Moorwood, N.M. Förster Schreiber, H.-W. Rix, P. van der Werf, H. Röttgering, L. van Starckenburg, A. van de Wel, I. Trujillo, and K. Kuijken: FIRES: Ultradeep Near-Infrared Imaging with ISAAC of the Hubble Deep Field South **110**, 38

OTHER ASTRONOMICAL NEWS

F. Paresce: Release of Scientific Data from VLTI Commissioning **107**, 41

A. Renzini: VLT Science Verification Policy and Procedures **107**, 41

D. Alloin: News from Santiago **107**, 42

ESO Studentship Programme **107**, 42

M. Dennefeld: The Third NEON Observing School **107**, 43

A. Bacher: "Life in the Universe" Winners on La Silla and Paranal **107**, 43

A. Bacher and L. Lindberg Christensen: In the Footsteps of Scientists – ESA/ESO Astronomy Exercise Series **107**, 44

Steve Warren: The UKIRT Infrared Deep Sky Survey becomes an ESO public survey **108**, 31

M. Jacob, P. Shaver, L. Dilella, A. Gimenez: Summary of the ESO-CERN-ESA Symposium on Astronomy, Cosmology and Fundamental Physics **108**, 35

M. Sterzik: IAOC Workshop in La Serena: Galactic Star Formation across the stellar Mass Spectrum **108**, 40

- Danielle Alloin and Luis Campusano: Astronomical Virtual Observatories discussed in Chile **108**, 40
- Andreas Glindemann: Hunting for Planets – GENIE Workshop at Leiden University **108**, 40
- Young Stars in Old Galaxies – a Cosmic Hide and Seek Game **108**, 41
- A. Bacher and R.M. West: Information from the ESO Educational Office **108**, 42
- C. Madsen: ESO in the European Parliament **108**, 43
- Rolf-Peter Kudritzki: Obituary Kurt Hunger **108**, 43
- German Foreign Minister Visits Paranal Observatory **108**, 45
- E. Mason and S. Howell: An Exciting Working Session on Cataclysmic Variables at ESO/Santiago **109**, 51
- W. Hillebrandt and B. Leibundgut: Conference Summary: From Twilight to Highlight: the Physics of Supernovae. ESO/MPA/MPE Summer Workshop 2002 **109**, 52
- J.R. Walsh and M.M. Roth: Developing 3D Spectroscopy in Europe **109**, 54
- D. Hofstadt, L.-A. Nyman: Obituary Guillermo Delgado (1961–2002) **109**, 55
- C. Madsen: Forty Years ESO – Public Anniversary Activities **109**, 56
- A. Bacher and R.M. West: First Teachers Training Course at ESO HQ was a Great Success **109**, 57
- M. Kissler-Patig: Summary of the Workshop on Extragalactic Globular Cluster Systems hosted by the European Southern Observatory in Garching on August 27–30, 2002 **110**, 42
- A. Glindemann: The VLTI: Challenges for the Future. Workshop at Jenam 2002 in Porto **110**, 44
- P. Shaver and E. Van Dishoek: Summary of a Meeting on Science Operations with ALMA, held on Friday, 8 November 200 **110**, 44
- C. Madsen: Celebrating ESO’s 40th Anniversary **110**, 45
- C. Madsen: Breaking the Ground for the European Research Area – The Conference ‘European Research 2002 **110**, 46
- A Nobel Prize for Riccardo Giacconi **110**, 47
- Agreement Between the Government of the Republic of Chile and ESO for Establishing a New Centre for Observation in Chile – ALMA **110**, 48
- Sara Ellison: Eighty Nights Up a Mountain **110**, 48
- ESO Fellowship Programme 2002/2003 **108**, 47
- List of Scientific Preprints (March–June 2001) **108**, 47
- A Note from the New Editor **108**, 48
- Workshop on “Structure Evolution and Cosmology: New synergy between ground-based observations, space observations and theory” to be held at ESO/Santiago **109**, 58
- Workshop on “Stellar Candles for the Extragalactic Distance Scale” to be held at the Universidad de Concepción **109**, 58
- Meeting on “Science Operations with the Atacama Large Millimeter Array” to be held at ESO, Garching **109**, 59
- ESO Vacancy: Editor (EDG604) **109**, 59
- Personnel Movements **109**, 59
- Corrigendum **109**, 59
- First Announcement of an ESO Workshop on High-Resolution Spectroscopy in Astronomy **110**, 50
- ESO Workshop on Large Programmes and Public Surveys **110**, 50
- Personnel Movements **110**, 50
- Daniel Hofstadt: Manfred Ziebell Retires **110**, 51
- Jacques Breysacher: Christa Euler – Thirty-Seven Years of Service with ESO! **110**, 51
- New ESO Proceedings **110**, 51
- ESO Workshop Proceedings Still Available **110**, 51

ANNOUNCEMENTS

- Personnel Movements **107**, 45
- List of Scientific Preprints **107**, 45
- The Very Large Interferometer: Challenges for the Future (A Jenam 2002 Workshop to be held at Porto, Portugal, on September 4–7) **108**, 46
- Personnel Movements **108**, 46

AUTHOR INDEX

A

- D. Alloin: News from Santiago **107**, 42
- D. Alloin and L. Campusano: Astronomical Virtual Observatories discussed in Chile **108**, 40

B

- D. Baade, T. Rivinius, S. Štefl: To Be or Not to Be and a 50-cm Post-Mortem Eulogy **107**, 24
- F. Courbin, G. Letawe, P. Magain, L. Wisotzki, P. Jablonka, D. Alloin, K. Jahnke, B. Kuhlbrodt, G. Meylan, D. Minniti: Spectroscopy of Quasar Host Galaxies at the VLT: Stellar Populations and Dynamics Down to the Central Kiloparsec **107**, 28
- A. Bacher: “Life in the Universe” Winners on La Silla and Paranal **107**, 43
- A. Bacher and L. Lindberg Christensen: In the Footsteps of Scientists – ESA/ESO Astronomy Exercise Series **107**, 44
- A. Bacher and R.M. West: Information from the ESO Educational Office **108**, 42
- A. Bacher and R.M. West: First Teachers Training Course at ESO HQ was a Great Success **109**, 57
- P. Benvenuti: Recovery of a historical document (ESO Turns 40. Some Snippets of History) **109**, 17
- Adriaan Blaauw: Reflections on ESO, 1957–2002 (ESO Turns 40. Perspectives from the Directors General, Past and Present) **109**, 7

C

- W. Brandner, G. Rousset, R. Lenzen, N. Hubin, F. Lacombe, R. Hofmann, A. Moorwood, A.-M. Lagrange, E. Gendron, M. Hartung, P. Puget, N. Ageorges, P. Bierichel, H. Bouy, J. Charton, G. Dumont, T. Fusco, Y. Jung, M. Lehnert, J.-L. Lizon, G. Monnet, D. Mouillet, C. Moutou, D. Rabaud, C. Röhrle, S. Skole, J. Spyromilio, C. Storz, L. Tacconi-Garman, G. Zins: NAOS+CONICA at YEPUN: First VLT Optics System Sees First Light **107**, 1
- J. Breysacher: Early days of the OPC (ESO Turns 40. Some Snippets of History) **109**, 12
- Jacques Breysacher: Christa Euler – Thirty-Seven Years of Service with ESO! **110**, 51
- L. Bronfman: A Panorama of Chilean Astronomy **107**, 14
- Catherine Cesarsky: United Kingdom Becomes Tenth Member of ESO **108**, 1
- Catherine Cesarsky: ESO Turns 40 **109**, 1
- Catherine Cesarsky, ESO Director General: Speech to mark the accession of the UK to ESO **109**, 3
- Catherine Cesarsky (ESO Turns 40. Perspectives from the Directors General, Past and Present) **109**, 11
- C. Cesarsky: First Light of UT4 (ESO Turns 40. Some Snippets of History) **109**, 17

D

- M. Dennefeld: The Third NEON Observing School **107**, 43

E

- Sara Ellison: Eighty Nights Up a Mountain **110**, 48
- D. Enard: The early days of instrumentation at La Silla (ESO Turns 40. Some Snippets of History) **109**, 13

F

- Dr. Arno Freytag, President of the ESO Council: Speech to mark the accession of the UK to ESO **109**, 3

G

- Carme Gallart, Robert Zinn, Frederic Pont, Eduardo Hardy, Gianni Marconi, Roberto Buonanno: Using color-magnitude diagrams and spectroscopy to derive star formation histories: VLT observations of Fornax **108**, 16
- L. Germany: News from the 2p2 Team **107**, 13
- L. Germany: News from La Silla **108**, 10
- L. Germany: 2.2-m Team **109**, 27
- Riccardo Giacconi (ESO Turns 40. Perspectives from the Directors General, Past and Present) **109**, 11

- Gerry Gilmore: ESO and the UK. Why Does the UK Need More Astronomy? (Speech to mark the accession of the UK to ESO) **109**, 4
- Roberto Gilmozzi and Jason Spyromilio: Paranal Observatory – 2002 **110**, 28
- Andreas Glindemann: Hunting for Planets – GENIE Workshop at Leiden University **108**, 40
- A. Glindemann et al.: First Fringes with ANTU and MELIPAL (ESO Turns 40. Some Snippets of History) **109**, 17
- A. Glindemann: The VLTI – 20 Months after First Fringes **110**, 18
- A. Glindemann: The VLTI: Challenges for the Future. Workshop at Jenam 2002 in Porto **110**, 44

H

- O. Hainaut: News from La Silla: Science Operations Department **110**, 30
- R. Hanuschik and D. Silva: VLT Quality Control and Trending Services **108**, 4
- Daniel Harbeck, Eva K. Grebel, Graeme H. Smith: Evidence for external enrichment processes in the globular cluster 47 Tuc? **108**, 26
- G. Hasinger, J. Bergeron, V. Mainieri, P. Rosati, G. Szokoly and the CDFS Team: Understanding the sources of the X-ray background: VLT identifications in the *Chandra/XMM-Newton* Deep Field South **108**, 11
- W. Hillebrandt and B. Leibundgut: Conference Summary: From Twilight to Highlight: the Physics of Supernovae. ESO/MPA/MPE Summer Workshop 2002 **109**, 52
- D. Hofstadt: Renata Scotto at La Silla (ESO Turns 40. Some Snippets of History) **109**, 12
- D. Hofstadt: La Silla vaut bien une Messe (ESO Turns 40. Some Snippets of History) **109**, 13
- D. Hofstadt, L.-Å. Nyman: Obituary Guillermo Delgado (1961–2002) **109**, 55
- Daniel Hofstadt: Manfred Ziebell Retires **110**, 51

J

- M. Jacob, P. Shaver, L. Dilella, A. Gimenez: Summary of the ESO-CERN-ESA Symposium on Astronomy, Cosmology and Fundamental Physics **108**, 35

K

- L. Kaper, A. Castro-Tirado, A. Fruchter, J. Greiner, J. Hjorth, E. Pian, M. Andersen, K. Beuermann, M. Boer, I. Burud, A. Jaunsen, B. Jensen, J.M. Castro-Ceron, S. Ellison, F. Frontera, J. Fynbo, N. Gehrels, J. Gorosabel, J. Heise, F. Hessman, K. Hurley, S. Kloise, C. Kouveliotou, N. Masetti, P. Möller, E. Palazzi, H. Pedersen, L. Piro, K. Reinsch, J. Rhoads, E. Rol, I. Salamanca, N. Tanvir, P.M. Vreeswijk, R.A.M.J. Wijers, T. Wiklind, A. Zeh, E.P.J. van den Heuvel: Gamma-Ray Bursts: the Most Powerful Cosmic Explosions **109**, 37
- M. Kissler-Patig: Summary of the Workshop on Extragalactic Globular Cluster Systems hosted by the European Southern Observatory in Garching on August 27–30, 2002 **110**, 42

- B. Koehler, C. Flebus, P. Dierickx, M. Dimmler, M. Duchateau, P. Duhoux, G. Ehrenfeld, E. Gabriel, P. Gloesener, V. Heinz, R. Karban, M. Kraus, J.M. Moresmau, N. Ninane, O. Pirnay, E. Quertemont, J. Strasser, K. Wirenstrand: The Auxiliary Telescopes for the VLTI: a Status Report **110**, 21
- Rolf-Peter Kudritzki: Obituary Kurt Hunger **108**, 43
- K. Kuijken et al.: OmegaCAM: the 16k × 16k CCD Camera for the VLT Survey Telescope **110**, 15
- R. Kurz, S. Guilloteau, P. Shaver: The Atacama Large Millimeter Array **107**, 7

L

- I. Labbé, M. Franx, E. Daddi, G. Rudnick, P.G. van Dokkum, A. Moorwood, N.M. Förster Schreiber, H.-W. Rix, P. van der Werf, H. Röttgering, L. van Starckenburg, A. van de Wel, I. Trujillo, and K. Kuijken: FIREs: Ultradeep Near-Infrared Imaging with ISAAC of the Hubble Deep Field South **110**, 38
- S. Laustsen: How ESO got its Optics Group (ESO Turns 40. Some Snippets of History) **109**, 12
- O. Le Fevre, D. Mancini, M. Saisse, S. Braun-Nogué, O. Caputi, L. Castinel, S. D’Odo-rico, B. Garilli, M. Kissler, C. Lucaix, G. Mancini, A. Pauget, G. Sciarretta, M. Scoddeggio, L. Tresse, D. Maccagni, J.-P. Picat, G. Vettolani: VIMOS Commissioning on VLT-Melipal **109**, 21

M

- C. Madsen: ESO in the European Parliament **108**, 43
- C Madsen: Forty Years ESO – Public Anniversary Activities **109**, 56
- C. Madsen: Celebrating ESO’s 40th Anniversary **110**, 45
- C. Madsen: Breaking the Ground for the European Research Area – The Conference ‘European Research 2002’ **110**, 46
- E. Mason and S. Howell: An Exciting Working Session on Cataclysmic Variables at ESO/Santiago **109**, 51
- M. McCaughrean, H. Zinnecker, M. Andersen, G. Meeus, N. Lodieu: Standing on the Shoulders of a Giant: ISAAC, Antu, and Star Formation **109**, 28
- R.E. Mennickent, C. Tappert, M. Diaz: Cataclysmic Variables: Gladiators in the Arena **109**, 41
- G. Monnet: Status of VLT 2nd Generation Instrumentation **108**, 2
- A. Moorwood: The early days of infrared instrumentation at ESO (ESO Turns 40. Some Snippets of History) **109**, 15

N

- W. Nees: ESO’s first step into the world of minicomputers (ESO Turns 40. Some Snippets of History) **109**, 16
- L.-Å. Nyman, P. Schilke and R.S. Booth: The Atacama Pathfinder Experiment **109**, 18

P

- F. Paresce: Release of Scientific Data from VLTI Commissioning **107**, 41

- L. Pasquini et al.: Installation and Commissioning of FLAMES, the VLT Multifibre Facility **110**, 1
- L. Pentericci, H.W. Rix, X. Fan, M. Strauss: The VLT and the most distant quasars **108**, 24
- F. Pepe, M. Mayor, G. Rupprecht: HARPS: ESO’s Coming Planet Searcher. Chasing Exoplanets with the La Silla 3.6-m Telescope **110**, 9

R

- A. Reisenegger, H. Quintana, D. Proust, E. Slezak: Dynamics and Mass of the Shapley Supercluster, the Largest Bound Structure in the Local Universe **107**, 18
- A. Renzini: VLT Science Verification Policy and Procedures **107**, 41
- Thomas Rivinius, Dietrich Baade, Stanislav Štefl, Monika Maintz, Richard Townsend: The ups and downs of a stellar surface: Nonradial pulsation modelling of rapid rotators **108**, 20
- G. Rupprecht: A Deep Look at an Active Galaxy **107**, 38

S

- Lord Sainsbury, UK Science Minister: Speech to mark the accession of the UK to ESO **109**, 2
- N.C. Santos, M. Mayor, D. Queloz, S. Udry: Extra-Solar Planets **110**, 32
- P. Shaver and E. Van Dishoek: Summary of a Meeting on Science Operations with ALMA, held on Friday, 8 November 2002 **110**, 44
- J. Sollerman and V. Flyckt: The Crab Pulsar and its Environment **107**, 32
- M. Sterzik: IAOC Workshop in La Serena: Galactic Star Formation across the stellar Mass Spectrum **108**, 40
- J.-P. Swings: First experience at La Silla, and some activities for the VLT (ESO Turns 40. Some Snippets of History) **109**, 13

V

- Harry van der Laan: From SEST to ALMA, from NTT to OWL: Of Vision, Dreams and Realities (ESO Turns 40. Perspectives from the Directors General, Past and Present) **109**, 10
- L. Vanzi, F. Mannucci, R. Maiolino, M. Della Valle: SOFI Discovers a Dust Enshrouded Supernova **107**, 35

W

- J.R. Walsh and M.M. Roth: Developing 3D Spectroscopy in Europe **109**, 54
- L. Wang, D. Baade, P. Höflich, J.C. Wheeler: Supernova Polarimetry with the VLT: Lessons from Asymmetry **109**, 47
- Steve Warren: The UKIRT Infrared Deep Sky Survey becomes an ESO public survey **108**, 31
- R. West: Memories of early times at ESO (ESO Turns 40. Some Snippets of History) **109**, 12
- R. Wilson: First Astronomical Light at the NTT (ESO Turns 40. Some Snippets of History) **109**, 16
- Lodewijk Woltjer (ESO Turns 40. Perspectives from the Directors General, Past and Present) **109**, 9

ESO, the European Southern Observatory, was created in 1962 to "... establish and operate an astronomical observatory in the southern hemisphere, equipped with powerful instruments, with the aim of furthering and organising collaboration in astronomy..." It is supported by ten countries: Belgium, Denmark, France, Germany, Italy, the Netherlands, Portugal, Sweden, Switzerland and the United Kingdom. ESO operates at two sites in the Atacama desert region of Chile. The new Very Large Telescope (VLT), the largest in the world, is located on Paranal, a 2,600 m high mountain approximately 130 km south of Antofagasta, in the driest part of the Atacama desert where the conditions are excellent for astronomical observations. The VLT consists of four 8.2-metre diameter telescopes. These telescopes can be used separately, or in combination as a giant interferometer (VLTI). At La Silla, 600 km north of Santiago de Chile at 2,400 m altitude, ESO operates several optical telescopes with diameters up to 3.6 m and a submillimetre radio telescope (SEST). Over 1300 proposals are made each year for the use of the ESO telescopes. The ESO headquarters are located in Garching, near Munich, Germany. This is the scientific, technical and administrative centre of ESO where technical development programmes are carried out to provide the Paranal and La Silla observatories with the most advanced instruments. There are also extensive astronomical data facilities. ESO employs about 320 international staff members, Fellows and Associates in Europe and Chile, and about 160 local staff members in Chile.

The ESO MESSENGER is published four times a year: normally in March, June, September and December. ESO also publishes Conference Proceedings, Preprints, Technical Notes and other material connected to its activities. Press Releases inform the media about particular events. For further information, contact the ESO Education and Public Relations Department at the following address:

EUROPEAN
SOUTHERN OBSERVATORY
Karl-Schwarzschild-Str. 2
D-85748 Garching bei München
Germany
Tel. (089) 320 06-0
Telefax (089) 3202362
ips@eso.org (internet)
URL: <http://www.eso.org>
<http://www.eso.org/gen-fac/pubs/messenger/>

The ESO Messenger:
Editor: Peter Shaver
Technical editor: Kurt Kjær

Printed by
Universitätsdruckerei
WOLF & SOHN
Heidemannstr. 166
D-80939 München
Germany

ISSN 0722-6691

ESO Workshop Proceedings Still Available

Many ESO Conference and Workshop Proceedings are still available and may be ordered at the European Southern Observatory. Some of the more recent ones are listed below.

No.	Title	Price
54	Topical Meeting on "Adaptive Optics", October 2–6, 1995, Garching, Germany. M. Cullum (ed.)	€ 40.–
55	NICMOS and the VLT. A New Era of High Resolution Near Infrared Imaging and Spectroscopy. Pula, Sardinia, Italy, May 26–27, 1998	€ 40.–
56	ESO/OSA Topical Meeting on "Astronomy with Adaptive Optics – Present Results and Future Programs". Sonthofen, Germany, September 7–11, 1999. D. Bonaccini (ed.)	€100.–
57	Bäckaskog Workshop on "Extremely Large Telescopes". Bäckaskog, Sweden, June 1–2, 1999. T. Andersen, A. Ardeberg, R. Gilmozzi (eds.)	€ 30.–
58	Beyond Conventional Adaptive Optics, Venice, Italy, May 7–10, 2001 E. Vernet, R. Ragazzoni, S. Esposito, N. Hubin (eds.)	€ 50.–

Contents

REPORTS FROM OBSERVERS

T. Ott et al.: Inward Bound: Studying the Galactic Centre with NAOS/CONICA	1
A. Stolte et al.: NAOS-CONICA Performance in a Crowded Field – the Arches Cluster	9
M. Pettini: Early Galactic Chemical Evolution with UVES	13
O. Le Fèvre et al.: The VIRMOS-VLT Deep Survey: a Progress Report	18
H. Boehnhardt et al.: Exploring the Icy World of the Edgeworth-Kuiper Belt – An ESO Large Programme	22
A. Cimatti et al.: The K20 Survey: New Light on Galaxy Formation and Evolution	29
B. Venemans, G. Miley, J. Kurk, H. Röttgering, L. Pentericci: Tracing the Formation and Evolution of Clusters and their Central Massive Galaxies to $z > 4$: a Progress Report	36

TELESCOPES AND INSTRUMENTATION

ESO and NSF Sign Agreement on ALMA. Green Light for World's Most Powerful Radio Observatory	39
New Vistas Open with MIDI at the VLT Interferometer	40
V. Doublier: TIMMI2 at the 3.6-m, or the Return of MIR	41

OTHER ASTRONOMICAL NEWS

NEWS FROM SANTIAGO

D. Alloin, M. Pierre, A. Refregier: International Workshop on "Structure Evolution and Cosmology: New Synergy Between Ground-Based Observations, Space Observations and Theory"	42
D. Alloin, W. Gieren: International Workshop on "Stellar Candles for the Extragalactic Distance Scale"	43
B. Leibundgut: Fellows at ESO: Aurore Bacmann, Maria-Rosa Cioni, Ivo Saviane and Petri Vaisanen	44
URANUS, Rings and Moons	45

ANNOUNCEMENTS

ESO Workshop on Large Programmes and Public Surveys	46
ESO Workshop on High-Resolution Infrared Spectroscopy in Astronomy	46
First Announcement of an ESO Workshop on Science with Adaptive Optics	47
Personnel Movements	47
Acronyms Used at ESO	48
ESO Studentship Programme	48

MESSENGER INDEX 2002 (Nos. 107–110)	49
-------------------------------------	----